AD_____

Award Number: DAMD17-99-1-9207

TITLE: The Role of a FGF-Binding Protein in Breast Cancer

PRINCIPAL INVESTIGATOR: Anton Wellstein, M.D., Ph.D.

CONTRACTING ORGANIZATION: Georgetown University Medical Center
Washingon, DC 20057

REPORT DATE: October 2003

TYPE OF REPORT: Final

PREPARED FOR: U.S. Army Medical Research and Materiel Command
Fort Detrick, Maryland 21702-5012

REPORT DOCUMENTATION PAGE

Form Approved
OMB No. 074-0188

1. AGENCY USE ONLY (Leave blank)	2. REPORT DATE	3. REPORT TYPE AND DATES COVERED
	October 2003	Final (15 Sep 99 - 14 Sep 03)

4. TITLE AND SUBTITLE
The Role of a FGF-Binding Protein in Breast Cancer

5. FUNDING NUMBERS
DAMD17-99-1-9207

6. AUTHOR(S)
Anton Wellstein, M.D., Ph.D.

7. PERFORMING ORGANIZATION NAME(S) AND ADDRESS(ES)
Georgetown University Medical Center
Washingon, DC 20057

E-MAIL:
wellstea@gunet.georgetown.edu

8. PERFORMING ORGANIZATION REPORT NUMBER

9. SPONSORING / MONITORING AGENCY NAME(S) AND ADDRESS(ES)
U.S. Army Medical Research and Materiel Command
Fort Detrick, Maryland 21702-5012

10. SPONSORING / MONITORING AGENCY REPORT NUMBER

11. SUPPLEMENTARY NOTES
Original contains color plates. All DTIC reproductions will be in black and white.

12a. DISTRIBUTION / AVAILABILITY STATEMENT
Approved for public release; distribution unlimited

12b. DISTRIBUTION CODE

13. ABSTRACT ***(Maximum 200 Words)***

Under this grant we studied the role and regulation of a secreted, fibroblast growth factor binding protein (FGF-BP) that can enhance angiogenesis and growth factor activity.

We found that FGF-BP is highly expressed in approximately 1/2 of invasive breast cancers and rarely in normal breast or in in situ carcinoma.

The FGF-BP gene is regulated in breast cancer cells by growth factors such as EGF. This regulation occurs at the transcriptional level and utilizes the transcription factor family C/EBPbeta as a major mechanism that involves interaction between activating and inhibitory isoforms of transcription factors.

Expression of FGF-BP as a transgene is lethal during embryogenesis in mice or in chicken embryos. Studies on mammary carcinogenesis in mice thus required the establishment of regulatable transgene expression and a tetracycline-regulated system was generated for this.

14. SUBJECT TERMS
Breast Cancer

15. NUMBER OF PAGES
72

16. PRICE CODE

17. SECURITY CLASSIFICATION OF REPORT	18. SECURITY CLASSIFICATION OF THIS PAGE	19. SECURITY CLASSIFICATION OF ABSTRACT	20. LIMITATION OF ABSTRACT
Unclassified	Unclassified	Unclassified	Unlimited

Table of Contents

INTRODUCTION

Hormones and growth factors define the capacity of human breast cancer to grow and metastasize. One of the essential requirements for the development of breast cancer are circulating steroid hormones and one of the most widely used drug therapies of breast cancer with the anti-estrogen tamoxifen is based on this fact. Furthermore, growth factor gene expression can supplement for hormone stimulation and thus contribute to hormone-independent cancer growth as well as to resistance to anti-hormone therapy or to cytotoxic drugs (reviewed e.g. in [1]).

Fibroblast growth factors (FGFs) and a potential function for a FGF-binding protein (BP)

Polypeptide growth factors of the FGF family regulate important developmental processes such as limb formation, mesoderm induction [2,3], show neurotrophic activities and stimulate the growth of new blood vessels in healing wounds or during tumor growth (reviewed in Ref. [4-6]). High concentrations of biologically active FGF-1 and FGF-2 (= aFGF and bFGF; Ref. [4]) are found in extracts of normal embryonic and adult tissues as well as in tumor tissues of different origin. However, the biological activities of both FGFs are quenched by tight binding to heparansulfate proteoglycans present in the extracellular matrix. It is only partly understood how these FGFs become solubilized and thus activated in embryonic or in tumor tissues that require angiogenesis for their growth. One established mechanism that can solubilize FGF-2 from this storage site is the digestion of the glycosaminoglycan portion of the cell attachment molecule by heparanases. An alternate mode of delivering active FGF-2 from the storage site to its receptor could be via non-covalent binding to a secreted carrier protein. Such a secreted binding protein for FGFs was described by D. Sato's laboratory in 1991 [7]. This protein was purified by from the supernatants of A431 cells. The purified protein protected FGF-2 from acid inactivation and FGF-2 bound to it retained its mitogenic activity. We hypothesized that this BP could be an important regulator that releases immobilized FGFs from their matrix storage site and thus activates them in vivo. Figure 1 (below) illustrates the proposed mechanism of action of BP that will be elucidated in more detail further below.

Growth factors, tumor angiogenesis and metastasis

One of the pivotal roles of locally-acting polypeptide growth factors is the induction of new blood vessels in a healing wound as well as in growing tumors. It has been shown in numerous studies with different approaches that a solid tumor cannot grow beyond a few millimeters in size without sufficient blood supply. In addition to the nourishing function of tumor blood vessels, they provide a pathway for the tumor cells to metastasize to distant organs. The most prominent and best studied angiogenesis factors are members of the FGF-family. Several members of the FGF family are very effective angiogenesis factors and have thus been a focus of research in tumor vascularization in the past decade. The FGF-family comprises >25 known distinct growth factors which can interact with their membrane receptors coded for by 4 separate receptor genes and numerous protein products due to alternative splicing (reviewed in [8,9]).

How do FGF's reach their receptors ?
For a growth factor to reach it's cognate receptor on the cell membrane it is usually released from cells into the extracellular space and then diffuses to the cognate receptor. Both FGF-1 and -2 lack a signal peptide and it is known that they are not released from cells into their media [4,8]. In contrast, these two growth factors are deposited into the extracellular membrane of the cells and are found tightly bound to membrane attached heparansulfates (HS). It is only partly understood how these FGFs become solubilized and thus activated in embryonic or in tumor tissues that require angiogenesis for their growth. One established mechanism that can solubilize FGF-2 from this storage site is the digestion of the heparansulfate by heparanases. Indeed tumor cells produce heparanase activities that can release active FGFs from the local storage in the extracellular matrix[9]. Furthermore, proteases that can digest the protein backbone of the proteoglycan could also release FGFs from the immobilized state and thus contribute to their activation.

The potential role of the secreted binding protein for FGF (BP) as a carrier for immobilized FGFs:
One alternative mode of delivering active FGF from the storage site to its receptor could be binding to a secreted carrier protein. The secreted FGF binding protein (BP) can serve as such an an extracellular chaperone molecule for FGFs[10] in support of the proposed mechanism of action (see Figure 1).

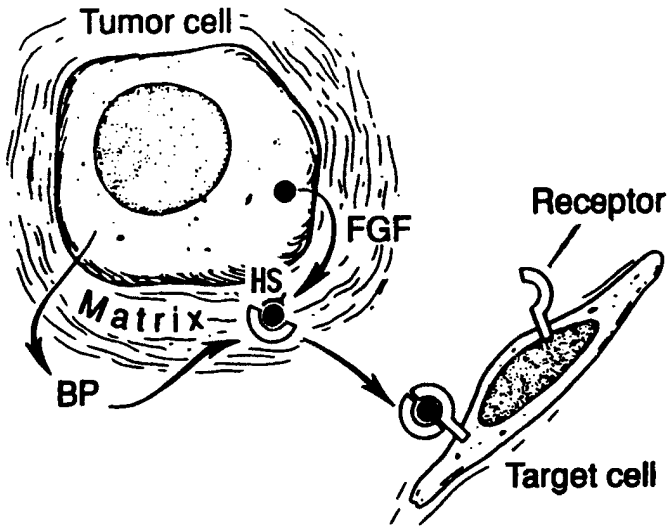

Figure 1. Model explaining the function of FGF-BP (BP) for the release of FGFs that are immobilized in the extracellular matrix. The secreted protein BP combined with high affinity into the immobilized FGS and release it in an active form. The BP / FGF complex can recognize the FGF receptor and signal through that in target cells or in the cells from which FGF is released (autocrine or paracrine mechanism) respectively.

We detected FGF-BP expression in a small series of invasive breast cancers. Furthermore, we found FGF-BP expressed in breast cancer cell lines. The hypothesis studied under this IDEA grant is that the induction of FGF-BP gene expression is an important pathway for the malignant progression of breast cancer. The induction of FGF-BP may provide a mechanism by which ubiquitously present FGF-2 or other FGF proteins can be mobilized to become mitogenic and angiogenic factor for this cancer. The major focus of this proposal is to explore the genetic basis for the activation of FGF-BP transcription during breast cancer progression and study the impact in an animal model. Towards this hypothesis we proposed to pursue the following aims:

Technial objectives:
Goal (1): To assess the significance of FGF-BP expression for the clinical course of breast cancer using archival samples with known outcome and defined pathological features. Task during Months 1 – 24.

Goal (2): To study which regulators of expression of the endogenous FGF-BP gene in FGF-BP-positive breast cancer cell lines. Task during Months 1 – 12.

Goal (3): To determine if the differential expression of FGF-BP in breast cancer cell lines is controlled at the transcriptional levels by examining the regulation of the FGF-BP gene promoter in cell lines. Task during Months 12 – 36.

Goal (4): To examine the direct impact of FGF-BP overexpression in transgenic animals. Task during Months 12 – 36.

BODY

TASK 1:
To assess the significance of FGF-BP expression for the clinical course of breast cancer using archival samples with known outcome and defined pathological features.

We had found expression of FGF-BP in a small series of breast cancer samples from our Cancer Center's tissue bank and from this proposed to study a larger set including non-malignant and premalignant lesions and compare this result to known pathological, molecular and clinical parameters.

TASK 1; Work accomplished during the first award cycle (Months 1-12):

Enhancing the method of detection of FGF-BP in the tumor cell compartment.

FGF-BP is a secreted protein that is released to the extracellular compartment (see Figure 1). Thus, detection of the protein in a given tissue does not reveal the cells producing the protein. This problem can be solved by detecting FGF-BP mRNA by in situ hybridization using tissue sections. We had already established in situ hybridization for FGF-BP mRNA in some tissues (frozen specimen, SCC, squamous cell carcinoma mostly). We first attempted to apply the method of detection to human breast cancer samples from the tissue archive. These are paraffin-embedded samples. Figure 1a shows an example of non-cancerous breast tissue and we found that this tissue rarely stains for FGF-BP mRNA and protein. Invasive carcinoma were found to stain positively for FGF-BP mRNA and protein in approximately 1/2 of the cases. Figure 1b shows an FGF-BP mRNA negative case and Figure 1c shows an FGF-BP mRNA positive case. The staining for mRNA is found in the cytosol of the positive cells - as expected - and the nuclei do not show a hybridization signal ("empty nuclei"). This is an important control to demonstrate a lack of non-specific cross-hybridization with DNA.

Details of the methods and of the approach are provided in the **appendix material**. It is planned to post the general method of in situ hybridization on the internet at the NIH/ Cooperative Breast Cancer Tissue Resource (CBCTR) website for use by other investigators that wish to utilize tissue microarrays for the detection of the expression of genes of interest.

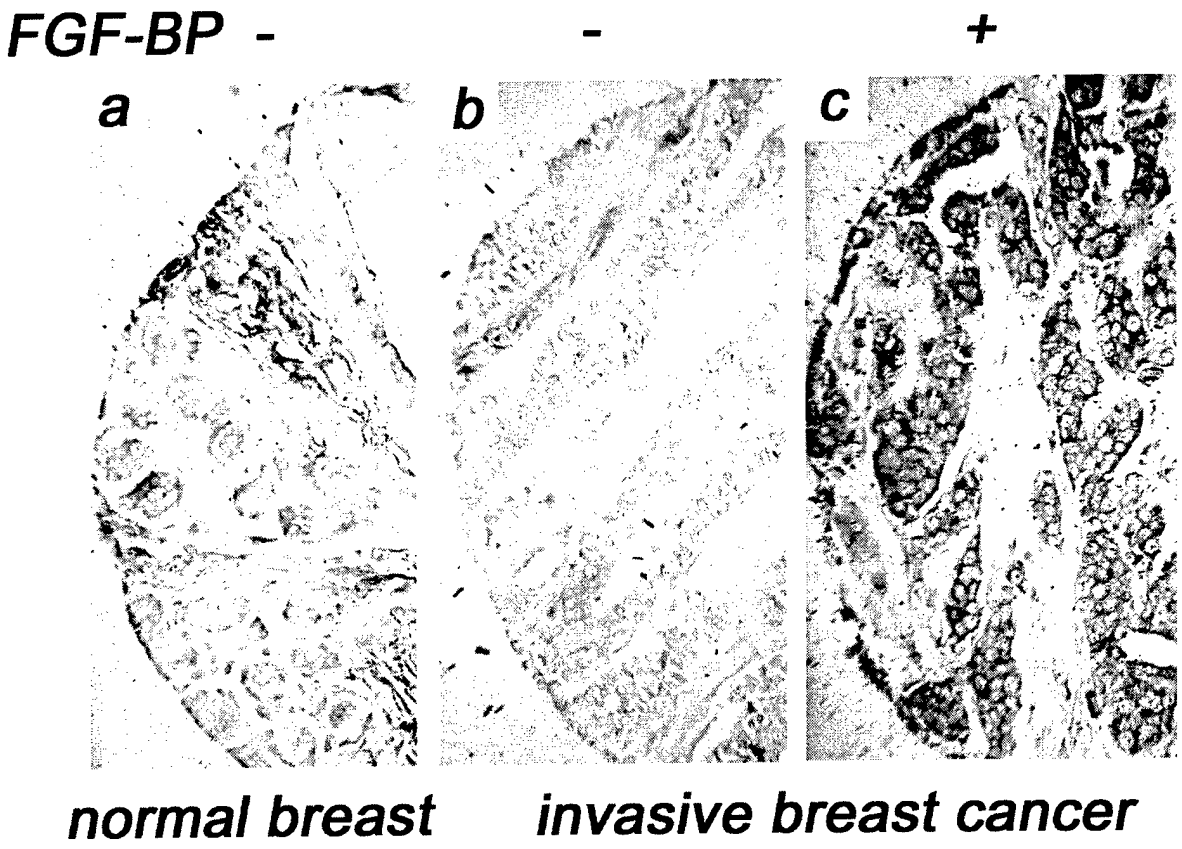

Figure 1. Expression of FGF-BP in human breast tissues.
In situ hybridization for FGF-BP mRNA using a tissue microarray (TMA) with paraffin-embedded normal breast (a) and invasive breast cancer (b,c) tissues. Normal breast and one of the breast cancer samples (b) were scored as negative for FGF-BP whereas the second breast cancer sample shown (c) was scored as positive.

Note: The FGF-BP mRNA expression is confined to the epithelial tissues. The nuclei of the positive cells do not stain for the mRNA.
(These samples were from a TMA obtained through the NIH Cooperative Breast Cancer Tissue Resource CBCTR. The samples shown were present on the same slide and were thus all hybridized at the same time.)

Conclusion:
In situ hybridization for FGF-BP is a selective method to detect the mRNA in paraffin-embedded, archival samples. In addition to the above breast tissues, other tissues were also stained with the same approach and showed a selective expression of FGF-BP e.g. in colon cancer versus normal colon archival tissues.

TASK 1; Work accomplished during the third award cycle:

An expansion of the number of samples as well as staining for other markers and analysis of available data was carried out. The overview and statistical analysis of results obtained from the stainings of a series of samples is given in the Tables 1, 2 below.

Table 1: Expression analysis for FGF-BP in human breast tissues.

FGF-BP	Negative	positive
Normal Breast	n = 24	4
In situ carcinoma	n = 26	8
Invasive cancer	n = 76	67

Statistical analysis of the data from Table 1 showed

1. a significant difference in the frequency of expression of FGF-BP amongst all groups ($p = 0.0008$; chi-square, Fisher's exact test);
2. a significant trend of increased frequency of expression from normal vs. in situ to invasive cancer ($p = 0.0002$ for trend; chi-square test).
3. a significant difference between normal and invasive cancer ($p = 0.0014$; chi-square, Fisher's exact test)
4. a significant difference between in situ carcinoma and invasive cancer ($p = 0.014$).
5. no significant difference between normal, non-malignant breast tissues and tissues with in situ carcinoma ($p = 0.36$; chi-square test).

The results from the expression studies of FGF-BP in breast cancer were correlated with available pathologic, clinical and molecular parameters.

1. Clinical and pathologic parameters were provided by CBCTR of NIH, who had the different samples characterized by expert pathologists from the NSABP (Dr. Soon Paik) and Baylor College of Medicine (Dr. Craig Allred).
2. Standard molecular parameters (ER, PR, HER-2) were generated by CBCTR and are provided by CBCTR.
3. Novel parameters that my laboratory studies, i.e. expression of the growth factor pleiotrophin (PTN) and its receptor anaplastic lymphoma kinase (ALK) were generated at the same time as the stainings for FGF-BP and are used as positive controls.

Table 2: Correlation of FGF-BP expression in invasive breast cancers with pathologic, clinical and molecular parameters.

Parameter	N	Spearman r (correlation)	p-value (two-tailed)	Significant (P<0.05)
T	113	-0.155	0.102	NS
N	96	-0.009	0.930	NS
M	119	-0.102	0.271	NS
# of LNodes	96	-0.019	0.854	NS
Stage	119	-0.083	0.372	NS
Grade	113	-0.116	0.222	NS
ER	116	0.205	0.027	Sig
PR	115	0.148	0.113	NS
HER-2	122	-0.126	0.167	NS
PTN*	126	0.610	<0.0001	Sig
ALK*	119	0.528	<0.0001	Sig
Overall Survival	119	0.085	0.357	NS

T, N, M is tumor size, nodal status (+/-) and existing distant metastasis; # of tumor positive lymph nodes, ER, PR (estrogen and progesterone receptor status) HER-2 overexpression of HER-2 growth factor receptor (immunohistochemistry).

Statistical analysis of the data was carried out using the Prism/Graphpad program. NS = not significant; sig = significant.

Methods:

Tissue samples.
Paraffin-embedded tissue samples were used for in situ hybridization as shown in Figure 1 and analyzed as described in the appendix materials. One set of tissue samples (n = 53) was from the Lombardi Cancer Center Tumor Repository. A second, independent set of samples (n = 152) was on tissue microarrays obtained through the NCI Cooperative Breast Cancer Tissue Resource (CBCTR). This tissue array contains samples from invasive breast cancer, in situ carcinoma as well as control breast tissues from reduction mammoplasty without malignancy (CBCTR Protocol # L-0060T to the P.I. of this grant, A.W.).

In situ Hybridization
The expression of FGF-BP mRNA in human breast tissue samples was assessed by in situ hybridization. The FGF-BP riboprobe consisted of a 668 bp internal sequence of FGF-BP cDNA [11], sub-cloned into the pRc/CMV vector (5.5 kb, Invitrogen). Digoxigenin-labeled antisense and sense riboprobes were made using the DIG RNA labeling kit (Roche) according to protocol. Tissue sections were cut (4 micrometers) and mounted on (+)-charged glass slides (Fisher Scientific; Pittsburgh, PA) using standard histology technique. In addition, tissue microarrays (TMAs) from the NCI Cooperative Breast Cancer Tissue Resource (CBCTR) were used. This TMA contained samples from invasive cancer as well as in situ carcinoma and control breast tissues from reduction mammoplasty.

Additional details and an overview of the method for *in situ* hybridization is described in the **appendix materials**.

TASK 1; INTERPRETATION OF THE DATA.

FGF-BP expression is detectable in close to 1/2 of breast cancer samples studied. The expression increases significantly from normal, non-malignant tissues and non-invasive in situ carcinoma to invasive cancers. However, there is no significant correlation of expression of FGF-BP in invasive cancers with overall survival of patients, tumor size or other clinico-pathological parameters (T, N, M, stage, grade). Only tumor size might have a potential negative correlation with FGF-BP expression ($r = -0.155$; $p = 0.102$), although the p-value is not significant (<0.05), but this could suggest that with increasing tumor size FGF-BP gets down-regulated.

With respect to standard molecular parameters used in routine analysis of breast cancers, a significant correlation between FGF-BP expression and ER was found although the correlation coefficient of 0.205 does not suggest a very strong correlation. This would suggest a reason why overall survival was not adversely correlated with FGF-BP since many of the ER-positive tumors have a good overall survival.

No significant correlation of FGF-BP expression with PR or HER-2 were found, although the correlation coefficient of 0.15 suggest a positive correlation for PR, but was not below the 0.05 level set for significance ($p = 0.11$). A positive correlation would be independently supportive of the notion of a positive correlation between active ER and FGF-BP expression.

Finally, a very strong correlation was apparent with respect to PTN and ALK expression with correlation coefficients above 0.50 and p-values of <0.0001. This does suggest that the malignant transformation process affects FGF-BP and these latter parameters in parallel.

TASK 2:
To study regulators of the endogenous FGF-BP gene in breast cancer cell lines.

Work accomplished during the first award cycle (Months 1 – 12):

MDA-MB468 human breast cancer cells as a model to study regulation of FGF-BP.

To find a tissue culture model that recapitulated the high FGF-BP expression that we observed in our preliminary studies with invasive breast cancer samples, we screened a number of cell lines for FGF-BP mRNA expression. We assayed FGF-BP mRNA expression, rather than protein expression, because FGF-BP is a secreted protein [12], and therefore is difficult to measure using whole cell extracts. We reported previously that most breast cancer cell lines (including MCF-7 cells) are negative for FGF-BP expression by Northern analysis [12], and we now found that MDA-MB-468 cells have high FGF-BP expression (Figure 1). Interestingly, MDA-MB-468 is a breast cancer cell line that can be invasive and metastatic *in vivo* when injected into mice along with angiogenesis-stimulating Matrigel [13]. In addition, MDA-MB-468 cells have been characterized as showing high expression of the EGF receptor [14] and are EGF responsive for invasion [15]. Overexpression of the EGF receptor is a poor prognostic indicator in breast cancer [16] presumably through EGF stimulation of a more invasive phenotype although the precise target genes are not yet defined.

FGF-BP expression MCF-7 cells was not detectable even when cells grown in full serum that contains estradiol and growth factors. However, one of the drug-resistant MCF-7 derivative cell lines, MCF-7/Adr, expresses detectable levels of FGF-BP by Northern blot (Fig. 1). This cell line has lost estrogen responsiveness and has a changed genotype relative to the original estrogen-responsive MCF-7 cell line.

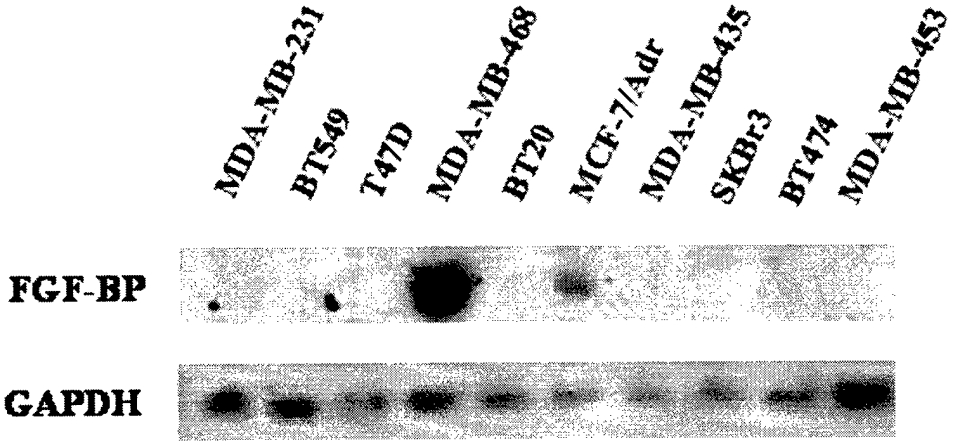

Figure 1. Northern blot analysis.
FGF-BP mRNA and a control (GAPDH mRNA) in human breast cancer cell lines is shown. Details at the end of this section under "Methods".

EGF effect on FGF-BP expression in MDA-MB-468 human breast cancer cells.
Treatment of MDA-MB-468 cells with 10 ng/ml EGF resulted in a rapid increase in the steady-state levels of FGF-BP mRNA (Figure 2A). Induction of FGF-BP mRNA was observed after 1 hour of treatment and was maximal after 6 hours with an average increase of 2.5- to 3-fold (Figure 2B).

To discern between the possible signaling pathways involved in EGF induction of FGF-BP in MDA-MB-468 cells, we tested pharmacological inhibitors of signal transduction molecules at various concentrations for their effect on FGF-BP regulation. Treatment with the EGFR tyrosine kinase inhibitor PD153035 resulted in a significant concentration dependent inhibition of EGF induction of FGF-BP mRNA (Figure 2C). In addition to EGFR tyrosine kinase activity, protein kinase C is also involved in the EGF effect since the bisindoylmaleimide PKC inhibitors Ro 31-8220 [17], at concentrations of 1 mM and 10 mM, and calphostin C [18] were both able to significantly inhibit the EGF induction of FGF-BP (Figure 2C).

To determine the role of the further downstream signaling pathways on EGF induction of FGF-BP, we utilized MAPK kinase (MEK1/2) and p38 MAP kinase inhibitors [19,20]. The MEK1/2 specific inhibitor U0126 was only effective at higher concentrations of 10 μM and 20 μM, and not at the concentration of 1 mM (Figure 2C); 1μM of U0126 is usually used to specifically inhibit MEK-induced signaling [21]. In contrast, treatment with increasing concentrations of the p38 MAPK inhibitor SB202190 resulted in a concentration-dependent inhibition of EGF-induced FGF-BP mRNA (Figure 2C).

Figure 2 is on the next page !

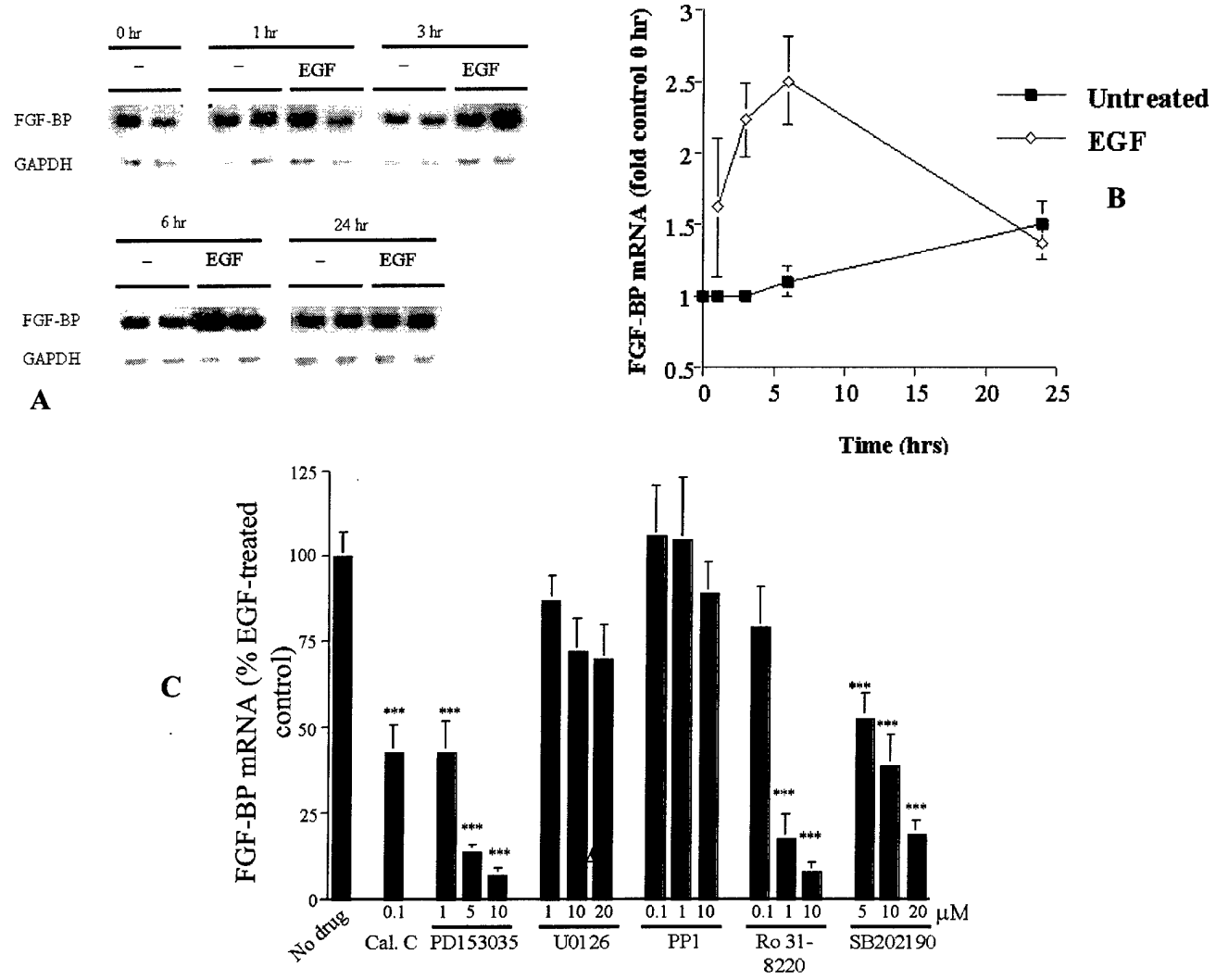

Figure 2. **Induction of FGF-BP mRNA by EGF in MDA-MB-468 cells.** *A*, A representative Northern blot analysis showing FGF-BP mRNA and a control (GAPDH mRNA) done in duplicate. MDA-MB-468 cells were treated with or without 10 ng/ml EGF for the indicated times. *B,C,* Results from quantation of Northern blots. Signal intensities were quantified by PhosphorImager and normalized to the control mRNA, GAPDH. *B, Closed squares*, represent control (untreated) levels, and open squares represent EGF treatment mRNA levels expressed as fold over control-0 hrs. Values represent the mean and S.D. of at least two separate experiments. *C,* FGF-BP mRNA levels from MDA-MB-468 cells treated with 10 ng/ml EGF for 6 hours. Cells were pretreated for 1 hour with vehicle alone or at the indicated concentrations of: Calphostin C (PKC inhibitor), PD153035 (EGFR tyrosine kinase inhibitor), U0126 (MEK1/2 inhibitor), PP1 (c-Src inhibitor), Ro 31-8220 (PKC inhibitor), SB202190 (p38 MAPK inhibitor). Values are expressed relative to mRNA levels after EGF treatment alone (without inhibitor), which was set to 100%. Basal FGF-BP level (without EGF or inhibitor) was approximately 30%. Values represent mean and S.E. from of at least three separate experiments. Statistically significant differences relative control conditions (EGF only) (***, $p<0.0001$, t-test or ANOVA; Prism/Graphpad Program).

TASK 2; Methods:

Cell Culture and Reagents
The MDA-MB-468 human breast cancer cell line, and the ME-180 human cervical squamous cell carcinoma cell line were obtained from American Type Culture Collection (ATCC; Manassas, VA). Cells were cultured in improved minimum essential medium (IMEM) with 10% fetal bovine serum (Invitrogen Inc.; Carlsbad, CA). Human recombinant EGF was purchased from Collaborative Biochemical Products (Bedford, MA). Tyrphostin AG1517 (PD153035), Ro 31-8220 (bisindoylmaleimide IX) and PP1 were purchased from Alexis Corp. SB202190 was purchased from Calbiochem (San Diego, CA). U0126 was purchased from Promega. Calphostin C was purchased Sigma-RBI (Natick, MA). Wortmannin was purchased from Biomol (Plymouth Meeting, PA). All compounds were dissolved in Me_2SO.

Northern Analysis-
MDA-MB-468 cells were grown to 80% confluence in 10-cm dishes, warmwashed twice in serum-free IMEM, and incubated for 16 hours in serum-free IMEM prior to treatment. Cells were pretreated for 1 hour with the indicated drug or with vehicle alone (Me_2SO; final concentration of 0.1%). EGF or anisomycin treatment was for 6 hours unless otherwise indicated. Total RNA was isolated with RNA STAT-60™ (Tel-Test Inc.; Friendswood, TX), and Northern analysis was carried out as described previously [22] using 20 mg of total RNA. Hybridization probes were prepared by random-primed DNA labeling (Amersham Biosciences; Piscataway, NJ) of purified insert fragments from human FGF-BP [12], and human GAPDH (Clontech; Palo Alto, CA). Quantification of mRNA levels was performed using a PhosphorImager (Amersham Biosciences).

TASK 2; INTERPRETATION OF THE DATA

These data suggest that p38 MAPK plays a dominant role in the induction of FGF-BP by EGF in MDA-MB-468 cells. Other intracellular targets for EGF receptor-induced intracellular signaling also potentially include members of the c-Src protein tyrosine kinase family. However, the c-Src family specific inhibitor PP1 [23] resulted only in a maximal 10% reduction in EGF-induced FGF-BP mRNA levels, only at the highest concentration used (10 μM (Figure 2C)). These data indicate only a minimal role for Src in EGF control of FGF-BP expression. The PI 3-kinase pathway also is not involved since treatment of MDA-MB-468 cells with 1 μM wortmannin did not have any significant effect on EGF induction of FGF-BP (data not shown). Overall, our pharmacological inhibitor data indicate major role for PKC, and more significantly, p38 MAPK in EGF effects on FGF-BP in breast cancer cells.

TASK 3:
To determine if the differential expression of FGF-BP in breast cancer cell lines is controlled at the transcriptional levels by examining the regulation of the FGF-BP gene promoter.

Work accomplished during the second award cycle (Months 12 – 24):

A series of FGF-BP promoter/ luciferase reporter constructs were tested for their basal activity and their EGF induction in MDA-MB 468 cells. Figure 1 shows the full length promoter as well as different deletion constructs to dissect out, which portions of the promoter are the most significant for basal and EGF induction.

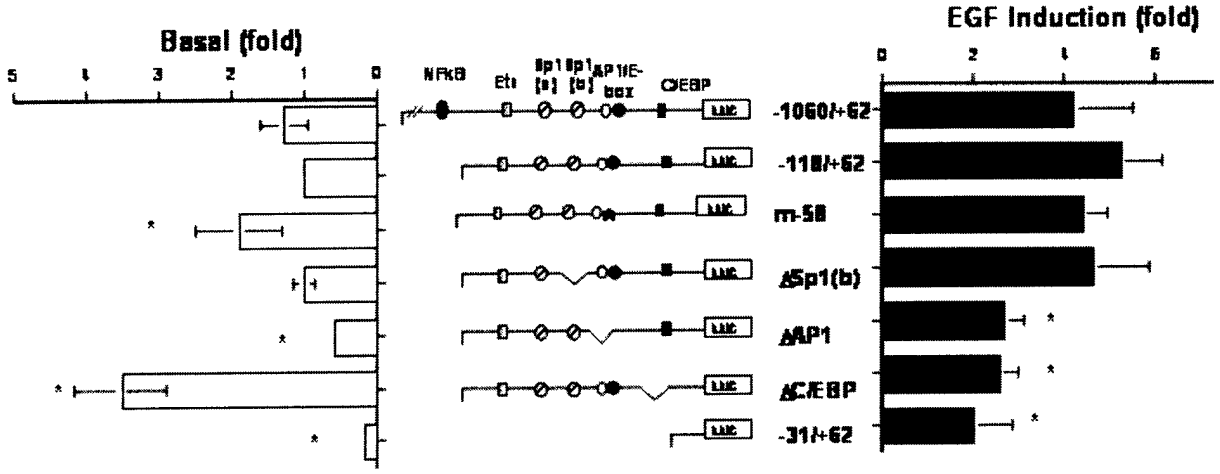

Figure 1. **FGF-BP promoter elements involved in EGF induction of FGF-BP in MDA-MB-468 cells.**
The *histogram* on the *left* shows the impact of each promoter deletion on the basal (uninduced) luciferase activity of each construct. The basal activity of the -118/+62 construct was set to 1. The *right* histogram shows the transcriptional activity in the presence of EGF and is expressed as -fold induction of EGF-treated over untreated for each construct. MDA-MB-468 cells were transiently transfected by electroporation with the indicated FGF-BP promoter luciferase constructs, and a CMV driven *Renilla* luciferase reporter vector for transfection efficiency, and were untreated or treated with 10 ng/ml of EGF for 18 h. Promoter constructs are described under "Methods" and in Ref. [22]. Values represent the mean and S.E. from at least three separate experiments, each done in triplicate wells. Statistically significant differences relative to the –118/+62 promoter construct are indicated (*, $p<0.05$, t test).

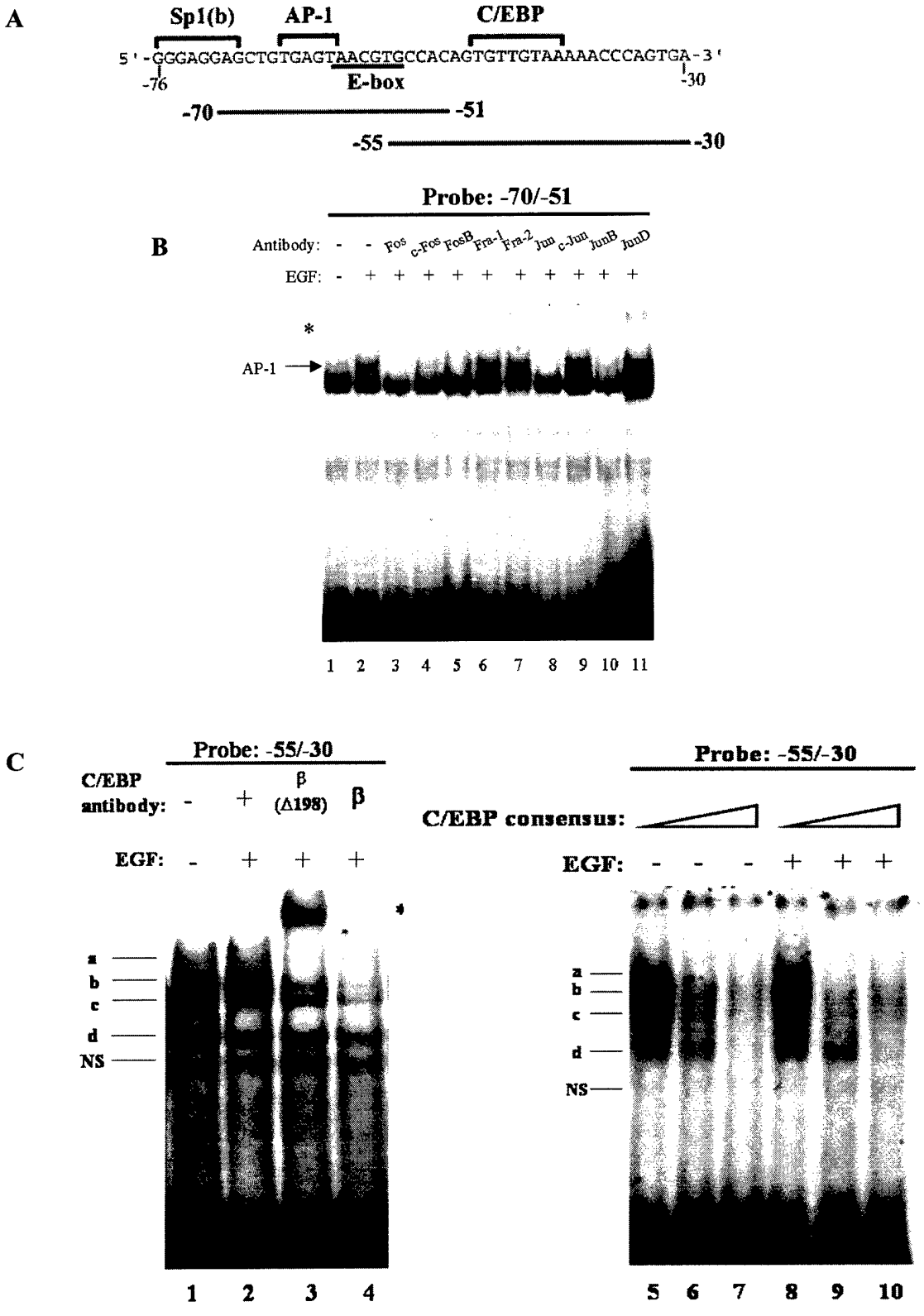

Figure 2. **Transcription factor binding to FGF-BP promoter ... (FULL TEXT OF THE LEGEND ON THE NEXT PAGE).**

Figure 2 (!graph on previous page !). **Transcription factor binding to FGF-BP promoter elements in MDA-MB-468 cells.** *A,* Double-stranded oligonucleotide sequences of promoter elements used for gel shift analysis. *B,* Supershift analysis of transcription factor binding to the AP-1, and *C,* C/EBP sites of the FGF-BP promoter. Labeled FGF-BP promoter sequences as indicated were incubated with nuclear extracts from untreated or EGF-treated MDA-MB-468 cells. Binding reactions were performed in the presence of "supershifting" antibodies as indicated. An arrow or bar to the left of each panel indicates specific binding of AP-1 and C/EBP. Asterisks indicate supershifted complexes.

Work accomplished during the third award cycle (Months 24 - 36):

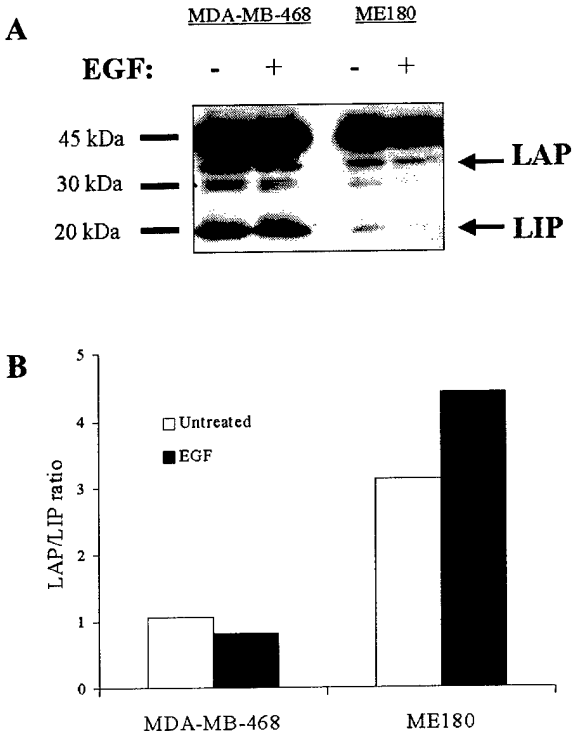

Figure 3. **Expression levels of endogenous C/EBPbeta in MDA-MB-468 breast cancer as compared to ME-180 squamous cell carcinoma cells.** *A*, A representative Western blot analysis of C/EBPb protein levels using 40 μg of nuclear extracts from untreated and EGF treated MDA-MB-468 and ME-180 cells. C/EBPb was specifically recognized using a polyclonal antibody specific for the C-terminus of the protein (C/EBPb (C-19)). The positions of LAP (35 kDa) and LIP (20 kDa) isoforms are indicated by *arrows*. *B,* Ratios of LAP to LIP in MDA-MB-468 and ME-180 cells. Levels of LAP and LIP were quantified from multiple exposures of Western blot analyses using densitometry, and corrected for levels of the 46 kDa nonspecific band. Values are expressed as actual ratios of LAP to LIP for each cell line.

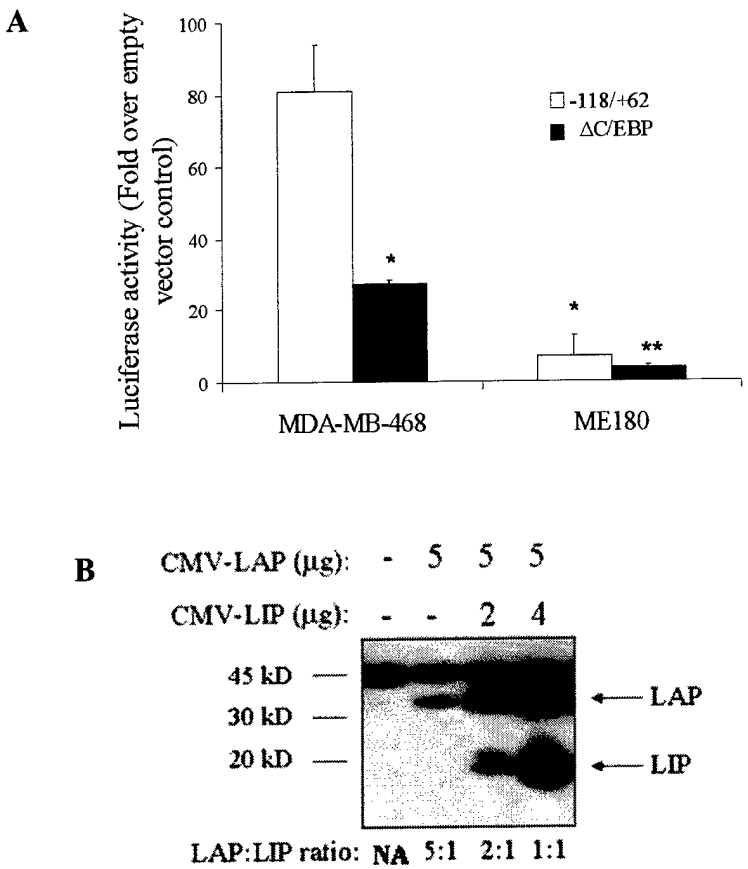

Figure 4. **Effects of LAP and LIP overexpression on the FGF-BP promoter activity (TEXT OF LEGEND ON THE NEXT PAGE).**

Figure 4 (graphs on previous page). **Effects of LAP and LIP overexpression on the FGF-BP promoter activity.** *A,* MDA-MB-468 cells and ME-180 were cotransfected with the indicated FGF-BP promoter constructs and 5 μg CMV-LAP. Relative luciferase activity of the cells transfected with ΔC/EBP (black bars) or -118/+62 (open bars) constructs are expressed as fold over control (empty vector transfected cell lines). *B,* Shown is a representative Western blot of C/EBPb protein levels in MDA-MB-468 cells transiently transfected with CMV-LIP and CMV-LAP. The levels of LAP and LIP were quantified from multiple exposures of Western blot analyses using densitometry, and corrected for levels of the 46 kDa band. Values are expressed as relative ratios of LAP to LIP for each transfection conditon. *C,* MDA-MB-468 cells were cotransfected with the -118/+62 or DC/EBP (*C, inset*) FGF-BP promoter constructs, 5 μg CMV-LAP, and the indicated amounts of CMV-LIP or empty vector (pcDNA3). MDA-MB-468 cells were treated were kept in serum free IMEM for 16 h. Values are expressed as the mean and S.E. of at least three experiments, each done in triplicate wells. Statistically significant differences relative to -118/+62 (*) or MDA-MB-468/DC/EBP (**) are indicated ($p<0.05$, t test).

Work accomplished during the last award cycle:

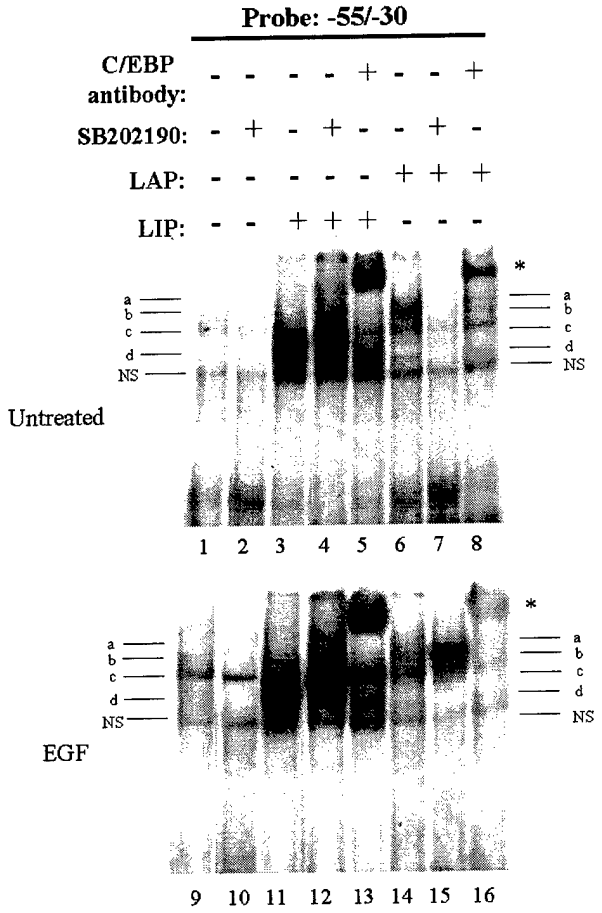

Figure 5. **Binding of C/EBPb-LAP and -LIP to the C/EBP site on the FGF-BP promoter.** ^{32}P labeled -55/-30 FGF-BP promoter sequence was incubated in the presence of nuclear extracts of MDA-MB-468 cells transfected with: empty vector, CMV-LAP, or CMV-LIP constructs. MDA-MB-468 cells were pretreated with vehicle alone (Me_2SO) or 10 μM SB202190 for 1 h and then treated with or without 10 ng/ml EGF for 1 h. Binding reactions were incubated with a C/EBP supershift antibody where indicated. Specific binding is indicated by bars (labeled a-d) to either side of each panel, non-specific binding is indicated (labeled NS), and supershifted complexes are indicated by an asterisk.

TASK 3; Methods:

Plasmids- Human FGF-BP promoter fragments were cloned into the pXP1 promoterless luciferase reporter vector and have been described previously [22]. The MEK2 (K101A) dominant negative construct was provided by Dr. J. Holt (Vanderbilt University). The expression plasmids containing wild-type p38 (pCDNA3-Flag-p38), and constitutively active MKK6 (pCDNA3-Flag-MKK6(Glu)) were provided by Dr. R. Davis (University of Massachusetts). The expression vectors for human CEBPb-LAP and C/EBPb-LIP (CMV-LAP and CMV-LIP, respectively) were gifts from Dr. U. Schibler (University of Geneva) courtesy of Dr. J. Schwartz (University of Michigan). Wildtype C/EBPb mRNA contains three inframe AUG translation start sites, from which LAP and LIP are translated from the second and third sites, respectively [24]. The second in frame AUG is flanked by an imperfect Kozak's sequence, GACCATGG [25], compared to the Kozak's consensus sequence of CCA/GCCAUGG [26,27], whereas the third inframe AUG is flanked by a perfect Kozak's sequence [24], resulting in translation of both LAP and LIP. The CMV-LAP construct contains only the second and third translation start sites, but both are flanked by perfectly matched Kozak's sequences resulting in the more efficient translation of LAP alone [24]. The effects of dominant negatives or activated constructs were compared to their empty vector control or with the empty vector pCDNA3 (Invitrogen).

Transient Transfections and Reporter Gene Assays- Twenty-four hours before transfection MDA-MB-468 cells were plated at a density of $3x10^6$ cells in 10-cm dishes. pRL-CMV *Renilla* luciferase reporter vector (Promega; Madison, WI) was included as a control for transfection efficiency. MDA-MB-468 cells were transfected by electroporation as described by Raja *et al.* [28]. Briefly, cells were trypsinized and washed twice by centrifugation in IMEM containing 10% FBS. The cells from each plate were then resuspended in 400 μl IMEM containing 20% FBS. A total of 30 μg plasmid DNA (29 μg of FGF-BP promoter construct, 3.0 ng of pRL-CMV) was added to the cell suspension 5 minutes before electroporation. For co-transfection, 24 μg of -118/+62Luc FGF-BP promoter construct, 5 μg or indicated amounts of expression vector, and 3.0 ng of pRL-CMV were added to cells. Electroporation of the entire cell sample was carried out in a cuvette with an electrode gap of 0.4 cm at 350 V and 500 mF, using a BioRad GenePulser II (Bio-Rad; Hercules, CA). The electroporated cells were then distributed equally to a 6-well plate, each well having been pre-filled with 3 ml of IMEM with 10% FBS. Cells were allowed to recover and attach for 16 hours before treatment. Transfected cells were washed twice with serum-free IMEM, treated with or without EGF (10 ng/ml) in serum-free IMEM for 16 hours, and then lysed in 150 μl of passive lysis buffer (Promega). 20 μl of extract was assayed for both firefly and *Renilla* luciferase activity using the Dual-Luciferase™ reporter assay system (Promega). To correct for transfection efficiency, and a small background induction (1.5-2.0 fold) of the pRL-CMV plasmid by EGF [29], *Renilla* luciferase values were corrected for protein content, and these numbers were then used to normalize firefly luciferase values. Protein content of cell extracts was determined by Bradford assay (Bio-Rad).

Gel Shift Assays- MDA-MB-468 cells were grown to 80% confluence on 150-mm dishes, serum starved for 16 hours, and treated with or without 10 ng/ml EGF for 1 hour. As a control, ME-180 SCC cells were treated with 5 ng/ml EGF for 1 hour. For gel shift assays using transiently transfected cells, MDA-MB-468 cells were plated at a density of $6x10^6$ cells in 150-mm dishes, and transfected with 10 mg of expression vector or empty vector by electroporation as described above. Cells were then either untreated or treated with 10ng/ml EGF for 1 hour. To study the effects of inhibition of p38 MAPK, cells were pretreated for 1 hour with 10 μM SB202190, then treated with or without 10 ng/ml EGF for 1 hour. Nuclear extracts were prepared as described previously [22]. Binding reactions with the -70/-51 and -55/-30 probe was carried out as described previously [22] with 6 μg of MDA-MB-468 nuclear extracts, binding buffer (20 mM Tris, pH 7.5, 60 mM KCl, 5% glycerol, 0.5 mM dithiothreitol, 2.0 mM EDTA), and 500 ng of poly(dI-dC).

Supershift antibodies (2 μg) were added to the binding reaction for 10 minutes on ice before adding 20 fmol of labeled probe. Reactions were carried out for 20 minutes at room temperature and analyzed by 6% polyacrylamide gel electrophoresis. Fos-specific antibodies c-Fos (K-25), c-Fos (4), Fos B (102), Fra-1 (R-20), and Fra-2 (Q-20); Jun-specific antibodies c-Jun/AP-1 (D), c-Jun/AP-1 (N), JunB (N-17), and JunD (329); and C/EBP specific antibodies C/EBPb (C-19), and C/EBPb (D198) were purchased from Santa Cruz Biotechnology (Santa Cruz, CA).

Western Analysis- 40 μg of crude nuclear extracts from untreated or EGF-treated MDA-MB-468 and ME-180 cells, or 20 μg of lysates from MDA-MB-468 transiently transfected cells were electrophoresed on Novex® precast 4-20% tris-glycine polyacrylamide gels (Invitrogen) at 150 V for 80 minutes. The protein was then transferred to polyvinylidene difluoride membranes (Millipore) for 2 hours at 200 mA. Blots were blocked for 1 hour in PBST (1x phosphate buffered saline, 0.5% Tween 20) containing 4% bovine serum albumin (Sigma; St. Louis, MO), and then incubated for 1 hour in 1x PBST/ 0.4% bovine serum albumin, containing antibodies (1 μg/ml) for C/EBPb (C-19) (Santa Cruz). Blots were washed with PBST (without bovine serum albumin) four times for 5 minutes each, with agitation. Blots were then incubated for 1 hour in antibody solution containing a 1:5000 dilution of horseradish peroxidase labeled donkey anti-rabbit immunoglobulin (Amersham) and washed as before. Lastly, blots were assayed for enhanced chemiluminescence using SuperSignal® West Pico Chemiluminescent Substrate (Pierce) and enhanced chemiluminescence film (Hyperfilm ECL; Amersham). Signal intensities of the 46, 36 (C/EBPb-LAP), and 20 kilodalton (C/EBPb-LIP) bands were measured by densitometry using multiple exposures to Hyperfilm ECL to assess the linear range. Expression of LAP and LIP were corrected for loading differences by comparing to the band intensity of the 46 kDa band, as described by Zahnow *et al.* [30].

Statistics – The GraphPad/Prism software package was used for graphics and data evaluation. ANOVA was applied for continuous variables and chi-square (Fisher's exact test) for discontinuous variables. p. values < 0.05 were considered significant.

TASK 3; INTERPRETATION OF THE DATA

Mutational analysis revealed that the AP-1 and C/EBP sites on the FGF-BP gene promoter were required for the EGF effect, whereas deletion of the C/EBP site resulted in a significant increase in promoter basal activity indicating a basal repressive control mechanism (Figure 1). This was corroborated by gel shift analysis showing binding of transcription factors to the C/EBP site (Figure 2). In composite these data suggest that the C/EBP site is a central regulatory element for the regulation of FGF-BP promoter activity in MDA-MB-468 cells.

We found that MDA-MB-468 cells express high endogenous levels of both the activating (LAP) and repressive (LIP) isoforms of C/EBPb (=C/EBPbeta) (Figure 3). Overexpression of C/EBPb-LAP in MDA-MB-468 cells resulted in a large 80-fold increase in FGF-BP promoter basal activity which was reversed by coexpression of LIP (Figure 4).

Gel shift analysis revealed that four LIP and LAP containing complexes (a-d) bind to the C/EBP site (Figure 5). DNA binding of the LIP and LAP-containing c complex and the b complex in the presence of EGF, was modulated by inhibition of p38 MAPK suggesting a role for these complexes in the EGF induction of the FGF-BP promoter.

This study suggests that, C/EBPbeta plays a role in the pathology of breast cancer, in particular in the control of FGF-BP that can drive angiogenesis and an invasive phenotype.

TASK 4:
To examine the direct impact of FGF-BP overexpression in the mammary epithelium using transgenic animals. Founder mice will be examined for aberrant mammary development as well as increased development of mammary tumors. The mice will also be used as a basis for longterm studies of bitransgenic animals to determine other genes which may co-operate with FGF-BP in breast cancer development.

We hypothesize that expression of FGF-BP as a transgene in a time- and tissue-dependent manner will shed light on its function in the intact organism, in particular the mamary gland. It was planned to generate transgenic animals and then study the impact on the mammary gland phenotype.

Work accomplished during the second award cycle (Months 12 – 24):

CMV-FGF-BP as a transgene:
We found in initial studies that human FGF-BP (hFGF-BP) transgene expression in mice using the CMV promoter/enhancer leads to embryonic lethality. No viable, transgenic offspring were obtained in a large series of embryo transfers (>20). The time of loss of embryos was around e12 to e15 and the cause of the loss of embryos was due to bleeding into the embryonic sac.

K14-FGF-BP as a transgene:
Based on the above data with CMV-FGF-BP we decided to utilize a more restricted promoter for expression of the transgene, i.e. K14. In 5 independent embryo transfer experiments with 2 to 3 foster mothers in each of the experiments and more than 20 embryos per foster mother, we only obtained a total of 10 live offspring. None of these were transgenic for hFGF-BP as assessed by genomic Southern blotting and PCR. However, the K14-hFGF-BP injected embryos did implant as evidenced by histologic sectioning of uteri from foster mothers that had failed to generate viable offsprings. Monitoring of the pregnant mice showed that the pregnancies were lost prior to day 15.

MMTV-hFGF-BP as a transgene:
In a separate experimental series we used the MMTV-LTR (abbreviated with"MMTV") to drive hFGF-BP expression as a transgene since its timing and tissue-specificity of expression is distinct from the K14-hFGF-BP. The MMTV-LTR promoter/enhancer construct was provided by our transgenic facility who obtained it from Dr. Phil Leder's laboratory. Studies by other laboratories have shown that the activates expression of a transgene in mostly epithelial tissues and as early as the four-cell-stage of embryogenesis. In two separate experiments with the MMTV-hFGF-BP transgene construct with a total of seven foster mothers and more than 20 embryos per foster mother, only 5 viable offspring were obtained. None of these were transgenic for hFGF-BP. From our preliminary assessment of these experiments the loss of the pregnancies also occurred before day e15. Whether implantation occurred was not checked in these two experiments.

Expression profile of the endogenous murine FGF-BP:
We found that mFGF-BP mRNA is barely above background on embryonic day e9, can be detected by day e12 and reaches its peak expression prenatally (day e16/17). The relative expression levels at these three time points are 1 / 4 / 20 for days e9 / e12 / e17 respectively. Most of the expression at day 12 was found in the basal layer of the skin and in the gut as assessed by in situ hybridization.

Conclusion: Obviously expression of hFGF-BP under the control of CMV, K14 or MMTV is embryonically lethal. Endogenous murine FGF-BP expression is initiated after day e8 and peaks prenatally. Gut, lung and skin are the major tissues of expression.

Alternative approaches taken due to embryonic lethality of FGF-BP:

1. **Conditional (Tetracycline regulated) FGF-BP transgene expression in mice**
2. **Transient expression model in chicken embryos**

Work accomplished during the third award cycle (Months 24 - 36):

1. **Conditional (Tetracycline regulated) FGF-BP transgene expression in mice**

To bypass embryonic lethality of FGF-BP expression in mice and study the effect of BP transgene expression in mature mice, we initiated the generation of mice with tetracycline-regulatable BP expression. As a first set of animals we generated mice containing FGF-BP under the control of a tetracyline response element (tetRE-FGF-BP). These mice still showed high lethality due to some leakage of the transgene tetRE promoter. But we were able to generate two distinct stable transgenic lines.

It is planned that these tetRE-FGF-BP mice will then be crossed with a second set of animals that express the tetracycline-regulatable transactivator (tTA). Depending on the promoter used to express the tTA (K14, MMTV or CMV), FGF-BP will then be regulatable in different tissues in the resulting bitransgenic animals by administration of doxycycline (a tetracycline derivative) and the resulting phenotypic effects studied.

Work accomplished during the most recent award cycle:

Most recently tetRE-FGF-BP mice were crossed with a second set of animals that express the tetracycline-regulatable transactivator under CMV control (CMV-tTA). These mice are available commercially. In these crosses FGF-BP should be regulatable in different tissues in the resulting bitransgenic animals by administration of doxycycline (a tetracycline derivative).

The bitransgenic lines were bred with CMV-tTA mice from Jackson Lab for inducibility studies. Initial studies show that FGF-BP is inducible in the skin (ear punches) of these mice as evidenced by the measurement of the transgene levels at the mRNA as well as protein level. Figure 1 shows the inducibility of the transgene expression in a skin biopsy due to doxycycline. Figure 2 shows the inducibility of the resulting protein using immunohistochemistry of a skin biopsy (dark stain).

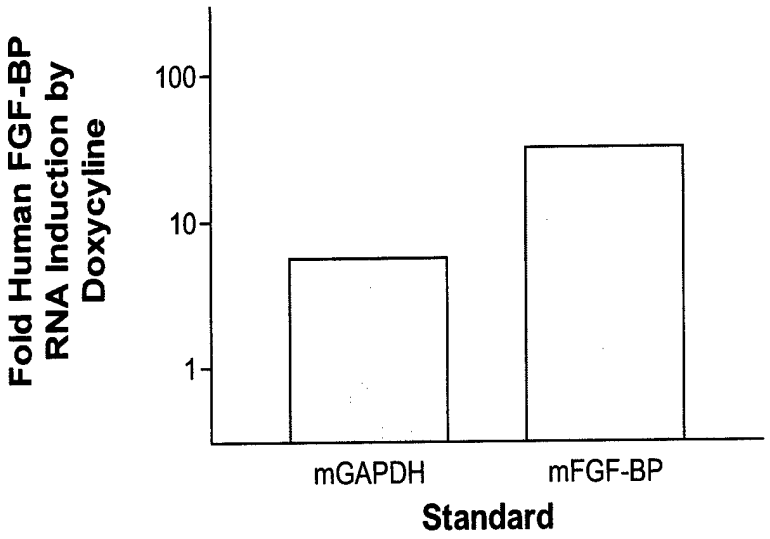

Figure 1. Induction of hFGF-BP mRNA in ear biopsies from tet-RE-hFGF-BP transgenic mice. Real-time PCR was used to measure the fold induction of hFGF-BP mRNA after induction of transgene expression for two days. The fold induction is expressed relative to mouse GAPDH as well as relative to the endogenous mFGF-BP to standardize the assay. Obviously the transgene is regulated >5-fold by doxycycline administration.

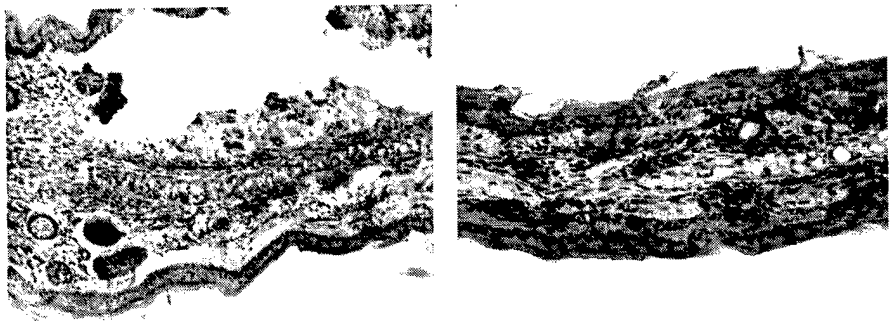

Figure 2. Induction of hFGF-BP protein in tet-RE-hFGF-BP transgenic mice. Immunohistochemistry for human FGF-BP (the transgene) was used. The left panel shows an ear biopsy before and the right punch after induction of transgene expression for two days. The dark purple stain represents FGF-BP. This experiment was repeated in a separate mouse line with a similar result (not shown).

Conclusions:

Obviously, we were able to generate tetracycline regulated FGF-BP transgenic mice. Now, further functional studies can be carried out as well as further crosses for tissue specific expression.

2. Transient expression of FGF-BP in chicken embryos

(Comment:
Although this is beyond the scope of this proposal, the following series of experiments was initiated due to the embryonically lethal phenotype generated by FGF-BP expression in mice and thus will be documented and commented on here.)

Chicken embryo studies have been used for many decades in biology. We have employed this model to study angiogenesis factors on the chorio-allantois membrane (CAM) of the embryos. More recent studies published e.g. in Cell (Li et al 1995) have demonstrated in this model that application of FGF can induce limb bud formation in chick embryos and have analyzed the signaling pathways for that. We set up a particular version of the chicken embryo as a model system which allows continuous microscopic monitoring of phenotypic effects in the live embryo. For this model, day 3-fertilized eggs are cracked and the contents placed on 10 ml of DMEM in 10 cm petri dishes (see Fig. 3A,B). In a humidified incubator at 39°C a high portion (>2/3) of the chicken embryos will grow on top of the yolk for at least another week and approximately 1/3 to 1/4 till day 12. Occasionally the embryos will even grow to full maturity if the experiment is allowed to continue and we have had viable, fully-matured chicks grown from this approach. Genes can be expressed for >4days after a single plasmid injection into the yolk sac (see Fig. 3C,D).

Phenotype of CMV-FGF-BP expression in chicken embryos:
Transient expression of human FGF-BP under a CMV promoter in the chicken embryo produces a lethal effect that is evident as early as 24 h after gene transfer. Gross examination of the transgenic embryos revealed a mottling of the skin characterized by erythema and dilated, prominent vasculature consistent with hemorrhage (Fig. 4). Intravascular injection of Evans blue dye with concomitant tissue extravasation among the FGF-BP transgenic embryos confirmed this hemorrhagic phenotype (not shown). Light and electron microscopic photomicrographic examination of the transgenic embryonic tissue demonstrated FGF-BP associated attenuation of endothelial cytoplasm together with a ruffled appearance of the cell membrane. Consistent with the occurrence of hemorrhage, erythrocytes appear extravascularly (not shown).

Taken together these data suggest a profound effect of FGF-BP upon embryonic vascular development characterized by compromised vascular formation and/or maintenance. It is likely that enhanced FGF activity due to FGF-BP expression also increases the expression of Ang-1, VPF/VEGF and/or their receptors as reported earlier[31-33]. This imbalance of vascular growth and differentiation signals was reported to lead to disruption of vascular integrity and to produce a phenotype reminiscent of that observed in the chicken embryos and probably also in the transgenic mouse embryos [34,35].

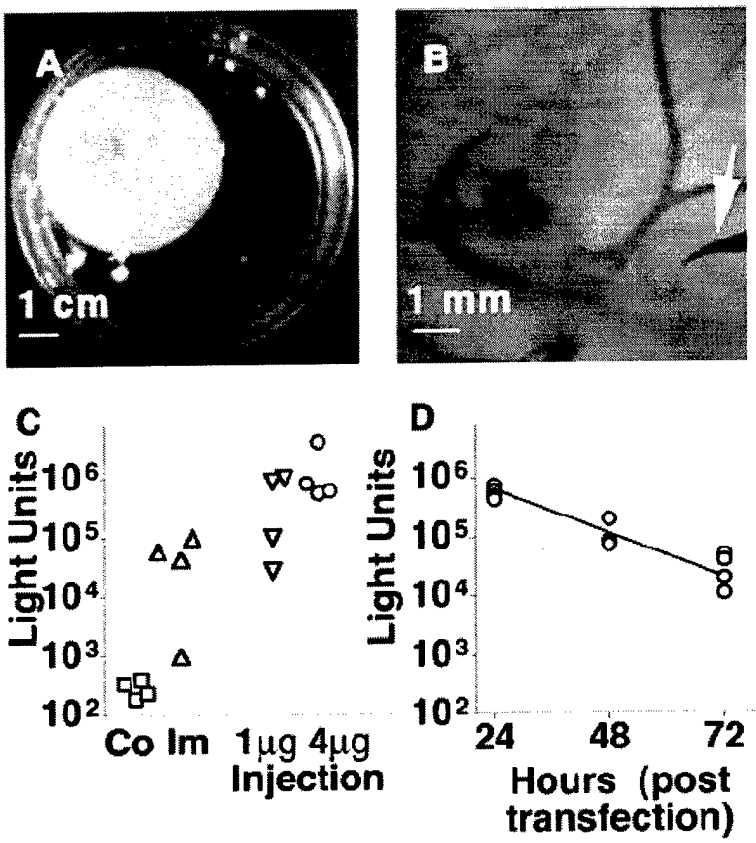

Figure 3. Gene Expression in the Chicken Embryo.
(A, B) Overview of the model. Different magnification of day 4 chicken embryos that were used for microinjection. The arrow in panel B points to the injection needle (black). **(C)** Embryos were microinjected with 25 ml of lipofectamine without (Control) or with 1 mg of CMV luciferase plasmid around the body of the embryo (Im = DNA immersion) or with 1 or 4 μg of the plasmid into the allantoic sac. Luciferase activity was measured 24 hours after microinjection. **(D)** Time course of luciferase activity after 4 μg of CMV luciferase injection into the allantoic sac. Each data point represents measurements from an individual embryo. Note the logarithmic scale of the Y-axis.

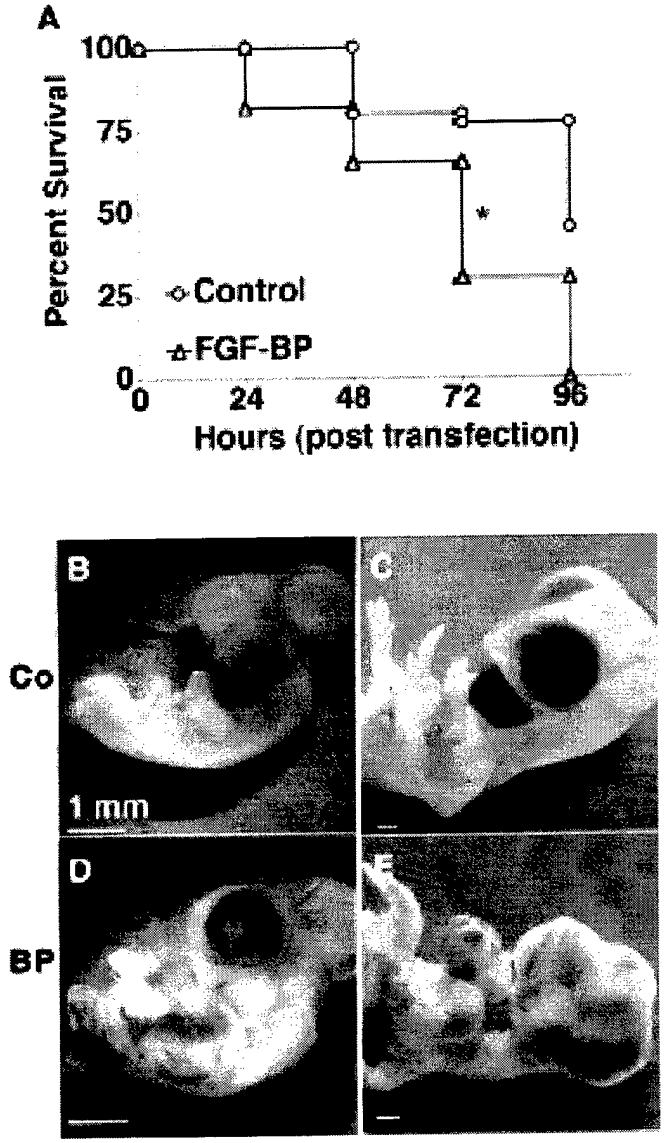

Figure 4. Effect of FGF-BP on Embryonic Survival and Development.
Day E4 embryos received microinjections of 4 μg CMV FGF-BP or CMV luciferase (= control) plasmid in 25 μl of lipofectamine into the allantoic sac. **(A)** Kaplan-Meier survival curves of the embryos. *, $p<0.05$ comparing the two groups (Prism/GraphPad program). **(B to D)** Embryos harvested 24 h (B, D) and 72 h (C, E) after administration of the expression vectors. Note the bleeding in the BP-transgenic embryos !

When scaled along days post conception, the development of chick embryos is shortend by approximately two days relative to mouse embryos. The experiments here thus cover the equivalent of murine days e6 to e15, when we observed embryonic lethality after FGF-BP expression.

TASK 4; Methods:

In Vitro Cultivation of Embryos. Three day old fertilized chicken (Gallus gallus) eggs (CBT Farms; Chestertown, Md.) were opened and intact embryos with yolk were placed in 10 x 2 cm polystyrene culture dishes (Corning; Corning, New York). Embryos were maintained in a humidified water-jacketed incubator at 39°C prior to and following transfection. The human FGF-BP (hFGF-BP), green fluorescent protein (GFP), luciferase and β-galactosidase expression vectors were constructed employing the pRc/CMV vector (Invitrogen, San Diego, CA). The hFGF-BP plasmid contained the hFGF-BP open reading frame and has been described previously[10]. Various concentrations of plasmid constructs were incubated with 25 μl Lipofectamine™ reagent (Life Technologies) at room temperature for 45 min. 25 μl of the liposomal mixture were injected into each embryo using a Hamilton syringe (Hamilton; Reno, NV) under 3X magnification with an Olympus SZH10 steromicroscope.

To quantitate gene transfer, CMV luciferase was used as a vector and embryos were harvested and homogenized in 150 μl Passive Lysis Buffer (Promega) at various time points following transfection. The Luciferase Reporter assay system (Promega) was used to detect firefly luciferase activity in 100 μl homogenate utilizing a Monolight 2010 luminometer.

TASK 4; INTERPRETATION OF THE DATA

In ongoing unpublished studies we found that expression of FGF-BP as a transgene in mice results in early embryonic lethality in the first half of gestation due to hemorrhage into the gestational sac. K14, MMTV or CMV-dependent transgene expression resulted in qualitatively the same phenotype that was only distinguished by a slightly different onset between days E6 and E10 (unpublished observation).

Due to this unexpected lethality of FGF-BP expression, we have now generated tetracycline-regulatable FGF-BP expression in transgenic animals.

Also, we established a method to express FGF-BP as a transient transgene in chicken embryos. This resulted in lethality of the chicken embryos within a few days after transgene expression due to vascular leakage.

KEY RESEARCH ACCOMPLISHMENTS

1. Increased expression of FGF-BP in invasive breast cancer
2. Significant positive correlation of expression of FGF-BP with ER as well as the growth factor pleiotrophin and receptor anaplastic lymphoma kinase.
3. Establishing a model breast cancer cell line (MDA-MB468) in which FGF-BP is regulatable by the growth factor EGF.
4. Analysis of the pathway of EGF regulation of FGF-BP
5. Analysis of the promoter elements driving EGF regulation of the FGF-BP gene in the breast cancer cell model.
6. Analysis of the transcription factor binding and interaction that drive EGF regulation of FGF-BP.
7. Finding that FGF-BP causes embryonic lethality during the second half of gestation of transgenic mice with K14, MMTV and CMV promoters used to drive FGF-BP transgene expression.
8. Initiation of tetracycline-regulatable transgene expression of FGF-BP in mice.
9. Demonstration that tetracycline-regulated FGF-BP transgene expression in mice is regulatable in vivo.
10. Establishing an alternative transient transgenic expression system for FGF-BP in chicken embryos.
11. Demonstration of vascular leakage and lethality of transgene expression of FGF-BP in chicken embryos.

- Task 1, which included expression and outcome studies with human breast cancer samples was thus completed and we were able to show the associations between FGF-BP expression and the invasive breast cancer phenotype.

- Tasks 2 and 3 which dealt with the regulation and molecular mechanisms of regulation of FGF-BP in a breast cancer cell model was thus completed and the pathway as well as cis-elements as well as trans-acting transcription factors were characterized.

- Task 4, which addressed the role of FGF-BP using a transgenic model ran into unpredicted embryonic lethality of the transgene and we had to resort to conditional transgene expression which was achieved successfully. We also generated a novel transient transgene chicken embryo model as an alternative to dissect the lethal phenotype induced by FGF-BP in mouse embryos.

REPORTABLE OUTCOMES

Publications (attached):

Tassi et al. (2001) J Biol Chem

Kagan et al. (2003) Cancer Research

Manuscripts (attached):

McDonnell et al; submitted to Nature Biotechnology

Henke et al.; CBCTR website NCI/NIH

Animal model:

Transgenic chicken embryo described in the manuscript: McDonnell et al; submitted to Nature Biotechnology

CONCLUSIONS

- FGF-BP is highly expressed in approximately 1/2 of invasive breast cancers and rarely in normal breast or in in situ carcinoma.

- The FGF-BP gene is regulated in breast cancer cells by growth factors such as EGF. This regulation occurs at the transcriptional level and utilizes the transcription factor family C/EBPbeta as a major mechanism that involves interaction between activating and inhibitory isoforms of transcription factors.

- The FGF-BP transgene is lethal when expressed during embryogenesis in mice or in chicken embryos. Studies on mammary carcinogenesis in mice thus requires the establishment of regulatable transgene expression and a tetracycline-regulated system was generated for this.

Future plans / suggestions and outlook:

Generation of an ELISA to detect the secreted FGF-BP protein in serum samples from patients could serve as an early marker for cancer detection or to monitor the success of chemotherapy or the recurrence of metastases.

REFERENCES

1. Dickson, R. & Lippman, M.E. Estrogenic regulation of growth and polypeptide growth factor secretion in human breast carcinoma. *Endocr.Rev.* **8**, 29-43 (1987).
2. Martin, G.R. The role of FGFs in the early development of vertebrate limbs. A Review. *Genes Dev.* **12**, 1571-1586 (1998).
3. Hogan, B.L.M. Morphogenesis. A Review. *Cell* **96**, 225-233 (1999).
4. Burgess, W.H. & Maciag, T. The heparin-binding (fibroblast) growth factor family of proteins. *Annu.Rev.Biochem.* **58**, 575-606 (1989).
5. Baird, A. & Böhlen, P. Fibroblast Growth Factors. in *Handbook of Experimental Pharmacology, Vol. 95/I* (eds. Sporn, M.B. & Roberts, A.B.) 369-418 (Springer, New York, Berlin, Heidelberg, 1990).
6. Hicks, K.K., Shin, J.T., Opalenik, S.R. & Thompson, J.A. Molecular mechanisms of angiogenesis: experimental models define cellular trafficking of FGF-1. *P.R.Health Sci.J* **15**, 179-186 (1996).
7. Wu, D.Q., Kan, M.K., Sato, G.H., Okamoto, T. & Sato, J.D. Characterization and molecular cloning of a putative binding protein for heparin-binding growth factors. *J.Biol.Chem.* **266**, 16778-16785 (1991).
8. Mason, I.J. The ins and outs of fibroblast growth factors. *Cell* **78**, 547-552 (1994).
9. Powers, C.J., McLeskey, S.W. & Wellstein, A. Fibroblast growth factors, their receptors and signaling. *Endocr Relat Cancer* **7**, 165-97 (2000).
10. Czubayko, F., Smith, R.V., Chung, H.C. & Wellstein, A. Tumor growth and angiogenesis induced by a secreted binding protein for fibroblast growth factors. *J.Biol.Chem.* **269**, 28243-28248 (1994).
11. Wu, D.Q., Kan, M.K., Sato, G.H., Okamoto, T. & Sato, J.D. Characterization and molecular cloning of a putative binding protein for heparin-binding growth factors. *J Biol Chem* **266**, 16778-85 (1991).
12. Czubayko, F., Smith, R.V., Chung, H.C. & Wellstein, A. Tumor growth and angiogenesis induced by a secreted binding protein for fibroblast growth factors. *J Biol Chem* **269**, 28243-8 (1994).
13. Bonfil, R.D. et al. Stimulation of angiogenesis as an explanation of Matrigel-enhanced tumorigenicity. *Int J Cancer* **58**, 233-9 (1994).
14. Filmus, J., Pollak, M.N., Cailleau, R. & Buick, R.N. MDA-468, a human breast cancer cell line with a high number of epidermal growth factor (EGF) receptors, has an amplified EGF receptor gene and is growth inhibited by EGF. *Biochem Biophys Res Commun* **128**, 898-905. (1985).
15. Shao, Z.M., Wu, J., Shen, Z.Z. & Barsky, S.H. Genistein inhibits both constitutive and EGF-stimulated invasion in ER-negative human breast carcinoma cell lines. *Anticancer Res* **18**, 1435-9 (1998).
16. Sainsbury, J.R., Farndon, J.R., Needham, G.K., Malcolm, A.J. & Harris, A.L. Epidermal-growth-factor receptor status as predictor of early recurrence of and death from breast cancer. *Lancet* **1**, 1398-402. (1987).
17. Davies, S.P., Reddy, H., Caivano, M. & Cohen, P. Specificity and mechanism of action of some commonly used protein kinase inhibitors. *Biochem J* **351**, 95-105. (2000).

18. Kobayashi, E. et al. Calphostins (UCN-1028), novel and specific inhibitors of protein kinase C. I. Fermentation, isolation, physico-chemical properties and biological activities. *J Antibiot (Tokyo)* **42**, 1470-4 (1989).
19. Cuenda, A. et al. SB 203580 is a specific inhibitor of a MAP kinase homologue which is stimulated by cellular stresses and interleukin-1. *FEBS Lett* **364**, 229-33 (1995).
20. Kumar, S. et al. Novel homologues of CSBP/p38 MAP kinase: activation, substrate specificity and sensitivity to inhibition by pyridinyl imidazoles. *Biochem Biophys Res Commun* **235**, 533-8 (1997).
21. Duncia, J.V. et al. MEK inhibitors: the chemistry and biological activity of U0126, its analogs, and cyclization products. *Bioorg Med Chem Lett* **8**, 2839-44 (1998).
22. Harris, V.K., Liaudet-Coopman, E.D., Boyle, B.J., Wellstein, A. & Riegel, A.T. Phorbol ester-induced transcription of a fibroblast growth factor- binding protein is modulated by a complex interplay of positive and negative regulatory promoter elements. *J Biol Chem* **273**, 19130-9 (1998).
23. Amoui, M., Draber, P. & Draberova, L. Src family-selective tyrosine kinase inhibitor, PP1, inhibits both Fc epsilonRI- and Thy-1-mediated activation of rat basophilic leukemia cells. *Eur J Immunol* **27**, 1881-6. (1997).
24. Descombes, P. & Schibler, U. A liver-enriched transcriptional activator protein, LAP, and a transcriptional inhibitory protein, LIP, are translated from the same mRNA. *Cell* **67**, 569-79 (1991).
25. Descombes, P., Chojkier, M., Lichtsteiner, S., Falvey, E. & Schibler, U. LAP, a novel member of the C/EBP gene family, encodes a liver-enriched transcriptional activator protein. *Genes Dev* **4**, 1541-51. (1990).
26. Kozak, M. Possible role of flanking nucleotides in recognition of the AUG initiator codon by eukaryotic ribosomes. *Nucleic Acids Res* **9**, 5233-62 (1981).
27. Kozak, M. Point mutations define a sequence flanking the AUG initiator codon that modulates translation by eukaryotic ribosomes. *Cell* **44**, 283-92 (1986).
28. Raja, R.H., Paterson, A.J., Shin, T.H. & Kudlow, J.E. Transcriptional regulation of the human transforming growth factor- alpha gene. *Mol Endocrinol* **5**, 514-20 (1991).
29. Harris, V.K. et al. Induction of the Angiogenic Modulator Fibroblast Growth Factor-binding Protein by Epidermal Growth Factor Is Mediated through Both MEK/ERK and p38 Signal Transduction Pathways. *J Biol Chem* **275**, 10802-10811 (2000).
30. Zahnow, C.A., Cardiff, R.D., Laucirica, R., Medina, D. & Rosen, J.M. A role for CCAAT/enhancer binding protein beta-liver-enriched inhibitory protein in mammary epithelial cell proliferation. *Cancer Res* **61**, 261-9. (2001).
31. Hata, Y., Rook, S.L. & Aiello, L.P. Basic fibroblast growth factors induce expresson of VEGF receptor KDR through a protein kinase C and p44/p42 mitogen-activated protein kinase-dependent pathway. *Diabetes* **48**, 1145-1155 (1999).
32. Mandriota, S.J. & Pepper, M.S. Regulation of angiopoietin-2 mRNA levels in bovine microvascular endothelial cells by cytokines and hypoxia. *Circ Res* **83**, 852-859 (1998).
33. Seghezzi, G. et al. Fibroblast growth factor-2 (FGF-2) induces vascular endothelial growth factor (VEGF) expression in the endothelial cells of forming capillaries: an autocrine mechanism contributing to angiogenesis. *J Cell Biol* **141**, 1659-1673 (1998).
34. Larcher, F., Murillas, R., Bolontrade, M., Conti, C.J. & Jorcano, J.L. VEGF/VPF overexpression in skin of transgenic mice induces angiogenesis, vascular hyperpermeability and accelerated tumor development. *Oncogene* **17**, 303-311 (1998).

35. Maisonpierre, P.C. et al. Angiopoietin-2, a natural antagonist for Tie2 that disrupts in vivo angiogenesis. *Science* **277**, 55-60 (1997).

APPENDICES

Personnel involved in the studies:

Ralf T. Henke, MD, postdoctoral fellow

Benjamin Kagan, graduate student

Kevin McDonnell, MD PhD, postdoctoral fellow

Anna T. Riegel, PhD, associate Professor

Elena Tassi, PhD, postdoctoral fellow

Anton Wellstein, MD PhD, Professor

Papers published and supported under this award

Tassi et al. (2001) J Biol Chem

Kagan et al. (2003) Cancer Research

Manuscripts supported under this award

Henke et al.; CBCTR website NCI/NIH

McDonnell et al; submitted to Nature Biotechnology (Title page and Abstract page)

(UNDER REVIEW FOR THE CBCTR WEBSITE AT NIH/NCI)

IN SITU HYBRIDIZATION WITH DIGOXIGENIN LABELED RNA PROBES

RALF T. HENKE, RANJAN RAY AND ANTON WELLSTEIN

LOMBARDI CANCER CENTER, GEORGETOWN UNIVERSITY, WASHINGTON, DC

CORRESPONDENCE TO: ANTON WELLSTEIN, MD, PHD GEORGETOWN UNIVERSITY, LOMBARDI CANCER CENTER, RESEARCH BUILDING E311, 3970 RESERVOIR RD. NW
WASHINGTON, DC 20057
EMAIL: WELLSTEA@GEORGETOWN.EDU

Introduction

When investigating the RNA expression in tissues one of the main concerns is to distinguish between expression levels in particular cell types and structures. When using northern blot or real time PCR with heterogeneous tissue samples it is often difficult to reach exact conclusions. The in situ hybridization (ISH) is established as a method allowing demonstration of the RNA expression by using specific probes without loosing the morphological information since the tissues are preserved in there structure.

The protocol described here uses Digoxigenin labeled RNA-Probes thus avoiding any radioactive isotopes and was used in our lab for more than 1000 slides including more than 100 tissue micro arrays. Positive staining results will appear as a violet to brown staining in individual cells, mainly in the cytoplasm. Normally unstained nuclei can be observed surrounded by stained cytoplasm (**Figure 1a**). Unspecific staining can be expected especially in collagen structures and usually appears blue rather than violet. Counterstaining with e.g. Haematoxilin is not necessary and not recommended since the low staining intensity of the ISH may otherwise be difficult to evaluate. Tissue structures can still be determined even in completely negative tissue (**Figure 1b**).

When staining tissue micro arrays we recommend establishing the method of ISH and the quality of each individual probe set (antisense and sense) first on an appropriate number of full sections of according pathological and reference tissues (e.g. for a breast cancer array: two sets of 10 invasive breast cancers and 10 normal breast samples, stained in the same batch. One set used for antisense and one for sense). This is especially important since due to their limited availability and high value usually only one tissue micro array will be stained with the antisense probe and no second array for the sense probe. When advancing to tissue micro arrays with established probes we also recommend to include several slides of previously tested tissues in the same batch with the array that are known to be positive or negative for the RNA of interest. Two sets of these should be stained with the antisense and sense probe. This provides appropriate external positive and negative controls for the array.

When evaluating the results of different batches of ISH high variation of staining intensity may be observed. When using tissue micro arrays each of them should be evaluated individually by first identifying the highest and lowest staining intensity on the slide.

To evaluate results we suggest using a relative scale for each array defining the highest observed staining as "+++" and the lowest as "-". Recommended coding to evaluate staining results of the individual cores is shown in **table 1**.

Table 1

Negative staining	-	no staining observed in this core
	+/-	slight signals but no certain positivity
Positive staining	+	certain positive staining in at least some cells
	++	medium staining in all cells or light staining in some cells and high staining in others
	+++	high staining in all cells and/or very high staining in at least 20% of the cells
N/A	x	core missing or the tissue of this core is necrotic and the RNA is degraded
	-NT	the appropriate cells (i.e. in breast arrays: cancer cells or breast epithelial cells) are not present in this core.

Figure 1a

1b

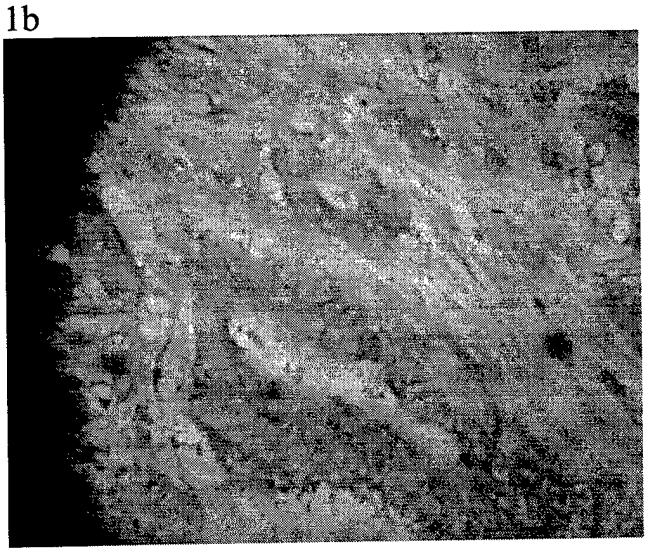

Representative staining results

1a) Colon Cancer stained with antisense RNA-probe. (400x)

1b) Sequential section stained with the according sense RNA-probe (negative control)

1. Solutions

SOLUTION (volumes are recommendations for 3-4 ISH)	NEEDED FOR
1) Digoxigenin labeled RNA-Probe / approx. 600 ng per slide (microarray)	
2) Xylene (RNA-grade)	Day 1
3) Ethanol 100% (RNA-grade)	Day 1
4) DEPC-H_2O (Diethyl Pyrocarbonate) / 8 liters for preparation of solutions - add 1ml DEPC per 1l H_2O, stir o/n then autoclave next morning	Day 1 and as stock
5) PBS 1x / 1 liter - dilute from 10x Stock with DEPC-H_2O	Day 1
6) PBS 10x / 500 ml - commercial or: - 80g NaCl, 2g KCl, 11.5g Na_2HPO_4*$7H_2O$ in 500 ml DEPC-H_2O	as stock
7) Proteinase K in PBS 1x / 200 ml per ISH - add on Day 1: 2 mg Proteinase K to 200ml PBS (final conc. 10 µg / ml)	prepare fresh on Day 1
8) SSC 2x / 1 liter - dilute from SSC 20x with DEPC-H_2O	Day 1
9) SSC 20x / 1 liter - commercial or: - 3M NaCl, 0,3 M Na-citrate, ad 1l DEPC-H_2O	as stock
10) 0,2M HCl / 1 liter - 1 Part 6N HCl, 29 Parts DEPC-H_2O	Day 1
11) TEA-HCl (0,1M Triethanolamine-HCl at ph 8,0) / 2 liters - dissolve 18,6 g TEA-HCl (RNA-grade) in 900 ml DEPC-H_2O - titrate to pH 8,0 with 10N NaOH (takes time, solution is a buffer!) - ad 1l DEPC-H_2O	Day 1
12) 0,25% Acetic anhydride in TEA-HCl / 200 ml per ISH - add on Day 1: 500 µl Acetic anhydride in 500ml in 200 ml TEA-HCl	prepare fresh on Day 1
13) Hybridization Solution / 200 µl (small sample) – 400 µl (tissue array) per slide - Sigma®, catalog number H7782 (calculate 200-400 µl/Tissue)	Day 1
14) dd-H_2O / several liters to prepare solutions and approx. 2 liters / ISH	Day 2 + Day 3
15) STE Buffer / 1 liter - 500 mM NaCl, 20 mM Tris-HCl pH 7,5, 1mM EDTA in dd-H_2O	Day 2
16) RNAse A in STE Buffer / 200 ml per ISH - ad 2g of RNAse to 200ml STE Buffer	prepare fresh on Day 2

17) SSC 2x / 2 liters - 200 ml SSC 20x, ad 2 liters dd-H_2O	Day 2
18) SSC 2x + Formamide (1:1) / 200 ml per ISH - 100 ml Formamide, 20 ml SSC 20x, 80 ml dd-H_2O	prepare fresh on Day 2
19) SSC 1x / 200 ml per ISH - 10 ml SSC 20x, 190 ml dd-H_2O	Day 2
20) SSC 0,5x / 200 ml per ISH - 5 ml SSC 20x, 195 ml dd-H_2O	Day 2
21) Buffer #1 / 3 liters - 100 mM Tris-HCl pH 7,5, 150 mM NaCl (8,77 g/l) in dd-H_2O - FILTER	Day 2 + Day 3
22) 2% Horse Serum in Buffer #1 - add 4 ml of Horse Serum to 200 ml Buffer #1	prepare fresh on Day 2
23) Anti-Digoxigenin antibody solution - dilute in Buffer #1: (calculate 500-700 µl / slide) 1:250 anti-DIG-FAB-AB-Fragments, 1:100 Horse Serum	prepare fresh on Day 2
24) Buffer #2 / 3 liters - 100 mM Tris-HCl pH 9,5, 100 mM NaCl, 50 mM $MgCl_2$ in dd-H_2O - FILTER	Day 3
25) NBT/BCIP Substrate Solution (**Light sensitive!** Wrap in aluminum-foil) - dilute in Buffer #2: (calculate 500 – 1000 µl / Tissue) 33,75µl / 10ml (3,75mg / 10ml) of NBT (nitroblue tetrazolium) 35µl / 10ml (1,75mg / 10ml) of BCIP (toluidinum salt)	prepare fresh on Day 3
26) Buffer #3 / 2 liters - 10mM Tris-HCl pH 8,0, 1mM EDTA in dd-H_2O - FILTER	Day 3
27) 0,5% Tween 20 in dd-H_2O / 200 ml per ISH	prepare fresh on Day 3
28) Sealing solution for microscopical slides	Stock

2. Material / Work environment

1) RNAse ZAP® Spray	
2) 20+ Plastic containers ("buckets") to hold the solutions during the ISH. Container-volume 200 ml	
3) Plastic slide holders for 24 slides	
4) Plastic trays ("slide chamber") to hold slides vertically during special steps like the o/n hybridization, the o/n antibody incubation and the NBT/BCIP staining	
5) Kimwipes®	
6) Parafilm®	
7) Plastic – Pasteur pipettes	
8) Vacuum system for at least 500 – 1000 ml of volume	
9) Empty drawer to develop during NBT/BCIP staining	
10) Workbench treated with RNAse ZAP®	
11) Sterile 1 liter vacuum filter system to prepare the solutions	
12) Ice on day one	
13) Water bath at 37°C	
14) Oven at 55°C and 65°C (do not use an incubator for cells or bacteria)	
15) Incubator at 42°C (do not use an incubator for cells or bacteria)	
16) Cover slips for microscopical slides	

3. Procedure

3.1. Preparations before the actual ISH

3.1.1. General considerations

- GLOVES MUST ALLWAYS BE WORN when handling the slides, any of the solutions or materials for day one or when handling the RNA-probes.
- Clean the workbench and all bottles, beakers and graded cylinders for solutions for day one with RNAse ZAP® and let them completely dry before proceeding further. Cover them with aluminum foil while drying.
- Whenever possible use sterile 15 ml or 50 ml Sarstedt® or Falcon® tubes for measuring and handling small volumes of solutions for day one. They can be considered RNAse free. Use them especially to prepare and store the hybridization solution with your RNA probe on day one.

3.1.2. Before Day 0

- Make at least 4 l of DEPC-H_2O (solution 4). If you prepare all solutions for the first time: 8 l.
- Clean the workbench with RNAse ZAP®
- Prepare solutions 5), 6), 8), 9), 10) and 11) with DEPC-H_2O
- Prepare solutions 15), 17), 21), 24) and 26) with dd-H_2O
- The three Buffer solutions must, all the others should be filtered (sterile1 liter vacuum filter system). Filter DEPC based solutions first if you want to use one filter for all. Wash filter between solutions for day one with DEPC-H_2O, later between solutions for day two and three with dd-H_2O

3.1.3. Day 0

- DO NOT MICROWAVE SLIDES, DO NOT KEEP SLIDES AT 55°C OVER NIGHT. Some other protocols recommend this preparation to remove excess paraffin. However this treatment reduces the RNA quality
- Clean the workbench (again), the plastic containers ("buckets") for day one and the slide holder with RNAse ZAP®. Place buckets and slide holder on and cover with aluminum foil. Let dry over night

3.1.4. Day 1

- ❑ Place slides in slide holder. Incubate slides in holder for 1 hour at 55°C
- ❑ Increase Oven to 65°C one hour before the first Xylene step and incubate slides for one more hour at 65°C
- ❑ Fill all **buckets for Day 1**:
  - Xylene I (Chemical hood!)
  - Xylene II (Chemical hood!)
  - Ethanol 100% I
  - Ethanol 100% II
  - DEPC-H_2O
  - PBS 1x
  - PBS 1x (later add: Proteinase K)
  - SSC 2x (DEPC-H_2O)
  - 0,2 M HCl
  - 0,1 M TEA-HCl pH 8,0
  - 0,5 ml acetic anhydride in 200 ml 0,1 M TEA-HCl pH 8,0
- ❑ Place the two PBS buckets in a 37°C water-bath
- ❑ Calculate RNA-probes and hybridization solution:
  a) needed volume of hybridization solution:
  200-400 µl/Tissue (200µl for small e.g. Cell pellets, 400 µl for Arrays)
  b) needed volume for antisense (and sense) RNA-probe:
  RNA-amount: The final RNA-concentration in the hybridization solution should be 1,5 µg RNA / 1,0 µl solution.

Example:
for 5 tissue array slides calculate 2000 µl hybridization solution and 3000 µg AS-RNA-Probe

3.1.5. Day 2

- ❑ Fill all **buckets for Day 2:**
  - SSC 2x I (dd-H_2O)
  - SSC 2x II (dd-H_2O)
  - STE Buffer
  - STE Buffer (add later: RNAse A)
  - SSC 2x + Formamide (1:1)
  - SSC 1x
  - SSC 0,5x
  - Buffer #1
  - Buffer #1 + 2% Horse serum (add later)
- ❑ Place the STE buffer buckets in 37°C water bath
- ❑ Place the SSC 2x + Formamide, the SSC 1x and the SSC 0,5x buckets in 42°C Incubator
- ❑ Take Horse Serum out of the Freezer (DO NOT heat over 37°C or microwave for thawing)

3.1.6. Day 3

- ❑ Fill all **buckets for Day 3:**
  - Buffer #1 I
  - Buffer #1 II
  - Buffer #2 I
  - Buffer #2 II
  - Buffer #3
  - 0,5% Tween
  - dd-H_2O

3.2. Day 1 – Protocol

3.2.1. De-Paraffination

- ❑ Pick up the slide holder from the 65°C oven (reset temperature to 55°C)
- ❑ Place the slide holder in Xylene I (Chemical hood!) ..... 5 min
- ❑ Xylene II (Chemical hood!) ..... 10 min
- ❑ Ethanol 100% I ..... 5 min
- ❑ Ethanol 100% II ..... 5 min
- ❑ DEPC-H_2O ..... 5 min

3.2.2. Protein-Digestion

- ❑ PBS I (37°C) ..... 5 min
- ❑ Add Proteinase K to PBS II (2 mg) while slides are in PBS I
- ❑ PBS II + Proteinase K (37°C) ..... 10 min
- ❑ PBS I (37°C) again ..... 5 min
- ❑ DEPC-H_2O (from here room temperature again) ..... 5 min

3.2.3. De-Proteinization

- ❑ 0,2 M HCl ..... 15 min
- ❑ While in HCl: add acetic anhydride to 0,1M TEA-HCl pH 8,0 bucket II
- ❑ While in HCl: pick up hybridization-solution from –20°C and RNA-probe(s) from –80°C PLACE BOTH ON ICE!
- ❑ While in HCl: prepare slide-chamber: double layer of wet filter paper, with Parafilm® on top

3.2.4. Acetylation

- ❑ 0,1M TEA-HCl pH 8,0 I ..... 5 min
- ❑ 0,1M TEA-HCl pH 8,0 II + 0,25% acetic anhydride ..... 15 min
- ❑ While in (TEA II + acet. anhy.): Mix needed volume hybridization solution with RNA-Probe. Keep ready solution on ice. Refreeze the remaining RNA-probe(s) at –80°C.

3.2.5. Hybridization

- ❑ SSC 2x (DEPC-H_2O) ..... 5 min
- ❑ Take out one slide at a time. Then do for each slide:
  - o Dry backside and front areas without tissue carefully with a Kimwipe®
  - o Place the slide vertically in the slide chamber
  - o Pipette the hybridization solution / RNA-probe mix on the tissue
- ❑ After the last Slide: seal the slide chamber with Parafilm® and place **O/N in 42°C Incubator**

3.3. Day 2 – Protocol

3.3.1. Post-Hybridization wash

- ❑ Pipette 1,0-2,0 ml of SSC 2x on each slide to dilute the hybridization solution. Use a plastic Pasteur pipette
- ❑ Suck tissues CAREFULLY almost dry with vacuum system (1 ml pipette-tip on the vacuum tube). Process one slide at a time. Do not allow the tissue to dry out completely
- ❑ Pipette 1,0-2,0 ml SSC 2x back on the tissue directly after the vacuum step
- ❑ After one complete round restart again to vacuum one slide at a time.
- ❑ Pick up the slide directly after the second vacuum step and dip it shortly in the SSC 2x I bucket. Then place it in an empty slide holder in the SSC 2x II bucket where you collect the slides
- ❑ When all slides are processed and collected in the SSC 2x II bucket, wait ..... 5 min

3.3.2. RNA-Digestion

- ❑ STE Buffer I (37°C) ..... 5 min
- ❑ While in STE Buffer I: Add 2mg RNAse A to STE Buffer II
- ❑ STE Buffer II + RNAse (37°C) ..... 10 min
- ❑ STE Buffer I (37°C) again ..... 5 min

3.3.3. Re-Fixation

- ❑ SSC 2x + Formamide (1:1) (42°C) ..... 10 min
- ❑ SSC 1x (42°C) ..... 5 min
- ❑ SSC 0,5x (42°C) 5min

3.3.4. Blocking

- ❑ Buffer #1 ..... 1 min
- ❑ Buffer #1 + 2% Horse Serum ..... 30 min
- ❑ While in Buffer #1 + HS: Prepare Antibody solution (Buffer #1 + AB + 1% Horse Serum)

3.3.5. DIG-Antibody-solution Application

- ❑ Take slides out of the blocking solution one after at a time and:
  - o Dry backside and front areas without tissue with a Kimwipe®
  - o Place slide in slide chamber
  - o Pipette Antibody solution (500+ µl / slide)
- ❑ After the last slide: seal the chamber with Parafilm®
- ❑ Place chamber in **4°C Fridge** ..... **overnight**

3.4. Day 3 – Protocol

3.4.1. Antibody washout

- Leave slides in the chamber and pipette 1000-2000µl Buffer #1 on each tissue (plastic pipette)
- After „full round" carefully vacuum liquid away and DIREKTLY re-pipette some Buffer #1
- Do a second round of vacuum. Each time a slide is finished dip it in Buffer #1 I and the place it in a slide holder in Buffer #1 II
- Once all are collected in the holder in Buffer #1 II: transfer the slides in the holder to Buffer #2 I
- Buffer #2 I ..... 5 min
- Buffer #2 II ..... 5 min
- While in Buffer #2: Prepare staining solution (NBCI/NBT in Buffer #2) (prepare in a Falcon® or Sarstedt® tube wrapped in aluminum foil)

3.4.2. Staining

- Take one slide at a time out of the Buffer #2 II, then:
  - Dry backside and front areas without tissue with a Kimwipe®
  - Place slide in the slide chamber
  - Pipette staining solution on tissues with a plastic pasteur pipette. *Note: Speed is crucial if multiple slides are processed since the first slides may already be fully stained before the last one is processed.*
- When all slides are in the chamber: Place it carefully in a drawer to develop in the dark
- Check every 10 min for staining process. If uncertain, take one of the first slides to the microscope to check and re-pipette staining solution afterwards if necessary

3.4.3. Stopping staining and cleaning

- When stained enough (usually after 20-30 min.), pick up the slides one at a time in the order they were processed, dip them in Buffer #2 and place them in a slide holder in Buffer #3
- When all slides are processed and in Buffer #3:..... wait 5 min
- 0,5% Tween 20 (move bucket carefully to wash slides)..... 5 min
- dd-H_2O: Place rack in bucket, go to the sink and wash under the dd-H_2O tap (slow flow) ...2 min
- Take slides out, place vertically on filter paper and let them COMPLETELY dry . at least 20 min
- Apply sealing solution on slides and cover with slip (Chemical hood)
- Wait at least 24hrs before storing slides upright in a box!

4. Further reference

Panoskaltis-Mortari, A. and R. P. Bucy (1995). "In situ hybridization with digoxigenin labeled RNA Probes: facts and artifacts." Biotechniques 18(2): 300-7

Vascular leakage in chick embryos after expression of a secreted binding protein for fibroblast growth factors.

Kevin McDonnell, Rafael Cabal-Manzano, Becky Hoxter, Emma T. Bowden

Anna T. Riegel, and Anton Wellstein*

Lombardi Cancer Center, Georgetown University, 3970 Reservoir Road

Washington, DC 20057, USA

*Correspondence should be addressed to A.W. (wellstea@georgetown.edu)

Phone: (202) 687-3672

Fax: (202) 687-4821

Keywords: chicken embryo, transgene, FGF, FGF-Binding Protein, vasculature

Abstract

Fibroblast growth factors (FGFs) have been implicated in a variety of physiologic and pathologic processes from embryonic development to tumor growth and angiogenesis. FGFs are immobilized in the extracellular matrix of different tissues and require release from this storage site to trigger a response. Secreted FGF-binding proteins (FGF-BPs) can release immobilized FGFs, enhance the activity of locally stored FGFs and can serve as an angiogenic switch molecule in cancer. Here we report the impact of expression of FGF-BP in a novel transgenic model, that allows continuous monitoring of effects in live chicken embryos. Microinjection of liposome-encapsulated plasmid expression vectors into the allantoic sac produces high levels of sustained gene expression. Expression of FGF-BP induces vascular permeability, hemorrhage and embryonic lethality. Light and electron microscopic studies suggest that this hemorrhage results from compromised microvascular structure. This model is a powerful tool in the real-time monitoring of transgene effects during embryogenesis.

THE JOURNAL OF BIOLOGICAL CHEMISTRY
Vol. 276, No. 43, Issue of October 26, pp. 40247–40253, 2001
Printed in U.S.A.

Enhancement of Fibroblast Growth Factor (FGF) Activity by an FGF-binding Protein*

Received for publication, May 30, 2001, and in revised form, July 29, 2001
Published, JBC Papers in Press, August 16, 2001, DOI 10.1074/jbc.M104933200

Elena Tassi‡§, Ali Al-Attar‡§, Achim Aigner‡¶, Matthew R. Swift‡, Kevin McDonnell‡, Alex Karavanov‖, and Anton Wellstein‡**

From the ‡Lombardi Cancer Center, Georgetown University, Washington, D.C. 20007 and ‖Ciphergen Biosystems, Palo Alto, California 94306

Fibroblast growth factor-binding protein (FGF-BP) 1 is a secreted protein that can bind fibroblast growth factors (FGFs) 1 and 2. These FGFs are typically stored on heparan sulfate proteoglycans in the extracellular matrix in an inactive form, and it has been proposed that FGF-BP1 functions as a chaperone molecule that can mobilize locally stored FGF and present the growth factor to its tyrosine kinase receptor. FGF-BP1 is up-regulated in squamous cell, colon, and breast cancers and can act as an angiogenic switch during malignant progression of epithelial cells. For the present studies, we focused on FGF-1 and -2 and investigated interactions with recombinant human FGF-BP1 protein as well as effects on signal transduction, cell proliferation, and angiogenesis. We show that recombinant FGF-BP1 specifically binds FGF-2 and that this binding is inhibited by FGF-1, heparan sulfate, and heparinoids. Furthermore, FGF-BP1 enhances FGF-1- and FGF-2-dependent proliferation of NIH-3T3 fibroblasts and FGF-2-induced extracellular signal-regulated kinase 2 phosphorylation. Finally, in the chicken chorioallantoic membrane angiogenesis assay, FGF-BP1 synergizes with exogenously added FGF-2. We conclude that FGF-BP1 binds directly to FGF-1 and FGF-2 and positively modulates the biological activities of these growth factors.

Fibroblast growth factors (FGFs)[1] represent a family of over 20 distinct proteins that are widely expressed in various tissues. FGFs have been reported to be involved in both development and adult tissue homeostasis, as well as in angiogenesis and cancer progression. FGF-2 (basic FGF), a 16–18-kDa protein, is one of the best-studied members of this family and has been shown to have a variety of biological effects in different cells and organ systems, including embryonic development, tumorigenesis, and angiogenesis (for a review, see Refs. 1 and 2).

FGF-2 interacts with low affinity cell surface and extracellular matrix heparan sulfate proteoglycans, which enable the growth factor to bind and activate its high affinity tyrosine kinase receptors (FGFRs), thereby forming a trimolecular active complex (3–6). It has been reported that cell surface heparan sulfate proteoglycans can modulate the action of FGF-2 by increasing its affinity for FGFRs (7). Moreover, heparan sulfate proteoglycans seem to protect FGF-2 from degradation by proteases in the extracellular environment (8, 9) and modulate the bioavailability of FGF-2, generating a local reservoir for the growth factor (10). The binding of FGF-2 to the cell surface receptor induces receptor tyrosine kinase dimerization and autophosphorylation (11). The phosphorylated FGFRs associate and subsequently activate SH2 domain-containing downstream signaling molecules, such as phospholipase Cγ (12, 13) and Src (14, 15). Moreover, upon ligand-dependent receptor autophosphorylation, adaptor proteins, such as Grb2 and Shc, link the FGFRs to the Ras/MAPK signaling cascade (16–18). Grb2 and Shc form a complex with the GDP/GTP exchange factor Son of Sevenless (Sos), which results in the translocation of Ras to the plasma membrane and its further activation by the exchange of GDP for GTP by Sos. Thus, activated Ras leads to the consecutive activation of a cascade of protein kinases involving Raf, MAPK/extracellular signal-regulated kinase kinase, and $p42/44^{MAPK}$, also known as extracellular signal-regulated kinase (ERK) 1 and 2 (16, 18).

FGF-2 lacks the classic leader sequence, which targets intracellular proteins for secretion to the extracellular environment, and several reports indicate that FGF-2 secretion occurs via endoplasmic reticulum- and Golgi-independent passive processes (19–21). In addition to the requirement for extracellular secretion, FGF-2 needs to be released and solubilized from the extracellular matrix (ECM) to act on its receptor. In comparison to other members of the FGF family, FGF-2 is tightly bound to the ECM and is a relatively abundant protein in numerous adult tissues, from which it can be extracted as a biologically active growth factor (22). In addition to FGF-2, several other less abundant members of this growth factor family are also stored in the ECM, although they have a lower affinity for glycosaminoglycans and are released more easily. Two distinct mechanisms by which locally stored FGF-2 can be released from the ECM have been described. One mechanism involves digestion of the sugar backbone in heparan sulfate proteoglycans by heparinases or other glycosaminoglycan-de-

* Supported by American Cancer Society Grant CB-202 (to A. W.), National Institutes of Health Grant CA71508 from the National Cancer Institute, Bethesda, Maryland (to A. W.), a grant from the US Army Medical Research Materiel Command Breast Cancer Program (to A. W. and A. A.-A.), and a grant from the Studienstiftung des Deutschen Volkes (to A. A.). The costs of publication of this article were defrayed in part by the payment of page charges. This article must therefore be hereby marked "*advertisement*" in accordance with 18 U.S.C. Section 1734 solely to indicate this fact.

The nucleotide sequence(s) reported in this paper has been submitted to the GenBank™/EBI Data Bank with accession number(s) M60047.

§ Both authors contributed equally to this work.

¶ Present address: Institute of Pharmacology, University of Marburg, 35035-Marburg, Germany.

** To whom correspondence should be addressed: Lombardi Cancer Center, Research Bldg. E311, Georgetown University; 3970 Reservoir Rd. NW, Washington, D.C. 20007. Tel.: 202-687-3672; Fax: 202-687-4821; E-mail: wellstea@georgetown.edu.

[1] The abbreviations used are: FGF, fibroblast growth factor; FGFR, FGF receptor; FGF-BP, FGF-binding protein; ERK, extracellular signal-regulated kinase; CAM, chorioallantoic membrane; MAPK, mitogen-activated protein kinase; ECM, extracellular matrix; TBS, Tris-buffered saline (50 mM Tris-HCl and 150 mM NaCl, pH 7.5); GST, glutathione *S*-transferase; SDS-PAGE, SDS-polyacrylamide gel electrophoresis.

grading enzymes (23–25). Binding of FGF-2 to an extracellular chaperone protein represents a separate mechanism for FGF-2 release and solubilization from the ECM. Studies from our laboratory have previously shown that the binding of FGF-2 to a secreted binding protein (FGF-BP) might represent such a mechanism (26, 27). Wu *et al.* (28) initially described FGF-BP as a low affinity heparin-binding protein isolated from human epidermoid carcinoma A431 cells. FGF-BP has been shown to bind to FGF-1 and -2 in a noncovalent, reversible manner. Moreover, FGF-BP protects and presents FGF-2 to its high affinity cell surface receptor (26, 27, 29), and a recent study (30) demonstrates the interaction of FGF-BP with perlecan, a heparan sulfate proteoglycan in the basement membrane. This most likely represents a local reservoir for FGF-BP. A related protein designated FGF-BP2 has recently been identified by our laboratory (2), and we will thus refer to the original protein as FGF-BP1.

FGF-BP1 is expressed below the level of detection by Northern blotting in normal adult human tissues, whereas its expression is significantly elevated in various tumors, including head and neck, skin, cervical, and lung squamous cell carcinomas (26, 30). In addition, FGF-BP1 is up-regulated in some colon cancers and breast adenocarcinomas (27). Furthermore, we have recently shown that phorbol esters as well as epidermal growth factor can up-regulate FGF-BP1 gene transcription (31–33). We reported previously (26) that expression of human FGF-BP1 cDNA in the FGF-2-positive SW-13 cells led these cells to grow anchorage independently. Likewise, whereas wild type SW-13 cells did not form tumors in nude mice, FGF-BP1-overexpressing SW-13 cells grew into highly vascularized tumors. Finally, we showed previously that the depletion of FGF-BP1 from squamous cell carcinoma and colon adenocarcinoma cell lines by ribozyme targeting resulted in a significant reduction of tumor growth and angiogenesis. In summary, these regulation, expression, and depletion experiments support a role for FGF-BP1 as a proangiogenic molecule in human tumors (27).

In the present study, we used recombinant FGF-BP1 protein to directly evaluate its binding to FGF-1 and -2 *in vitro* and study the functions of the protein. We found that FGF-BP1 was able to bind ^{125}I-FGF-2 in a dose-dependent and specific manner and can be competed by FGF-1 and FGF-2 as well as by different heparinoids. Furthermore, we studied the role of FGF-BP1 on the activation of the Ras/MAPK signaling pathway and on the mitogenic response of FGF-1- and FGF-2-treated NIH-3T3 fibroblasts. We demonstrate that FGF-2-induced ERK2 phosphorylation and proliferation were enhanced by the addition of FGF-BP1. Finally, in chorioallantoic membrane (CAM) assays, we found a significant FGF-BP1-dependent increase of FGF-2-mediated angiogenesis. Thus, our results indicate that the FGF-BP1 protein positively modulates the biochemical and biological activity of FGF-2 in multiple models.

MATERIALS AND METHODS

Cell Cultures—NIH-3T3 cells were maintained in Dulbecco's modified Eagle's medium (Life Technologies Inc.) supplemented with 10% (v/v) calf serum. Sf-9 cells (BD PharMingen, San Diego, CA) were cultured in EX-Cell 400 media (JRH Bioscience, Lenexa, KS) supplemented with 5% (v/v) fetal calf serum in a humidified incubator at 27 °C in the absence of CO_2.

Recombinant Histidine-tagged FGF-BP1 Protein Purification—The His-tagged FGF-BP1 protein was produced by infecting Sf-9 cells with a baculovirus vector that contains an expression cassette for human FGF-BP1 (BAC-TO-BAC Baculovirus Expression System; Life Technologies Inc.). The baculovirus construct contains nucleotides 197–799 of the human FGF-BP1 cDNA, flanked bilaterally by cDNAs encoding six histidine residues. The FGF-BP1 cDNA fragment was inserted into pFASTBAC HTb donor plasmid, which was then transformed into bacmid-containing DH10BAC competent cells. LacZ-negative clones containing the recombinant bacmid were identified. The bacmid DNA was isolated and then transfected into Sf-9 cells to generate baculovirus. Infected Sf-9 cells were grown for 5 days, pelleted, and lysed in a buffer containing 6 M guanidine-HCl, 0.01 M Tris-HCl, and 0.1 M sodium phosphate, pH 8.0. Cell lysates were homogenized and then incubated for 1 h on ice. Cellular debris was removed by centrifugation at 10,000 × *g* for 15 min. Supernatant was loaded onto a Ni-NTA-Sepharose column (Qiagen, Hilden, Germany). The column was sequentially washed with buffers containing 30 mM sodium citrate, 300 mM NaCl, and decreasing pH values of 8, 6.3, 5.9, and 5.7, respectively. His-tagged FGF-BP1 was then eluted with three aliquots of 0.5 ml of the buffer at pH 4.5. Eluates were neutralized immediately and stored at 4 °C.

Silver Staining and Western Blot Analysis—30 μl of recombinant FGF-BP1 were resuspended with 5× Laemmli's buffer, boiled at 95 °C for 5 min, and separated by electrophoresis on a 4–20% gradient polyacrylamide gel. The protein was then detected by silver staining and after immunoblotting. Silver staining was performed as suggested by the manufacturer (Bio-Rad). The His-tagged protein was detected with a rabbit polyclonal anti-FGF-BP1 (27) or a mouse monoclonal anti-His antibody (Invitrogen Corp., Carlsbad, CA) that was then visualized by enhanced chemiluminescence detection using horseradish peroxidase-linked donkey anti-rabbit or anti-mouse immunoglobulin G as the secondary antibodies, respectively (Amersham Pharmacia Biotech).

Phosphorylation Studies—50% confluent NIH-3T3 cells were serum-deprived overnight and treated for 5 min with 2 and 10 ng/ml FGF-2 (Invitrogen Corp.) and recombinant FGF-BP1. Controls were left untreated. Cells were then washed with cold phosphate-buffered saline, pH 7.4, and subsequently lysed at 4 °C in a buffer containing 50 mM Tris-HCl, pH 8, 150 mM NaCl, 40 mM β-glycerophosphate, 1 mM EGTA, 0.25% sodium deoxycholate, 1% Nonidet P-40, 50 mM sodium fluoride, 20 mM sodium pyrophosphate, 1 mM sodium orthovanadate, 2 μg/ml leupeptin, 2 μg/ml aprotinin, 1 μg/ml pepstatin, and 100 μg/ml pefabloc. Cellular debris was removed by centrifugation at 14,000 rpm for 15 min. Phosphorylated proteins were immunoprecipitated from the cleared lysates by incubation with agarose-conjugated anti-phosphotyrosine (4G10; Upstate Biotechnology, Lake Placid, NY) monoclonal antibody for 2 h at 4 °C. Immunocomplexes were recovered by centrifugation and washed five times with cold lysis buffer. Samples were then resuspended with 15 μl of 2× Laemmli's buffer and boiled for 5 min at 95 °C. Alternatively, 10–50 μg of total protein cell extracts were resuspended with 5× Laemmli's buffer and heated for 5 min at 95 °C. Both immunoprecipitates and total cell lysates were separated on 10% SDS-polyacrylamide gels, transferred onto polyvinylidene difluoride membranes, and analyzed by immunoblot analysis. Tyrosine-phosphorylated proteins and ERK2 were detected with the corresponding mouse monoclonal antibody and then visualized by enhanced chemiluminescence detection using horseradish peroxidase-linked goat anti-mouse antibody (Amersham Pharmacia Biotech), respectively. Monoclonal anti-pan ERK antibody was purchased from BD Transduction Laboratories (Lexington, KY).

FGF/FGF-BP1 Binding Assays—100 ng/ml His-BP1 (a bilaterally hexahistidine-tagged FGF-BP1 protein) diluted in Tris-buffered saline (TBS) was incubated overnight in 96-well plates (EIA/RIA Strip Plate; Corning Inc., Corning, NY) at 4 °C with constant rocking. Excess unbound His-BP1 was removed by washing the wells twice with TBS. Nonspecific binding was blocked by the addition of 300 μl of LB medium (Bio 101, Carlsbad, CA) to the wells for 1 h at room temperature. Wells were then washed five times with TBS. ^{125}I-FGF-2 (1–20 ng/ml) was added to the wells and incubated for 2 h at room temperature with constant rocking. Unbound ^{125}I-FGF-2 was removed by washing the wells five times with TBS containing 2% Tween 20. In the competition assays, different amounts of FGF-1, FGF-2, His-BP1, pentosanpolysulfate (bene Chemie, Munich, Germany), and heparin or heparan sulfate (Sigma) were simultaneously added with ^{125}I-FGF-2. Binding of radiolabeled FGF-2 to His-BP1 was measured by counting the radioactive emission from the individual wells. ^{125}I-FGF-2 was purchased from Amersham Pharmacia Biotech. Human recombinant FGF-1 and FGF-2 were purchased from Life Technologies, Inc.

Protein-protein Interaction Studies on Protein Arrays (Protein Chip Assay)—The analysis was performed with a surface-enhanced laser desorption/ionization (34) (Protein Biology System I; Ciphergen, Palo Alto, CA). The different FGF-BP1-containing preparations (1 μl of a 20 mg/ml solution) were placed on a normal-phase protein array, which was then washed, and 1 μl of a-cyano-4-hydroxy cinnamic acid (2 mg/ml) in 50% (v/v) acetonitrile and 0.5% (w/v) trifluoroacetic acid was added to the spot. The retained proteins were then subjected to mass spectrometry. For the analysis of the interaction of FGF-BP1 with

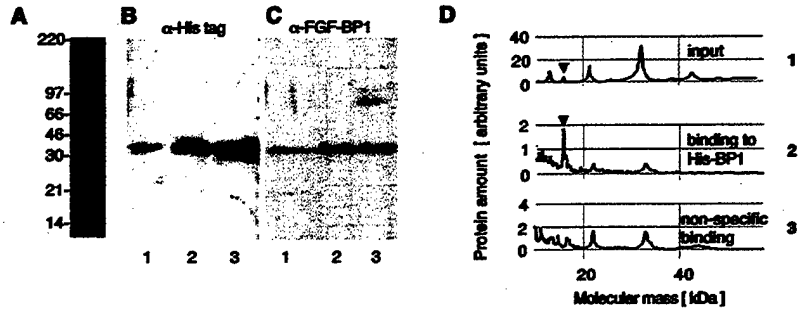

FIG. 1. **Silver stain, Western blots, and binding of FGF-2 to the recombinant His-BP1 protein.** *A*, silver stain of 30 μl of a pooled, chelate affinity-purified His-BP1 preparation separated by a 4–20% gradient SDS-PAGE. *B* and *C*, Western blots of 30-μl aliquots from consecutive affinity chromatography fractions loaded onto 4–20% SDS-PAGE. A blot with anti-His tag (*B*) and anti-BP1 (*C*) antibodies is shown. *D*, protein chip analysis using surface-enhanced laser desorption/ionization to assess FGF-2 binding to immobilized His-BP1. Mass spectrometry analysis of proteins is shown. *1*, input FGF-2 ligand preparation (FGF-2 spiked into cell growth media with 10% fetal calf serum). *2* and *3*, proteins present in the input preparation that bound to immobilized His-BP1 (*2*) or to background (*3*), respectively. The *arrowheads* indicate the peak corresponding to the FGF-2 protein used as a ligand.

FGF-2, 3 μl of a 240 mg/ml solution of FGF-BP1 in phosphate-buffered saline were applied to a preactivated protein array, which was then incubated overnight in a humidified chamber at 4 °C. The protein solution was removed, 3 ml of 1 M ethanolamine (pH 8.2) were added to each spot, and the array was incubated for an additional 30 min at room temperature. For further details, see Ref. 35.

Proliferation Assay—5 × 10^3 NIH-3T3 fibroblasts were seeded in three replicates in 96-well plates for 8 h. Cells were serum-deprived for 16 h and then treated with human recombinant FGF-1 (10 ng/ml), FGF-2 (5 ng/ml), anti-FGF-2 (15 μg/ml), and His-BP1 (6 ng/ml), unless indicated otherwise. The proliferation rate was evaluated after 48 h by the addition of 10 μl/well WST-1 reagent, as suggested by the manufacturer (Roche Molecular Biochemicals). Rabbit polyclonal anti-FGF-2 was purchased from R&D Systems (Minneapolis, MN).

CAM Assay—The CAM assay was carried out as described previously (36). In brief, 2-day-old fertilized chicken eggs were broken open into 35 × 10-mm Petri dishes and incubated at 37 °C for 48 h. Sterile Whatmann filter disks (8 mm in diameter) were prewetted in TBS solution and placed peripherally on the CAM of viable embryos, in between adjacent visible blood vessels. FGF-2 and His-BP1 were placed on the disks as indicated. CAMs were photographed using a digital camera at 0, 12, 24, and 36 h after disk placement. The degree of angiogenesis around each disk was measured using a score from 1 (minimal angiogenesis) to 4 (maximal angiogenesis, with directional growth of new vasculature toward the disk). Scoring was carried out blinded, and the results were averaged. Baseline (no treatment) was subtracted from the average score as indicated.

Statistics and Data Analysis—Graphpad/Prism Software (San Diego, CA) was used for statistical analysis as well as curve fitting to obtain half-maximal inhibitory concentrations (IC_{50}) from binding studies. From this, K_d values for FGF-2 were derived by using the Cheng-Prusoff equation ($K_d = IC_{50}/(1 + L/K_d)$), (37) where L is the concentration of the FGF-2 radioligand, and IC_{50} is the half-maximal inhibitory concentration calculated from the competition isotherm of the unlabeled FGF-2.

RESULTS

Generation of Recombinant FGF-BP1 Protein—In previous studies, we investigated the effects of FGF-BP1 by overexpression experiments in FGF-BP1-negative cells or by depletion of endogenous FGF-BP1 from cells using ribozyme targeting (26, 27, 29). Because FGF-BP1 is secreted from cells and acts as an extracellular chaperone, we sought to examine the biological effects of a human recombinant FGF-BP1 when added to the extracellular milieu. For this purpose, two recombinant human FGF-BP1 proteins were produced *in vitro*. A bilaterally hexahistidine-tagged FGF-BP1 protein (His-BP1) was purified from Sf-9 insect cells infected with a baculovirus construct containing nucleotides 197–799 of human FGF-BP1 cDNA (GenBank™ accession number M60047). This protein was used for the functional assays, and its purification is shown in Fig. 1. In addition a glutathione *S*-transferase (GST)-tagged FGF-BP1 designated GST-BP1 was generated in BL21 bacteria using a pGEX-2TK construct that contains the same nucleotides (data not shown). This protein was used to generate antibodies and used in some of the initial protein-protein interaction studies (see below). To determine whether the protein generated in the Sf-9 cells did indeed represent FGF-BP1, serial elutions obtained from the final affinity chromatography were separated by SDS-PAGE, and a single protein was detected by silver staining and Western blotting with anti-BP1 as well as anti-histidine tag antibodies (Fig. 1, *A–C*). The BP1 protein ran at 34 kDa apparent molecular mass, and the silver staining of a pooled sample shows that the purity of the preparation is >90% (Fig. 1*A*). The electrophoretic mobility of the His-BP1 protein is slower than that predicted by its molecular mass (26.9 kDa), most likely due to its basic nature, a feature also reported for the bovine BP1 protein (see Ref. 38).

FGF Binding to FGF-BP1 in Cell-free Assays—We first asked whether the recombinant His-BP1 will specifically recognize FGF-2 when the FGF-2 ligand is present at low abundance in a diverse mixture of molecules comprising fetal calf serum. To address this question, we used surface-enhanced laser desorption/ionization protein chip technology coupled with mass spectrometry (34) (see Fig. 1*D*). This approach was previously applied by us to characterize ligand-receptor interaction when studying pleiotrophin and its receptor, anaplastic lymphoma kinase (35). In the present experimental series, the His-BP1 protein was immobilized on a protein chip and incubated with FGF-2 that had been mixed with growth media containing 10% fetal calf serum. FGF-2 comprised only a very small portion of the overall preparation used as the input (*arrowhead* in Fig. 1*D*, *1*, *input*). However, FGF-2 was specifically recognized by the immobilized His-BP1 in this mixture (*arrowhead* in Fig. 1*D*, *2*), and only nonspecific binding was observed without the immobilized His-BP1 (Fig. 1*D*, *3*). From this, we conclude that FGF-2 does indeed bind specifically to His-BP1, even when the growth factor is only present at very low abundance in a complex mixture of proteins and other molecules, and that no other ligand for His-BP1 is present in fetal calf serum.

We next sought to quantitate FGF binding to the His-BP1 recombinant protein. For this, a cell-free 96-well binding assay was established using immobilized His-BP1 as a bait and ^{125}I-FGF-2 as a ligand. As shown in Fig. 2*A*, His-BP1 (*bottom panel*) and GST-BP1 (*top panel*) bound to the radiolabeled FGF-2 in a dose-dependent manner. The bacterial GST-BP1 displayed less specific and more nonspecific binding to ^{125}I-FGF-2 per unit of protein in comparison with the eukaryotic His-BP1, and we thus decided to use the latter as the major tool for our additional studies. To support the specificity of His-BP1 binding to the FGF-2 radioligand, competition assays were performed with excess cold FGF-2, FGF-1, or His-BP1 as well as epider-

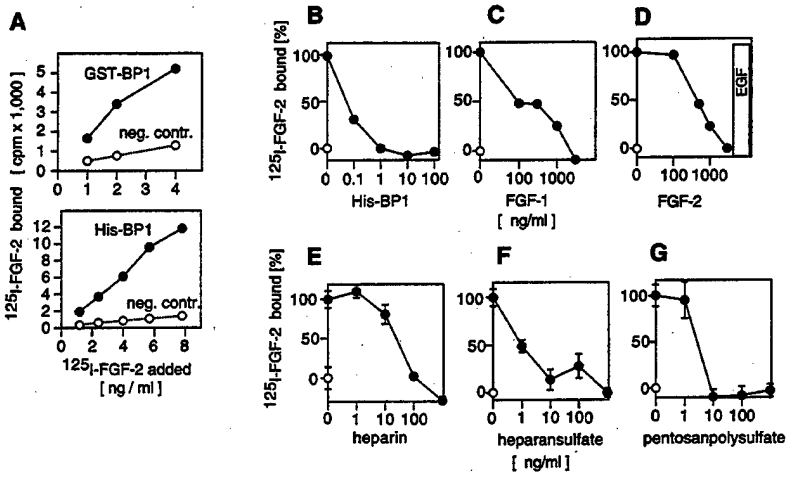

FIG. 2. **Binding of FGF-2 to His-BP1 and competition by different agents.** *A*, binding of different concentrations of ^{125}I-FGF-2 to GST-BP1 (*top panel*) and His-BP1 (*bottom panel*) immobilized in 96-well plates. *B–G*, competition of His-BP1, FGF-1, FGF-2, heparin, heparan sulfate, and pentosanpolysulfate for ^{125}I-FGF-2 binding to immobilized His-BP1. ^{125}I-FGF-2 binding obtained from wells containing immobilized His-BP1 (●; 100%) in comparison to blocking solution only (○; 0%) is shown. The data are representative of at least four independent experiments, in which each sample was run in triplicate.

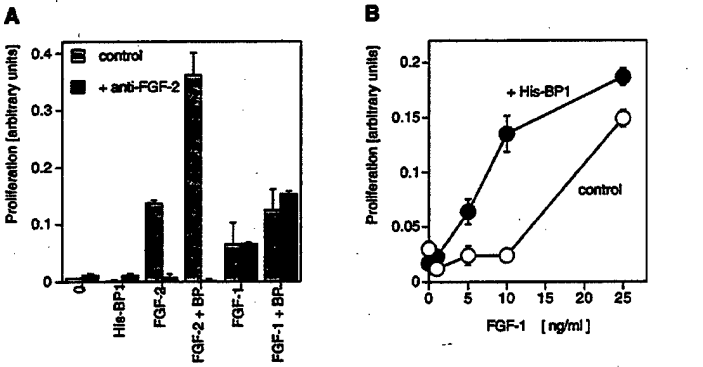

FIG. 3. **Effect of His-BP1 on FGF-1- and FGF-2-mediated mitogenesis in NIH-3T3 fibroblasts.** *A*, cells were treated for 48 h with FGF-1 (10 ng/ml) or FGF-2 (5 ng/ml) ± His-BP1 (6 ng/ml) in the absence (▨) or presence (■) of anti-FGF-2 antibody. *B*, concentration-response curve of FGF-1 in the absence (○) or presence of His-BP1 (●). The proliferation rate was measured as described under "Materials and Methods," and the data shown are representative of three independent experiments.

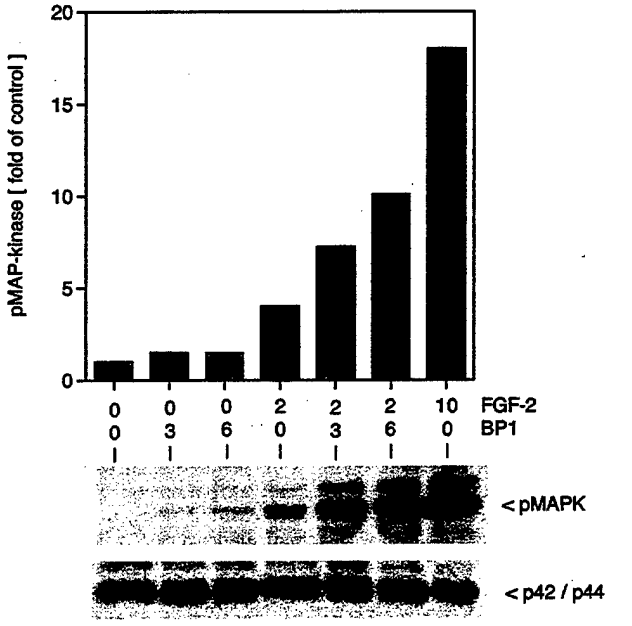

FIG. 4. **Effect of His-BP1 on FGF-2-induced ERK2 activation in NIH-3T3 fibroblasts.** Cells were starved overnight and treated for 5 min with different concentrations of FGF-2 and/or His-BP1, as indicated (ng/ml). Controls were left untreated. 50 μg of total cell lysates were separated by 10% SDS-PAGE, transferred onto polyvinylidene difluoride membranes, and immunoblotted with anti-phosphotyrosine monoclonal antibody (*pMAPK*). Detection of endogenous ERK2 in the protein extracts was determined by Western blot analysis, using anti-pan ERK monoclonal antibodies (*p42/44*). Quantitation of bands was obtained by densitometry and is expressed relative to control (*bar graph*).

mal growth factor as a nonspecific growth factor control. As shown in Fig. 2*B*, increasing concentrations of His-BP1 were able to inhibit the binding of ^{125}I-FGF-2 to the immobilized His-BP1, and an ~10-fold excess of the His-BP1 in solution completely inhibited FGF-2 binding. FGF-2 also competed for FGF-2 radioligand binding (Fig. 2*D*). From a series of such competition assays, we calculated an apparent dissociation constant (K_d) value of ~10 nM for FGF-2 binding to His-BP1 (for details, see "Materials and Methods"). Furthermore, in support of the original report on FGF-BP1 by Wu *et al.* (28), we found that FGF-1 also competed with FGF-2 for its binding to His-BP1 (Fig. 2*C*). Epidermal growth factor was used as a negative control and did not did not inhibit FGF-2 binding to the immobilized His-BP1 even at 10 μg/ml (*bar* in Fig. 2*D*), supporting a specific interaction of FGF-BP1 and FGF-2.

Earlier studies from our laboratory have shown that FGF-BP1 lowers the affinity of heparin for FGF-2 (29) in support of the notion that FGF-BP can release FGF-2 from its local storage on glycosaminoglycans in the extracellular matrix (27). Conversely, based on this mechanism of action of FGF-BP1, we speculated that glycosaminoglycans in solutions should be able to disrupt binding of FGF-2 to FGF-BP. We thus studied the effects of heparin, heparan sulfate, and pentosanpolysulfate on the binding of FGF-2 to His-BP1 (Fig. 2, *E–G*). The extracellular matrix glycosaminoglycan heparan sulfate inhibited binding of FGF-2 to the immobilized His-BP1 at very low concentrations (IC_{50} = 1 ng/ml), and the semisynthetic heparinoid pentosanpolysulfate (39–41) and the anticoagulant heparin were somewhat less potent (IC_{50} = 3 and 30 ng/ml). All of these heparinoids completely inhibited binding of FGF-2 to the immobilized His-BP1, and we propose from these data that the heparin-binding domain in FGF-2 overlaps with the binding domain that interacts with FGF-BP. Also, this mutually exclusive binding of FGF-2 to FGF-BP or to a glycosaminoglycan supports the notion of FGF-BP as an extracellular chaperone molecule that releases locally stored FGFs (26, 27, 30, 42).

FGF-BP1 Enhances FGF-induced Proliferation in NIH-3T3 Fibroblasts—After we demonstrated the ability of the recombinant human FGF-BP1 to specifically bind FGF-1 and -2 in a cell-free system, we sought to determine the effect of this interaction on biological activity *in vitro*. FGF-1 and -2 are potent mitogens for a number of cell lines, including fibroblasts and

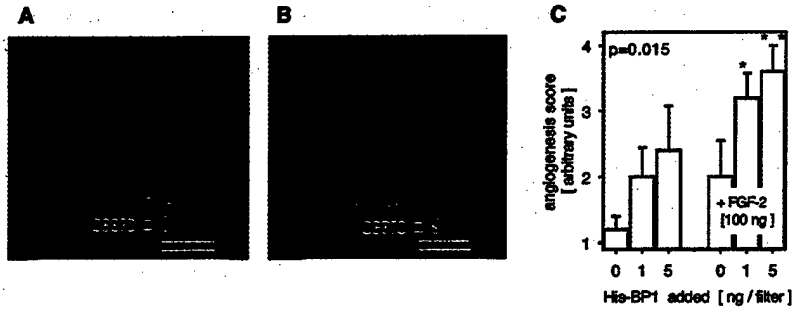

FIG. 5. **Effect of His-BP1 on FGF-2-induced angiogenesis in the CAM assay.** Filter disks with FGF-2 (100 ng) ± His-BP1 (as indicated) were placed on CAMs of 4-day-old chicken embryos. *A* and *B*, photograph of angiogenesis on the CAMs scored as 1 (*A*) and 3 (*B*) at 24 h. *Bar*, 1 mm. *C*, quantitation of the assays; $p = 0.015$ is the overall p value from analysis of variance. *, $p < 0.05$; **, $p < 0.01$ (comparison relative to the respective control sample).

endothelial cells (17), and we used NIH-3T3 fibroblasts as an experimental model system to study the effect of His-BP1 on FGF-induced proliferation (Fig. 3). To control the effectiveness of FGF-2 mitogenic action, we first assessed the ability of the growth factor to induce cell proliferation. NIH-3T3 cells were serum-deprived overnight and grown for 48 h in the presence or absence of different concentrations of FGF-2 to establish a dose-response curve (data not shown). We then stimulated the cells with a submaximally effective concentration of FGF-2 (5 ng/ml) and added His-BP1 (6 ng/ml) (Fig. 3*A*). Whereas no proliferation was detected when cells were grown in the presence of His-BP1 alone, the addition of FGF-2 enhanced the mitogenic activity of the growth factor. To rule out the possibility that interaction of His-BP1 with a mitogenic factor other than FGF-2 was responsible for the His-BP1-mediated effect, we included an FGF-2-specific antibody. The anti-FGF-2 antibody blocked the FGF-2-dependent cell growth and completely inhibited the synergistic effect of His-BP1 and FGF-2. As a control, the anti-FGF-2 antibody failed to reduce FGF-1-dependent cell growth as well as the synergistic effects between His-BP1 and FGF-1. As for FGF-2, a concentration-response curve for FGF-1 showed that His-BP1 enhances the effects of low concentrations of FGF-1 ($p < 0.01$; analysis of variance) and does not increase the maximal effect of the growth factor (Fig. 3*B*). Taken together, these results establish that the synergistic interaction between His-BP1 and FGF-1- or FGF-2-stimulated NIH-3T3 mitogenesis is specific and dependent on the presence of the respective growth factor.

FGF-BP1 Positively Modulates FGF-2-induced ERK2 Activation in a Dose-dependent Fashion—ERK2 plays an important role in transducing proliferative signals from receptor tyrosine kinases (18). In particular, engagement of FGFRs by their extracellular ligands, such as FGF-1 and FGF-2, has been extensively reported to induce activation of the Ras/ERK2 cascade (16, 43). Consistent with these observations and in light of our results, we next decided to examine the early signaling events elicited by the specific interaction between FGF-2 and His-BP1 (Fig. 4). Interestingly, we found that FGF-2-dependent ERK2 activation, as determined by immunoblot analysis with an anti-phosphotyrosine antibody, was significantly enhanced in NIH-3T3 fibroblasts when cells were co-stimulated for 5 min with different concentrations of FGF-2 and His-BP1. In particular, 3 and 6 ng/ml His-BP added to FGF-2 (2 ng/ml) exhibited an enhancement of phosphorylation of 1.8- and 2.5-fold, respectively, when compared with the levels obtained with FGF-2 alone (Fig. 4, *bar graph*). The same results were obtained in immunoprecipitation studies (data not shown). In addition, as shown in the *bottom panel* of Fig. 4, the levels of expression of ERK2 were not affected by these treatments and, consistent with the phospho-MAPK blots, a mobility shift of the lower ERK2 band due to phosphorylation was obvious. From these findings, we conclude that FGF-2-dependent phosphorylation of ERK2 is synergistically modulated by His-BP1.

FGF-BP1 Enhances FGF-2-dependent Angiogenesis in Vivo—FGF-2 has been shown to be a powerful inducer of angiogenesis both *in vitro* and *in vivo* (2, 21, 44). As an experimental approach to investigate the effects of FGF-BP1 on FGF-2-mediated angiogenesis *in vivo*, we used the chick embryo CAM assay. As shown in Fig. 5, FGF-2 and His-BP1 induce an angiogenic response on their own. The baseline effect of FGF-BP1 on its own is likely due to locally stored FGFs from the chicken embryo. However, simultaneous stimulation with both FGF-2 and FGF-BP1 resulted in a significant enhancement of this response. These findings support the notion that FGF-BP1, by its cooperative interaction with FGF-2, is a positive regulator of FGF-2-mediated angiogenesis *in vivo*.

DISCUSSION

FGF-BP1 is a secreted protein that binds FGF-2 and is hypothesized to mobilize FGF-2 from its storage in the ECM (28). Previous studies have found that endogenous FGF-BP1 is overexpressed in several cancers (26, 27, 30). Additionally, depletion of FGF-BP1 mRNA has been shown to abrogate the angiogenesis-dependent growth of ME-180 squamous cell carcinoma and Ls174T colon cancer cells when implanted in athymic nude mice (27). Because endogenous FGF-BP1 plays a critical role in tumor growth and angiogenesis, we set out to explore the effects of exogenously added FGF-BP1 protein on FGF-dependent cellular responses.

For our experiments, we produced and purified human recombinant, polyhistidine-tagged FGF-BP1. This His-BP1 protein gave a single band after SDS-PAGE by silver staining as well as by immunoblotting, and recombinant His-BP1 binds radiolabeled FGF-2 *in vitro*. This binding is specific because it is competed by excess concentrations of cold FGF-1 and -2 or recombinant FGF-BP1 and not by an unrelated growth factor, epidermal growth factor. Heparinoids inhibit binding between FGF-2 and FGF-BP1 at low concentrations (nanograms/milliliter), and we conclude from this that binding of FGF-2 to heparinoids and to FGF-BP1 is mutually exclusive. This lends additional support to the role of FGF-BP1 as a chaperone that can shuttle FGFs from their glycosaminoglycan storage. The His-BP1 purified as a monomeric protein and chemical cross-linking studies of radiolabeled FGF-2 with His-BP1 suggested that these proteins bind at a 1:1 ratio.[2]

There have been conflicting reports with regard to whether FGF-BP1 binds FGF-1. In the original description of FGF-BP1, Wu *et al.* (28) found that FGF-BP1 purified from the media of A431 human epidermoid carcinoma cell cultures was also able to bind FGF-1. In contrast, Lametsch *et al.* (38) reported that FGF-BP1 purified from bovine prepartum mammary secretion binds FGF-2, but not FGF-1. Nevertheless, in our experiments, FGF-1 completely inhibited FGF-2 binding to the human recombinant FGF-BP1, thus demonstrating an interaction of FGF-1 with FGF-BP1. Furthermore, FGF-BP1 synergized with FGF-1 as well as with FGF-2 in the proliferation assays with

[2] A. Al-Attar and A. Wellstein, unpublished data.

NIH-3T3 cells (Fig. 3), and the effect of FGF-BP1 on both of these FGFs was indistinguishable.

The MAPK pathway has been studied extensively in the stimulation of quiescent cells with mitogenic factors and is generally considered to be responsible for the initiation of cellular growth. Of note, in different cellular systems, it has been shown that the specific interaction of FGF-2 with its receptor and the subsequent FGFR activation trigger a downstream signal cascade that culminates with the activation and phosphorylation of ERK2 (16). To investigate the role of recombinant exogenous FGF-BP1 on FGF-2-mediated early intracellular biological responses, phosphoprotein analysis was performed in NIH-3T3 murine fibroblasts. Consistent with previous findings that demonstrated the physical interaction of FGF-BP1 with FGF-2 (28), we now provide evidence that FGF-BP1 exerts positive and synergistic modulation of FGF-2-mediated signaling by enhancing the growth factor-dependent ERK2 phosphorylation. Interestingly, we show that at concentrations of FGF-2 not sufficient to elicit maximal ERK2 activation, FGF-BP1 significantly amplifies the FGF-2-mediated response in a dose-dependent manner. Sustained activation of the ERK2 signal transduction pathway often controls the stimulation of cell proliferation (45, 46), and ERK2 activation is required for proliferation of fibroblasts *in vitro* (43). In addition to ERK2, FGF-2-dependent mitogenic signal transduction pathways lead to the activation of phospholipase Cγ and p70S6K, respectively. However, it has been observed that phospholipase Cγ activation is likely not to be responsible for FGF-2-mediated NIH-3T3 mitogenesis, nor is the signal that emanates from p70S6K sufficient to induce cell proliferation (47–49). Indeed, coincident with the ERK2 activation, we found that the interaction of FGF-BP1 with FGF-2 also elicits a dramatic enhancement of FGF-2-mediated NIH-3T3 proliferation. This supports the notion of FGF-BP1 as a chaperone molecule that will serve as a positive modulator of FGF-2-dependent growth controlled by the ERK2 pathway.

FGF-2 is a potent angiogenic molecule, and previous studies have shown that it can induce neovascularization in the chicken embryo CAM assay. Here, we use this experimental model to address whether recombinant FGF-BP1 can act synergistically with FGF-2 to cause new and directed blood vessel growth. We found that the angiogenic response seen with the addition of both recombinant FGF-BP1 and FGF-2 was significantly greater than that seen with the addition of FGF-2 alone. Furthermore, FGF-BP1 treatment led to a more rapid establishment of directed blood vessel growth when added to FGF-2 (see Fig. 5*A, left versus right panel*). Interestingly, we found that FGF-BP1 added to the CAM, without exogenous FGF-2, was able to induce angiogenesis in a dose-dependent manner on its own; we speculate that this is due to endogenous FGFs present in the CAM. This finding is also consistent with an earlier report in which transfection of FGF-BP1 into a human adrenocortical carcinoma cell line (SW-13) induced the growth of highly vascularized tumors in athymic nude mice (26), and reduction of FGF-BP1 message in ME-180 cells reduced their angiogenic stimulus during tumor growth (27). In addition, all-*trans*-retinoic acid has been shown to down-regulate FGF-BP1 mRNA levels in tumors grown from the ME-180 cells and, coincident with that, the extent of tumor angiogenesis (50).

Binding proteins have been described for other cytokines, and the most relevant two binding protein families are those for insulin-like growth factor and transforming growth factor β. Latent transforming growth factor β-binding proteins and insulin-like growth factor-binding proteins have been shown to bind and protect their respective ligands from degradation and can positively or negatively modulate their ligands' functional activities (51, 52). Each of these binding proteins represents a family of multiple proteins, with homologous members found in different tissues and species. Similarly, human FGF-BP1 has homologues in chicken, zebrafish, cow, mouse, and rat (2, 28, 29, 38). Recently, we found a novel FGF-BP, designated FGF-BP2, that is also located on chromosome 4p16, in close proximity to FGF-BP1. The amino acid sequences of these two proteins contain eight cysteine residues that are conserved across different species and between the FGF-BP genes. This suggests identical disulfide bond formation and similar tertiary structure. It will be interesting to see to what extent the different FGF-BPs contribute to the diversity of activities by the more than 20 FGFs (2).

In conclusion, our studies suggest that FGF-BP1 represents an important regulatory factor that positively modulates FGF-mediated cellular responses, such as signaling, proliferation, and angiogenesis.

REFERENCES

1. Basilico, C., and Moscatelli, D. (1992) *Adv. Cancer Res.* **59,** 115–165
2. Powers, C. J., McLeskey, S. W., and Wellstein, A. (2000) *Endocr. Relat. Cancer* **7,** 165–197
3. Yayon, A., Klagsbrun, M., Esko, J. D., Leder, P., and Ornitz, D. M. (1991) *Cell* **64,** 841–848
4. Klagsbrun, M., and Baird, A. (1991) *Cell* **67,** 229–231
5. Rapraeger, A. C., Krufka, A., and Olwin, B. B. (1991) *Science* **252,** 1705–1708
6. Rapraeger, A. C., Guimond, S., Krufka, A., and Olwin, B. B. (1994) *Methods Enzymol.* **245,** 219–240
7. Roghani, M., Mansukhani, A., Dell'Era, P., Bellosta, P., Basilico, C., Rifkin, D. B., and Moscatelli, D. (1994) *J. Biol. Chem.* **269,** 3976–3984
8. Damon, D. H., Lobb, R. R., D'Amore, P. A., and Wagner, J. A. (1989) *J. Cell. Physiol.* **138,** 221–226
9. Sommer, A., and Rifkin, D. B. (1989) *J. Cell. Physiol.* **138,** 215–220
10. Rusnati, M., and Presta, M. (1996) *Int. J. Clin. Lab. Res.* **26,** 15–23
11. Klint, P., and Claesson-Welsh, L. (1999) *Front. Biosci.* **4,** D165–D177
12. Burgess, W. H., Dionne, C. A., Kaplow, J., Mudd, R., Friesel, R., Zilberstein, A., Schlessinger, J., and Jaye, M. (1990) *Mol. Cell. Biol.* **10,** 4770–4777
13. Mohammadi, M., Honegger, A. M., Rotin, D., Fischer, R., Bellot, F., Li, W., Dionne, C. A., Jaye, M., Rubinstein, M., and Schlessinger, J. (1991) *Mol. Cell. Biol.* **11,** 5068–5078
14. Zhan, X., Plourde, C., Hu, X., Friesel, R., and Maciag, T. (1994) *J. Biol. Chem.* **269,** 20221–20224
15. Landgren, E., Blume-Jensen, P., Courtneidge, S. A., and Claesson-Welsh, L. (1995) *Oncogene* **10,** 2027–2035
16. Lewis, T. S., Shapiro, P. S., and Ahn, N. G. (1998) *Adv. Cancer Res.* **74,** 49–139
17. Boilly, B., Vercoutter-Edouart, A. S., Hondermarck, H., Nurcombe, V., and Le Bourhis, X. (2000) *Cytokine Growth Factor Rev.* **11,** 295–302
18. Schlessinger, J. (2000) *Cell* **103,** 211–225
19. McNeil, P. L., Muthukrishnan, L., Warder, E., and D'Amore, P. A. (1989) *J. Cell Biol.* **109,** 811–822
20. Mignatti, P., Morimoto, T., and Rifkin, D. B. (1992) *J. Cell. Physiol.* **151,** 81–93
21. Bikfalvi, A., Klein, S., Pintucci, G., and Rifkin, D. B. (1997) *Endocr. Rev.* **18,** 26–45
22. Burgess, W. H., and Maciag, T. (1989) *Annu. Rev. Biochem.* **58,** 575–606
23. Bashkin, P., Doctrow, S., Klagsbrun, M., Svahn, C. M., Folkman, J., and Vlodavsky, I. (1989) *Biochemistry* **28,** 1737–1743
24. Saksela, O., and Rifkin, D. B. (1990) *J. Cell Biol.* **110,** 767–775
25. Buczek-Thomas, J. A., and Nugent, M. A. (1999) *J. Biol. Chem.* **274,** 25167–25172
26. Czubayko, F., Smith, R. V., Chung, H. C., and Wellstein, A. (1994) *J. Biol. Chem.* **269,** 28243–28248
27. Czubayko, F., Liaudet-Coopman, E. D., Aigner, A., Tuveson, A. T., Berchem, G. J., and Wellstein, A. (1997) *Nat. Med.* **3,** 1137–1140
28. Wu, D. Q., Kan, M. K., Sato, G. H., Okamoto, T., and Sato, J. D. (1991) *J. Biol. Chem.* **266,** 16778–16785
29. Kurtz, A., Wang, H. L., Darwiche, N., Harris, V., and Wellstein, A. (1997) *Oncogene* **14,** 2671–2681
30. Mongiat, M., Otto, J., Oldershaw, R., Ferrer, F., Sato, J. D., and Iozzo, R. V. (2001) *J. Biol. Chem.* **276,** 10263–10271
31. Harris, V. K., Liaudet-Coopman, E. D., Boyle, B. J., Wellstein, A., and Riegel, A. T. (1998) *J. Biol. Chem.* **273,** 19130–19139
32. Harris, V. K., Coticchia, C. M., List, H. J., Wellstein, A., and Riegel, A. T. (2000) *J. Biol. Chem.* **275,** 39801
33. Harris, V. K., Coticchia, C. M., Kagan, B. L., Ahmad, S., Wellstein, A., and Riegel, A. T. (2000) *J. Biol. Chem.* **275,** 10802–10811
34. Dove, A. (1999) *Bio/Technology* **17,** 233–236
35. Stoica, G. E., Kuo, A., Aigner, A., Sunitha, I., Souttou, B., Malerczyk, D., Caughey, D. J., Wen, D., Karavanov, A., Riegel, A. T., and Wellstein, A. (2001) *J. Biol. Chem.* **276,** 16772–16779
36. Auerbach, R., Kubai, L., Knighton, D., and Folkman, J. (1974) *Dev. Biol.* **41,** 391–394
37. Cheng, Y., and Prusoff, W. H. (1973) *Biochem. Pharmacol.* **22,** 3099–3108
38. Lametsch, R., Rasmussen, J. T., Johnsen, L. B., Purup, S., Sejrsen, K., Petersen, T. E., and Heegaard, C. W. (2000) *J. Biol. Chem.* **275,** 19469–19474

39. Wellstein, A., Zugmaier, G., Califano, J. A., III, Kern, F., Paik, S., and Lippman, M. E. (1991) *J. Natl. Cancer Inst.* **83,** 716–720
40. Zugmaier, G., Lippman, M. E., and Wellstein, A. (1992) *J. Natl. Cancer Inst.* **84,** 1716–1724
41. Wellstein, A., and Czubayko, F. (1996) *Breast Cancer Res. Treat.* **38,** 109–119
42. Liu, X. H., Aigner, A., Wellstein, A., and Ray, P. E. (2001) *Kidney Int.* **59,** 1717–1728
43. Pages, G., Lenormand, P., L'Allemain, G., Chambard, J. C., Meloche, S., and Pouyssegur, J. (1993) *Proc. Natl. Acad. Sci. U. S. A.* **90,** 8319–8323
44. Moscatelli, D. A., Presta, M., Mignatti, P., Mullins, D. E., Crowe, R. M., and Rifkin, D. B. (1986) *Anticancer Res.* **6,** 861–863
45. Cano, E., and Mahadevan, L. C. (1995) *Trends Biochem. Sci.* **20,** 117–122
46. Thomson, S., Mahadevan, L. C., and Clayton, A. L. (1999) *Semin. Cell Dev. Biol.* **10,** 205–214
47. Friesel, R. E., and Maciag, T. (1995) *FASEB J.* **9,** 919–925
48. Kanda, S., Hodgkin, M. N., Woodfield, R. J., Wakelam, M. J., Thomas, G., and Claesson-Welsh, L. (1997) *J. Biol. Chem.* **272,** 23347–23353
49. Bailly, K., Soulet, F., Leroy, D., Amalric, F., and Bouche, G. (2000) *FASEB J.* **14,** 333–344
50. Liaudet-Coopman, E. D. E., and Wellstein, A. (1996) *J. Biol. Chem.* **271,** 21303–21308
51. Mangasser-Stephan, K., and Gressner, A. M. (1999) *Cell Tissue Res.* **297,** 363–370
52. Baxter, R. C. (2000) *Am. J. Physiol. Endocrinol. Metab.* **278,** E967–E976

[CANCER RESEARCH 63, 1696–1705, April 1, 2003]

Complex Regulation of the Fibroblast Growth Factor-binding Protein in MDA-MB-468 Breast Cancer Cells by CCAAT/Enhancer-binding Protein β[1]

Benjamin L. Kagan, Ralf T. Henke, Rafael Cabal-Manzano, Gerald E. Stoica, Quang Nguyen, Anton Wellstein, and Anna Tate Riegel[2]

Departments of Pharmacology [B. L. K., A. W., A. T. R.] and Oncology [R. T. H., R. C-M., G. E. S., Q. N., A. W., A. T. R.], Vincent T. Lombardi Cancer Center, Georgetown University, Washington, DC 20057

ABSTRACT

The fibroblast growth factor-binding protein (FGF-BP) binds and activates fibroblast growth factors in the extracellular matrix, and can have a rate-limiting role in tumor angiogenesis. Here we demonstrate high levels of FGF-BP expression in invasive human breast cancer, relative to normal breast and *in situ* carcinoma, and in MDA-MB-468 human breast cancer cells. In these cells, FGF-BP was up-regulated by treatment with epidermal growth factor (EGF), dependent on protein kinase C and p38 mitogen-activated protein kinase signaling. Mutational analysis revealed that the activator protein 1 and CCAAT/enhancer binding protein (C/EBP) sites on the FGF-BP gene promoter were required for the EGF effect, whereas deletion of the C/EBP site resulted in a significant increase in promoter basal activity indicating a basal repressive control mechanism. These data suggest that the C/EBP site is a central regulatory element for the regulation of FGF-BP promoter activity in MDA-MB-468 cells. We found that MDA-MB-468 cells express high endogenous levels of both the activating (LAP) and repressive (LIP) isoforms of C/EBPβ. Overexpression of C/EBPβ-LAP in MDA-MB-468 cells resulted in a large 80-fold increase in FGF-BP promoter basal activity, which was reversed by coexpression of LIP. Gel-shift analysis revealed that four LIP- and LAP-containing complexes (a-d) bind to the C/EBP site. DNA binding of the LIP and LAP-containing c complex and the b complex in the presence of EGF was modulated by inhibition of p38 mitogen-activated protein kinase, suggesting a role for these complexes in the EGF induction of the FGF-BP promoter. This study suggests that along with its well-defined role in mammary gland development, C/EBPβ may well play a role in the pathology of breast cancer, in particular in the control of angiogenesis in the invasive phenotype.

INTRODUCTION

Paracrine and autocrine growth factors have many functions, including a crucial role in inducing the formation of new blood vessels in a healing wound, as well as in a growing tumor. Many studies have demonstrated that a solid tumor mass cannot grow beyond a few millimeters in size without a sufficient supply of blood to the tumor. Tumor blood vessels provide a pathway for tumor cells to metastasize to distal sites, as well as a source of nourishment (1–4). The most important and best-studied angiogenic factors belong to the family of FGFs[3] (5, 6). FGF-1 and FGF-2 are unique in that their biological activities can be quenched by binding tightly to heparansulfate proteoglycan molecules in the extracellular matrix (7–10). A mechanism by which FGF can be activated involves the binding of FGF to a secreted carrier protein delivering the activated FGF to its target receptor. This secreted carrier protein, called the FGF-BP, is able to bind to FGF-1 and FGF-2 in a noncovalent, reversible manner (11). FGF-2 bound to FGF-BP protein is not subject to degradation (12) and can enhance the mitogenic activity of FGF-2 in mouse fibroblasts (13).

Expression of FGF-BP in cell lines that express FGF-2 results in these cells having a tumorigenic and angiogenic phenotype (12). FGF-BP-transfected cells are able to release the protein into their medium along with FGF-2 in a noncovalently bound form; the released FGF-2 is then biologically active (14). FGF-BP mRNA is expressed in SCC and colorectal carcinoma tumor tissue (12). FGF-BP mRNA is up-regulated in the skin of mice during embryonic development but drops to low levels in adult skin. In both mouse and human skin, FGF-BP mRNA and protein levels increase at least 3-fold on treatment with the PKC-activating phorbol ester TPA, and increase additionally in 7,12-dimethylbenz(*a*)anthracene/TPA-induced papillomas and carcinomas (15). We have also determined that FGF-BP can be up-regulated in SCC by EGF (16), and both TPA and EGF regulation of FGF-BP are dependent on an AP-1 and a C/EBP site in the FGF-BP promoter (16, 17).

C/EBPβ is a member of the C/EBP family of transcription factors (C/EBPα, C/EBPβ, C/EBPγ, C/EBPδ, C/EBPε, and C/EBPζ) that bind to consensus DNA sequences as homo- and heterodimers, and affect the transcription of various genes involved in proliferation and differentiation, especially in the liver and the immune system (18, 19). A variant of C/EBPβ, the C/EBPβ-LIP, translated from the same mRNA as the full-length protein (also called C/EBPβ-LAP), has been described (20, 21). The LIP variant is similar to LAP, except that it does not contain a transactivating domain. The C/EBPβ-LIP-LAP dimer is able to bind to its normal consensus site on a promoter, with greater affinity than LAP-LAP dimers, but is not able to promote transcription, therefore acting as a dominant-negative factor (20). C/EBPβ, especially LIP, may have a central role in mouse mammary gland differentiation and proliferation (22, 23), and C/EBPβ-LIP is expressed in human breast cancer samples that are both estrogen receptor- and progesterone receptor-negative (24).

Like many other growth factors, EGF plays a role in the tumorigenesis of many different types of cancers such as SCCs (reviewed in Refs. 25–27) and in the tumorigenesis of breast cancer (28). Expression of the EGF receptor and other members of the EGF receptor family, especially HER2, has been associated with poor prognosis in breast cancer (28, 29). In SCC, FGF-BP is an EGF target gene, whereas in colon cancer cells we do not observe induction of FGF-BP by EGF.[4] Therefore, it was of interest to determine the level of

Received 8/19/02; accepted 1/31/03.

The costs of publication of this article were defrayed in part by the payment of page charges. This article must therefore be hereby marked *advertisement* in accordance with 18 U.S.C. Section 1734 solely to indicate this fact.

[1] Tissue microarrays with breast tissues were provided through the National Cancer Institute CBCTR (U-0060T to A. W.). Supported by grants from the Department of Defense Breast Cancer Program (to A. W., Q. N., B. L. K.), the NIH (CA71508, to A. W.), the Susan G. Komen Foundation, (to G. E. S., A. T. R.), and the German Ministry for Research and Education (to R. T. H.).

[2] To whom requests for reprints should be addressed, at Department of Oncology, Vincent T. Lombardi Cancer Center, Research Building, E307, Georgetown University, 3970 Reservoir Road NW, Washington, DC 20057. Phone: (202) 687-1479; Fax: (202) 687-4821; E-mail: ariege01@georgetown.edu.

[3] The abbreviations used are: FGF, fibroblast growth factor; FGF-BP, fibroblast growth factor-binding protein; SCC, squamous cell carcinoma; PKC, protein kinase C; TPA, 12-*O*-tetradecanoylphorbol-13-acetate; EGF, epidermal growth factor; AP-1, activator protein 1; C/EBP, CCAAT/enhancer binding protein; LIP, liver-enriched inhibitory protein; LAP, liver-enriched activating protein; IMEM, improved minimum essential medium; ISH, *in situ* hybridization; TMA, tissue microarray; CBCTR, Cooperative Breast Cancer Tissue Resource; CMV, cytomegalovirus; GAPDH, glyceraldehyde-3-phosphate dehydrogenase; FBS, fetal bovine serum; MAPK, mitogen-activated protein kinase; EGFR, epidermal growth factor receptor; MEK, mitogen-activated protein kinase kinase.

[4] R. Ray and A. T. Riegel, unpublished observations.

expression of FGF-BP in human breast cancer, and to determine the EGF and basal regulation of this gene in this setting.

MATERIALS AND METHODS

Cell Culture and Reagents. The MDA-MB-468 human breast cancer cell line and the ME-180 human cervical SCC cell line were obtained from American Type Culture Collection (Manassas, VA). Cells were cultured in IMEM with 10% FBS (Invitrogen Inc., Carlsbad, CA). Human recombinant EGF was purchased from Collaborative Biochemical Products (Bedford, MA). Tyrphostin AG1517 (PD153035), Ro 31–8220 (bisindoylmaleimide IX) and PP1 were purchased from Alexis Corp. SB202190 was purchased from Calbiochem (San Diego, CA). U0126 was purchased from Promega. Calphostin C was purchased Sigma-RBI (Natick, MA). Wortmannin was purchased from Biomol (Plymouth Meeting, PA). All of the compounds were dissolved in Me_2SO.

Case Samples. A total of 205 paraffin-embedded tissue blocks from patients with breast cancer who had undergone surgery were obtained from the Lombardi Cancer Center/Georgetown University Medical Center. Pathology reports and clinical histories at the time of admission were reviewed to determine the nature of the lesion and tumor staging. The samples were classified as follows: 143 *in situ*, 34 invasive, and 28 normal, noncancerous breast tissue. Serial recuts of 4-μm paraffin-embedded tissue sections were used for detecting FGF-BP mRNA expression by ISH. In addition, TMAs from the National Cancer Institute CBCTR were used. This TMA contained samples from invasive cancer, as well as *in situ* carcinoma and control breast tissues from reduction mammoplasty.

ISH. The expression of FGF-BP mRNA in human breast tissue samples was assessed by ISH. The FGF-BP riboprobe consisted of a 668-bp internal sequence of FGF-BP cDNA (11), subcloned into the pRc/CMV vector (5.5 kb; Invitrogen). Digoxigenin-labeled antisense and sense riboprobes were made using the DIG RNA labeling kit (Roche) according to protocol. Tissue sections were cut (4-μm) and mounted on (+)-charged glass slides (Fisher Scientific, Pittsburgh, PA) using standard histology technique.

The protocol used for ISH has been described previously (30–32). Briefly, tissues were microwaved (high) for 3 min, and incubated at 56°C overnight and at 65°C 1 h before deparaffination. Paraffin was removed by two 5-min immersions in xylene followed by two 5-min washes in ethanol, and one wash in diethylpyrocarbonate-treated water. After deparaffination, samples were digested in a 1× PBS/10 μg/ml proteinase K solution at 37°C for 10 min. The slides were washed once in diethyl pyrocarbonate water and once in 2× SSC [0.9 M NaCl and 0.09 M sodium citrate (pH 7.0)]. For tissue deproteinization, slides were immersed in 0.2 M HCl (15 min) and rinsed in 0.1 M triethanolamine (pH 8.0). Acetic anhydride (0.25%) was then added to the triethanolamine for 15 min to deacetylate the samples. Tissue sections were washed in 2× SSC and hybridized with probes (1 ng/μl) overnight at 42°C. After incubation, the samples were washed with 2× SSC then treated with a STE [10 mM Tris (pH 7.5), 10 mM NaCl, and 1 mM EDTA] buffer/RNase A (10 μg/ml) solution for 10 min. After RNase A treatment, sections were washed with increasing stringency (2× SSC/formamide, 1× SSC, and 0.5× SSC) at 42°C. Digoxigenin was detected with an alkaline phosphatase-coupled antidigoxigenin monoclonal antibody (Roche) diluted in Buffer A [100 mM Tris-HCL (pH 7.5) and 150 mM NaCl]/1% horse serum. The alkaline phosphatase-tag was visualized by the nitroblue tetrazolium/5-bromo-4-chloro-3-indolyl phosphate detection system (Roche; Indianapolis, IN), which was in solution with Buffer B [100 mM Tris-HCl (pH 9.5), 100 mM NaCl, and 50 mM $MgCl_2$]. The chromogen color reaction was terminated with Buffer C [10 mM Tris-HCl (pH 8.0) and 1 mM EDTA). Usually, if the size of the section allowed, we ran two sections per slide with antisense and sense, because this makes the evaluation of the ISH assay easier. Slides were evaluated for staining of the cytosolic RNA, and Fig. 1*A* shows an example of negative staining in normal breast and breast cancer, as well as positive staining (Fig. 1*A i, ii,* and *iii,* respectively).

Northern Analysis. MDA-MB-468 cells were grown to 80% confluence in 10-cm dishes, washed twice in serum-free IMEM, and incubated for 16 h in serum-free IMEM before treatment. Cells were pretreated for 1 h with the indicated drug or with vehicle alone (Me_2SO; final concentration of 0.1%). EGF or anisomycin treatment was for 6 h unless otherwise indicated. Total RNA was isolated with RNA STAT-60 (Tel-Test Inc., Friendswood, TX), and

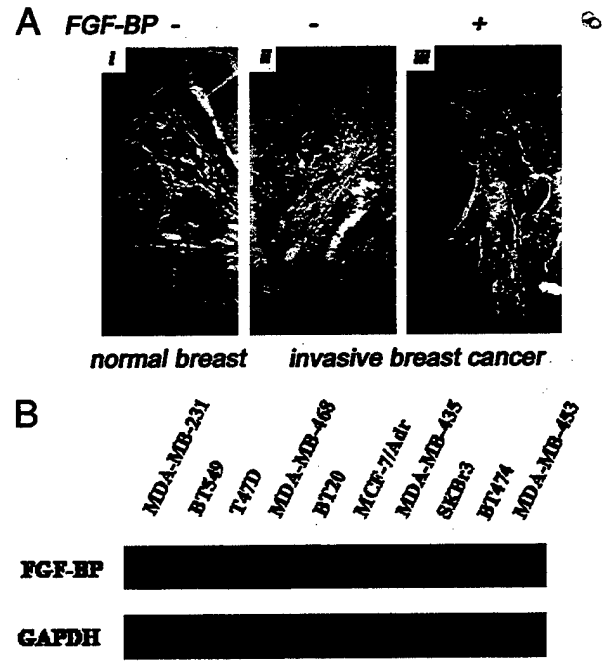

Fig. 1. Expression of FGF-BP mRNA in human breast cancer tissues and cell lines. *A,* ISH for FGF-BP mRNA using a TMA with paraffin-embedded normal breast (*i*) and invasive breast cancer (*ii* and *iii*) tissues. Normal breast and one of the breast cancer samples (*ii*) were scored as negative for FGF-BP, whereas the second breast cancer sample shown (*iii*) was scored as positive. Note that the FGF-BP mRNA expression is confined to the epithelial tissues. The TMA was obtained through the NIH CBCTR. The samples shown are selected from the same slide. Overview and statistical analysis of results is given in Table 1. *B,* Northern blot analysis showing FGF-BP mRNA and a control (GAPDH mRNA) in human breast cancer cell lines. Additional details under "Experimental Procedures."

Northern analysis was carried out as described previously (17) using 20 μg of total RNA. Hybridization probes were prepared by random-primed DNA labeling (Amersham Biosciences, Piscataway, NJ) of purified insert fragments from human FGF-BP (12) and human GAPDH (Clontech, Palo Alto, CA). Quantification of mRNA levels was performed using a PhosphorImager (Amersham Biosciences).

Plasmids. Human FGF-BP promoter fragments were cloned into the pXP1 promoterless luciferase reporter vector and have been described previously (17). The MEK2 (K101A) dominant-negative construct was provided by Dr. J. Holt (Vanderbilt University, Nashville, TN). The expression plasmids containing wild-type p38 (pCDNA3-Flag-p38) and constitutively active MKK6 (pCDNA3-Flag-MKK6(Glu)) were provided by Dr. R. Davis (University of Massachusetts, Boston, MA). The expression vectors for human CEBPβ-LAP and C/EBPβ-LIP (CMV-LAP and CMV-LIP, respectively) were gifts from Dr. U. Schibler (University of Geneva, Geneva, Switzerland) courtesy of Dr. J. Schwartz (University of Michigan, Ann Arbor, MI). Wild-type C/EBPβ mRNA contains three in-frame AUG translation start sites, from which LAP and LIP are translated from the second and third sites, respectively (20). The second in-frame AUG is flanked by an imperfect Kozak's sequence, GACCATGG (21), compared with the Kozak's consensus sequence of CCA/GCCAUGG (33, 34), whereas the third in-frame AUG is flanked by a perfect Kozak's sequence (20), resulting in translation of both LAP and LIP. The CMV-LAP construct contains only the second and third translation start sites, but both are flanked by perfectly matched Kozak's sequences resulting in the more efficient translation of LAP alone (20). The effects of dominant negatives or activated constructs were compared with their empty vector control or with the empty vector pCDNA3 (Invitrogen).

Transient Transfections and Reporter Gene Assays. Twenty-four h before transfection, MDA-MB-468 cells were plated at a density of 3×10^6 cells in 10-cm dishes. pRL-CMV *Renilla* luciferase reporter vector (Promega, Madison, WI) was included as a control for transfection efficiency. MDA-MB-468 cells were transfected by electroporation as described by Raja *et al.* (35). Briefly, cells were trypsinized and washed twice by centrifugation in IMEM containing 10% FBS. The cells from each plate were then resuspended

in 400 μl of IMEM containing 20% FBS. A total of 30 μg of plasmid DNA (29 μg of FGF-BP promoter construct and 3.0 ng of pRL-CMV) was added to the cell suspension 5 min before electroporation. For cotransfection, 24 μg of −118/+62Luc FGF-BP promoter construct, 5 μg or indicated amounts of expression vector, and 3.0 ng of pRL-CMV were added to cells. Electroporation of the entire cell sample was carried out in a cuvette with an electrode gap of 0.4 cm at 350 V and 500 μF, using a Bio-Rad GenePulser II (Bio-Rad, Hercules, CA). The electroporated cells were then distributed equally to a six-well plate, each well having been prefilled with 3 ml of IMEM with 10% FBS. Cells were allowed to recover and attach for 16 h before treatment. Transfected cells were washed twice with serum-free IMEM, treated with or without EGF (10 ng/ml) in serum-free IMEM for 16 h, and then lysed in 150 μl of passive lysis buffer (Promega). Twenty μl of extract was assayed for both firefly and *Renilla* luciferase activity using the Dual-Luciferase reporter assay system (Promega). To correct for transfection efficiency and a small background induction (1.5–2.0-fold) of the pRL-CMV plasmid by EGF (16), *Renilla* luciferase values were corrected for protein content, and these numbers were then used to normalize firefly luciferase values. Protein content of cell extracts was determined by Bradford assay (Bio-Rad).

Gel-Shift Assays. MDA-MB-468 cells were grown to 80% confluence on 150-mm dishes, serum starved for 16 h, and treated with or without 10 ng/ml EGF for 1 h. As a control, ME-180 SCC cells were treated with 5 ng/ml EGF for 1 h. For gel-shift assays using transiently transfected cells, MDA-MB-468 cells were plated at a density of 6×10^6 cells in 150-mm dishes and transfected with 10 μg of expression vector or empty vector by electroporation as described above. Cells were then either untreated or treated with 10 ng/ml EGF for 1 h. To study the effects of inhibition of p38 MAPK, cells were pretreated for 1 h with 10 μM SB202190, then treated with or without 10 ng/ml EGF for 1 h. Nuclear extracts were prepared as described previously (17). Binding reactions with the −70/−51 and −55/−30 probe was carried out as described previously (17) with 6 μg of MDA-MB-468 nuclear extracts, binding buffer [20 mM Tris (pH 7.5), 60 mM KCl, 5% glycerol, 0.5 mM DTT, and 2.0 mM EDTA], and 500 ng of poly(dI·dC).

Supershift antibodies (2 μg) or cold consensus oligonucleotide (20- and 50-fold molar excess) were added to the binding reaction for 10 min on ice before adding 20 fmol of labeled probe. Reactions were carried out for 20 min at room temperature and analyzed by 6% PAGE. Fos-specific antibodies c-Fos (K-25), c-Fos (4), Fos B (102), Fra-1 (R-20), and Fra-2 (Q-20); Jun-specific antibodies c-Jun/AP-1 (D), c-Jun/AP-1 (N), JunB (N-17), and JunD (329); and C/EBP-specific antibodies C/EBPβ (C-19) and C/EBPβ (Δ198) were purchased from Santa Cruz Biotechnology (Santa Cruz, CA). The C/EBP consensus oligonucleotide (Santa Cruz Biotechnology) had a sequence of 5′-TGCAGATTGCGCAATCTGCA-3′.

Western Analysis. Forty μg of crude nuclear extracts from untreated or EGF-treated MDA-MB-468 and ME-180 cells, or 20 μg of lysates from MDA-MB-468 transiently transfected cells were electrophoresed on Novex precast 4–20% Tris-glycine polyacrylamide gels (Invitrogen) at 150 V for 80 min. The protein was then transferred to polyvinylidene difluoride membranes (Millipore) for 2 h at 200 mA. Blots were blocked for 1 h in PBST (1× PBS and 0.5% Tween 20) containing 4% BSA (Sigma, St. Louis, MO), and then incubated for 1 h in 1× PBST/0.4% BSA, containing antibodies (1 μg/ml) for C/EBPβ (C-19; Santa Cruz). Blots were washed with PBST (without BSA) four times for 5 min each, with agitation. Blots were then incubated for 1 h in antibody solution containing a 1:5000 dilution of horseradish peroxidase-labeled donkey antirabbit immunoglobulin (Amersham) and washed as before. Lastly, blots were assayed for enhanced chemiluminescence using SuperSignal West Pico Chemiluminescent Substrate (Pierce) and enhanced chemiluminescence film (Hyperfilm ECL; Amersham). Signal intensities of the M_r 46,000, 36,000 (C/EBPβ-LAP), and 20,000 (C/EBPβ-LIP) bands were measured by densitometry using multiple exposures to Hyperfilm ECL to assess the linear range. Expression of LAP and LIP were corrected for loading differences by comparing to the band intensity of the M_r 46,000 band, as described by Zahnow *et al.* (23).

Statistics. The GraphPad Prism software package was used for graphics and data evaluation. Student *t* test was applied for continuous variables and χ^2 (Fisher's exact test) for discontinuous variables. Values of $P < 0.05$ were considered significant.

RESULTS

Expression of FGF-BP Correlates with Invasive Breast Cancer. In this study, we assessed the expression of FGF-BP in 205 (cancer and noncancer) paraffin-embedded tissue samples from breast surgical patients. ISH was performed using an FGF-BP-specific digoxigenin-labeled antisense riboprobe, and case samples were categorized by status (*in situ* or invasive) to correlate FGF-BP with cancer grade. Fig. 1*A* shows a representative example of parallel staining for FGF-BP mRNA expression in normal breast (negative) as well as breast cancer (one positive and one negative). FGF-BP mRNA expression was detected in 47% (67 of 143) of invasive cases, 23% (8 of 34) of *in situ* cases, and 14% (4 of 28) of normal and noncancerous breast (Table 1). These data show that expression of FGF-BP is associated with malignant transformation ($P = 0.0002$ for trend normal *versus in situ versus* invasive) and with invasiveness of human breast cancer ($P = 0.014$ *in situ versus* invasive; Table 1).

EGF Treatment Increases FGF-BP mRNA in MDA-MB-468 Human Breast Cancer Cells through PKC and p38 MAPK Signaling. To find a tissue culture model that recapitulated the high FGF-BP expression that we observed in invasive breast cancer, we screened a number of cell lines for FGF-BP mRNA expression. In this study and as reported previously (16, 36, 37), we have assayed FGF-BP mRNA expression, rather than protein expression, because FGF-BP is a secreted protein (12), and therefore is difficult to measure using whole cell extracts. Although it has been shown previously that most breast cancer cell lines are negative for FGF-BP expression (12), we have found that MDA-MB-468 cells have high FGF-BP expression (Fig. 1). Interestingly, MDA-MB-468 is a breast cancer cell line that can be invasive and metastatic *in vivo* when injected into mice along with angiogenesis-stimulating Matrigel (38). In addition, MDA-MB-468 cells have been characterized as showing high expression of the EGF receptor (39) and are EGF-responsive for invasion (40). Overexpression of the EGF receptor is a poor prognostic indicator in breast cancer (28) presumably through EGF stimulation of a more invasive phenotype, although the precise target genes are not yet defined. Treatment of MDA-MB-468 cells with 10 ng/ml EGF resulted in a rapid increase in the steady-state levels of FGF-BP mRNA (Fig. 2*A*). Induction of FGF-BP mRNA was observed after 1 h of treatment and was maximal after 6 h with an average increase of 2.5–3-fold (Fig. 2*B*). To discern between the possible signaling pathways involved in EGF induction of FGF-BP in MDA-MB-468 cells, we tested pharmacological inhibitors of signal transduction molecules at various concentrations for their effect on FGF-BP regulation. Treatment with the EGFR tyrosine kinase inhibitor PD153035 resulted in a significant concentration dependent inhibition of EGF induction of FGF-BP mRNA (Fig. 2*C*). In addition to EGFR tyrosine kinase activity, PKC is also involved in the EGF effect, because the bisindoylmaleimide PKC inhibitors Ro 31–8220 (41), at concentrations of 1 μM and 10 μM, and calphostin C (42) were both able to significantly inhibit the EGF induction of FGF-BP (Fig. 2*C*).

To determine the role of the additional downstream signaling pathways on EGF induction of FGF-BP, we used MEK1/2 and p38 MAPK inhibitors (43, 44). The MEK1/2-specific inhibitor U0126 was

Table 1 *Expression analysis for FGF-BP in human breast tissues*

	FGF-BP	
	Negative	Positive
(1) Normal breast ($n = 28$)	24	4
(2) *In situ* carcinoma ($n = 34$)	26	8
(3) Invasive cancer ($n = 143$)	76	67[a]

[a] $P = 0.0014$ and 0.014 relative to (1) and (2), respectively.

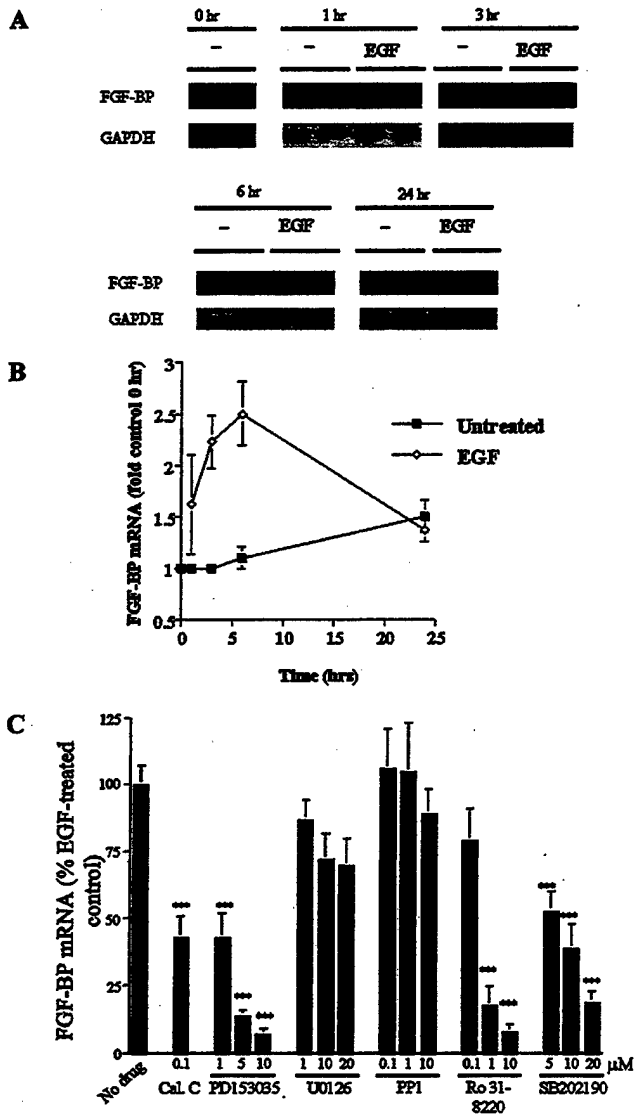

Fig. 2. Induction of FGF-BP mRNA by EGF in MDA-MB-468 cells. *A*, a representative Northern blot analysis showing FGF-BP mRNA and a control (GAPDH mRNA) done in duplicate. MDA-MB-468 cells were treated with or without 10 ng/ml EGF for the indicated times. *B* and *C*, results from quantitation of Northern blots. Signal intensities were quantified by PhosphorImager and normalized to the control mRNA, GAPDH. *B*, ■, represent control (*untreated*) levels, and □ represent EGF treatment mRNA levels expressed as fold over control-0 h. Values represent the mean of at least two separate experiments; *bars*, ±SD. *C*, FGF-BP mRNA levels from MDA-MB-468 cells treated with 10 ng/ml EGF for 6 h. Cells were pretreated for 1 h with vehicle alone or at the indicated concentrations of: Calphostin C (PKC inhibitor), PD153035 (EGFR tyrosine kinase inhibitor), U0126 (MEK1/2 inhibitor), PP1 (c-Src inhibitor), Ro 31–8220 (PKC inhibitor), and SB202190 (p38 MAPK inhibitor). Values are expressed relative to mRNA levels after EGF treatment alone (without inhibitor), which was set to 100%. Basal FGF-BP level (without EGF or inhibitor) was ~30%. Values represent mean from of at least three separate experiments; *bars*, ±SE. Statistically significant differences relative control conditions (EGF only; ***, $P < 0.0001$, *t* test).

only effective at higher concentrations of 10 μM and 20 μM, and not at the concentration of 1 μM (Fig. 2*C*); 1 μM of U0126 is usually used to specifically inhibit MEK-induced signaling (45). In contrast, treatment with increasing concentrations of the p38 MAPK inhibitor SB202190 resulted in a concentration-dependent inhibition of EGF-induced FGF-BP mRNA (Fig. 2*C*). These data suggest that p38 MAPK plays a dominant role in the induction of FGF-BP by EGF in MDA-MB-468 cells. Other intracellular targets for EGF receptor-induced intracellular signaling also potentially include members of the c-Src protein tyrosine kinase family. However, the c-Src family-specific inhibitor PP1 (46) resulted only in a maximal 10% reduction in EGF-induced FGF-BP mRNA levels, only at the highest concentration used (10 μM; Fig. 2*C*). These data indicate only a minimal role for Src in EGF control of FGF-BP expression. The phosphatidylinositol 3′-kinase pathway also is not involved because treatment of MDA-MB-468 cells with 1 μM wortmannin did not have any significant effect on EGF induction of FGF-BP (data not shown). Overall, our pharmacological inhibitor data indicate a major role for PKC, and more significantly, p38 MAPK in EGF effects on FGF-BP in breast cancer cells.

EGF Regulation of the FGF-BP Gene Promoter in MDA-MB-468 Cells Is Mediated through AP-1 and C/EBP Sites on the FGF-BP Promoter. The promoter of the human FGF-BP gene was cloned previously (17), and functional analysis of the promoter in ME-180 SCC cells revealed that activity is mediated through the first 118 bp of the proximal promoter sequence (16, 17). In contrast, in colon cancer cells the first 1060 bp of the promoter is involved in basal and regulated expression of the FGF-BP promoter.[5] The important regulatory sites within this region are shown in Fig. 3, *center panel,* and include two Sp1 binding sites [Sp1(a) and Sp1(b)], AP-1, E-box, and C/EBP binding sites. We examined the promoter elements involved in the basal activity and EGF regulation of the FGF-BP promoter in MDA-MB-468 cells using a series of promoter mutant or deletion constructs linked to a luciferase reporter gene. After transfection into MDA-MB-468 cells, the fold activity or induction of each construct in the presence or absence of EGF treatment was determined. As shown in Fig. 3, *left histogram,* basal activity of the promoter was not significantly affected when deleted from −1060 to −118. In contrast, the −118 construct harboring a deletion of the AP-1 site (ΔAP-1) resulted in a significant decrease in basal promoter activity. Surprisingly, deletion of the C/EBP site resulted in a significant increase in basal activity of ~3.5-fold equivalent to that seen with EGF treatment of the promoter. This suggested that the C/EBP site acts as a repressor element for FGF-BP promoter basal activity in breast cancer cells. This effect of deletion of the C/EBP site on the FGF-BP promoter was not seen in ME-180 cells (16, 17), suggesting a tissue-specific mechanism by which FGF-BP basal promoter activity is regulated.

Consistent with the response of the endogenous FGF-BP gene to EGF, the FGF-BP promoter was induced 4-fold by EGF in MDA-MB-468 cells, and this effect was still evident within the first 118 bp upstream of the transcription start site (Fig. 3, *right histogram*). Deletion of the AP-1 or C/EBP site on the FGF-BP promoter resulted in a 50% decrease in EGF induction (Fig. 3, *right histogram*), suggesting that in combination these sites constitute the majority of the transcriptional effects of EGF on the FGF-BP gene promoter in MDA-MB-468 cells. Consistent with this conclusion, deletion of the Sp1(b) site did not affect the ability of EGF to induce the FGF-BP promoter in MDA-MB-468 cells (Fig. 3, *right histogram*), nor did mutation of the E-box site centered at −58. This mutation has resulted previously in superinduction of promoter activity in both TPA and EGF-treated SCC cells (47). Interestingly, this mutation did increase basal promoter activity to 2-fold over control (Fig. 3, *right histogram*). The necessity of the C/EBP site on the FGF-BP promoter for both basal and EGF-induced activity in MDA-MB-468 cells may represent a novel phenomenon, specific to the transcriptional regulation of FGF-BP in breast cancer cells.

Contribution of the p38 Pathway to FGF-BP Promoter Activity. Inhibition of p38 MAPK with pharmacological agents demonstrated the importance of this kinase in mediating the induction of FGF-BP by

[5] R. Ray, R. Cabal-Mazano, A. Moser, S. W. Byers, A. T. Riegel, and A. Wellstein. Gene expression of fibroblast growth factor-binding protein 1 is regulated by beta-catenin in the APC Min/+ mouse, submitted for publication.

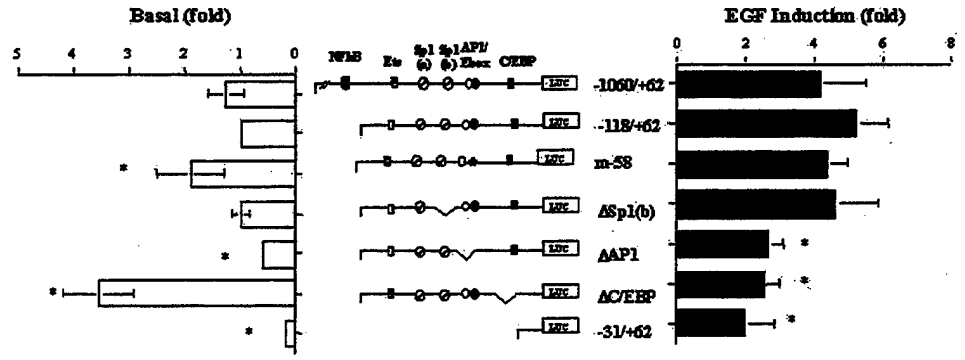

Fig. 3. FGF-BP promoter elements involved in EGF induction of FGF-BP in MDA-MB-468 cells. The histogram on the *left* shows the impact of each promoter deletion on the basal (uninduced) luciferase activity of each construct. The basal activity of the −118/+62 construct was set to 1. The *right* histogram shows the transcriptional activity in the presence of EGF and is expressed as fold induction of EGF-treated over untreated for each construct. MDA-MB-468 cells were transiently transfected by electroporation with the indicated FGF-BP promoter luciferase constructs and a CMV driven *Renilla* luciferase reporter vector for transfection efficiency, and were untreated or treated with 10 ng/ml of EGF for 18 h. Promoter constructs are described under "Experimental Procedures" and by Harris *et al.* (17). Values represent the mean from at least three separate experiments, each done in triplicate wells; *bars*, ±SE. Statistically significant differences relative to the −118/+62 promoter construct are indicated (*, $P < 0.05$, *t* test).

EGF in MDA-MB-468 cells. To confirm this result, we demonstrated that expression vectors for p38 MAPK or a constitutively active mutant of MKK6 [MKK6(Glu)], a MEK that specifically phosphorylates p38 MAPK (48), along with the FGF-BP promoter luciferase construct (−118/+62) into MDA-MB-468 cells, resulted consistently in a significantly higher level of EGF induction of FGF-BP transcription as compared with empty vector transfected cells (Fig. 4*A*). These data underscore the role of p38 MAPK signaling for the full induction

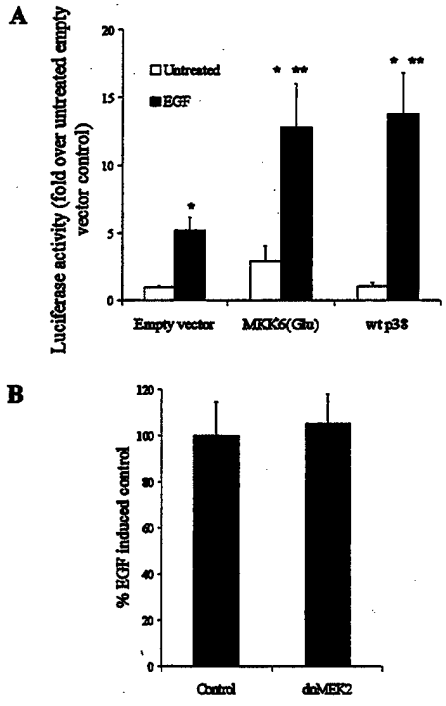

Fig. 4. Effects of MAPK signaling on the EGF induction of FGF-BP promoter activity. *A*, MDA-MB-468 cells were transiently cotransfected with the −118/+62 FGF-BP promoter construct, and either empty vector or expression vectors for p38 MAPK or MKK6(Glu). Transfected cells were either untreated or treated with 10 ng/ml EGF for 18 h. FGF-BP promoter activity is shown relative to the untreated empty vector control. Values represent the mean of at least three separate experiments, each done in triplicate wells; *bars*, ±SE. *B*, MDA-MB-468 cells were transiently cotransfected with the −118/+62 FGF-BP promoter construct along with either empty vector or a dominant-negative construct for MEK2. Cells were treated as in *A*, and EGF induction is determined by the fold increase in luciferase activity and expressed relative to empty vector control, which is set at 100%. Basal (uninduced) promoter activity was ~25% of EGF-treated. Values represent the mean of at least three separate experiments, each done in triplicate wells; *bars*, ±SE. Statistically significant differences relative to untreated (*) or EGF-treated (**) empty vector control are indicated ($P < 0.05$, *t* test).

of FGF-BP transcription by EGF in MDA-MB-468 cells. In contrast, expression of dominant-negative MEK2 did not change the ability of EGF to induce the activity of the FGF-BP promoter consistent with our earlier conclusion (from Fig. 2*C*) that MEK1/2 does not play a predominant role in EGF induction of FGF-BP (Fig. 4*B*). These activities of the p38 MAPK and MKK6 expression vectors were demonstrated to be specific in parallel experiments using the p38 MAPK-specific inhibitor SB202190 and a Stratagene AP-1 responsive reporter (data not shown).

AP-1 and C/EBP Factors Bind to the FGF-BP Promoter in MDA-MB-468 Cells. To determine which AP-1 factors bind to the promoter in EGF-treated MDA-MB-468 cells, gel-shift analysis was carried out using labeled promoter sequence fragment −70 to −51 (Fig. 5*A*), and nuclear extracts from untreated or EGF-treated MDA-MB-468 cells. Protein binding in the uppermost complex, shown previously to represent AP-1 (16, 17, 37), is induced by EGF in MDA-MB-468 cells (Fig. 5*B*, *Lanes 1* and *2*, *arrow*). Incubation with an antibody for Fos family members resulted in a supershifted complex, and incubation with antibodies specific for c-Fos and FosB inhibited the formation of the AP-1 complex, suggesting that c-Fos and FosB bind to the AP-1 site on the FGF-BP promoter in MDA-MB-468 cells. The AP-1 complex was also blocked when EGF-treated MDA-MB-468 nuclear extracts were incubated with antibodies specific for Jun family members and JunB, suggesting that JunB also binds to the AP-1 site on the FGF-BP promoter (Fig. 5*B*, *Lanes 8* and *10*).

To demonstrate C/EBP binding to the FGF-BP promoter in MDA-MB-468 cells, we carried out gel-shift analysis using a labeled promoter sequence fragment from −55 to −30 (Fig. 5*A*), which was incubated in the presence of nuclear extracts from untreated or EGF-treated MDA-MB-468 cells. As shown in Fig. 5*C* (*Lanes 1* and *2*) and Fig. 8 (*Lanes 1–3* and *12–14*), we observed four specific complexes in nuclear extracts from MDA-MB-468 cells. However, no qualitative differences in any of these C/EBP complexes were observed between untreated and EGF-treated cells (Fig. 5*C*, *Lanes* 1, 2, 5, and *8*). Complexes a-d, formed in MDA-MB-468 cells, were confirmed to bind C/EBPβ by supershift analysis using antibodies C/EBPβ (Δ198) and C/EBP β (C-19), as well as by competition with a cold excess C/EBP consensus oligonucleotide (Fig. 5*C*, *Lanes* 6, 7, 9, and *10*). Incubation with the Δ198 antibody, which recognizes all of the C/EBP family members, resulted in one supershifted band and the disappearance of band a when extracts from EGF-treated MDA-MB-468 cells were used (Fig. 5*C*, *Lane 3*). The C-19 antibody, which is specific for only C/EBPβ, resulted in a decrease in binding of complexes a and b

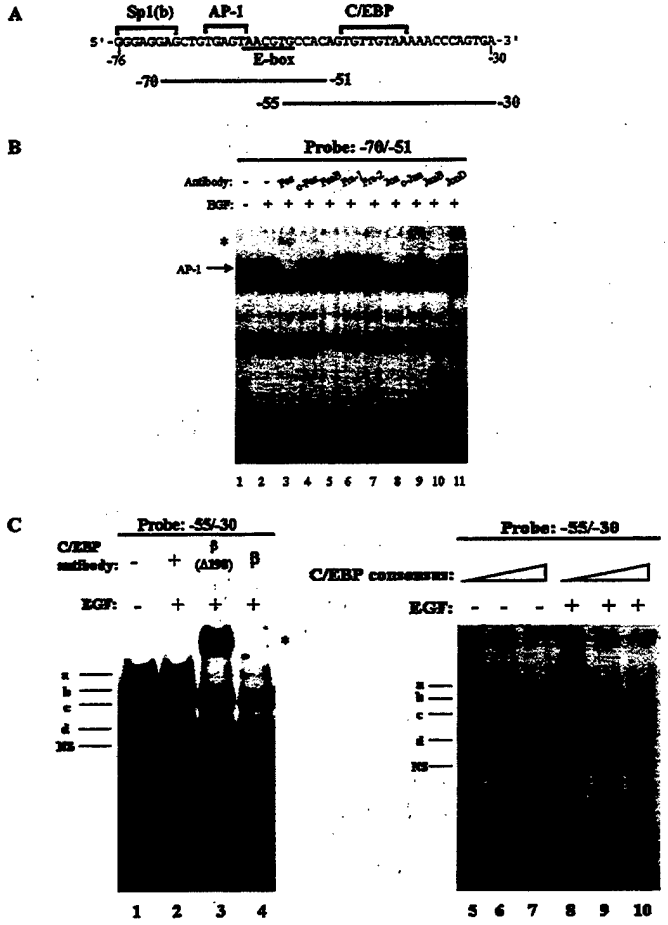

Fig. 5. Transcription factor binding to FGF-BP promoter elements in MDA-MB-468 cells. *A*, double-stranded oligonucleotide sequences of promoter elements used for gel-shift analysis. *B*, supershift analysis of transcription factor binding to the AP-1, and *C*, C/EBP sites of the FGF-BP promoter. Labeled FGF-BP promoter sequences as indicated were incubated with nuclear extracts from untreated or EGF-treated MDA-MB-468 cells. Binding reactions were performed in the presence of "supershifting" antibodies or cold excess consensus oligonucleotide as indicated. An *arrow* or *bar* to the *left* of each panel indicates specific binding of AP-1 and C/EBP. * indicate supershifted complexes.

(Fig. 5*C*, *Lane 4*). These data suggest that C/EBPβ binding to the FGF-BP promoter in MDA-MB-468 cells is complex, but specific, and that the degree of binding is independent of EGF treatment.

C/EBPβ-LAP and C/EBPβ-LIP Are Expressed in MDA-MB-468. As shown in Fig. 3, deletion of the C/EBP site on the FGF-BP promoter results in a significant increase in basal promoter activity in MDA-MB-468 cells. This suggests that a transcription factor complex that binds to this site might act as a repressor, reducing the basal activity of the FGF-BP promoter, which is a unique aspect of regulation of FGF-BP promoter activity not observed previously. A variant of C/EBPβ, the C/EBPβ-LIP, translated from the same mRNA as the full-length protein but at a downstream start codon (also called C/EBPβ-LAP), has been described (20, 21). The LIP variant is similar to LAP, except that it does not contain a transactivating domain. The C/EBPβ-LIP-LAP dimer is able to bind to its normal consensus site on a promoter, with greater affinity than LAP-LAP dimers, but is not able to promote transcription, therefore acting as a dominant negative (20).

To determine whether differences in C/EBPβ isoform expression could account for the tissue-specific variations observed, we compared the levels of C/EBPβ isoform expression in MDA-MB-468 (where the C/EBP site is repressive) and ME-180 cells (where the C/EBP site has no impact on basal activity). Immunoblot analysis using an antibody specific for the COOH terminus of C/EBPβ revealed that MDA-MB-468 cells express higher levels of LIP relative to LAP (Fig. 6*A*, M_r 20,000 band) as compared with ME-180 cells. In fact, as shown in Fig. 6*B*, ME-180 cells have a 3–4-fold higher LAP:LIP ratio than MDA-MB-468 cells, and we conjectured that these differences in LAP:LIP ratios might explain the differences in basal activity seen with the ΔC/EBP promoter construct (Ref. 16; Fig. 3).

Effect of C/EBPβ Isoforms on the Activity of the FGF-BP Promoter. C/EBPβ-LIP has been shown to have a higher DNA-binding affinity than LAP, and that small increases in the levels of LIP present, relative to levels of LAP, confer a significant increase in the ability of transcriptional repression to occur (20). These results are consistent with the notion that the ratio of LAP:LIP present in a cell is an important factor that determines the transactivating ability of a C/EBPβ complex. To determine whether changes in C/EBPβ isoform levels impacted on the activity of the FGF-BP promoter, we transiently cotransfected expression vectors for either LAP alone or LAP and LIP together (CMV-LAP and CMV-LIP, respectively) along with FGF-BP promoter constructs in MDA-MB-468 cells. Overexpression of LAP alone resulted in a significant increase of 80-fold in the basal activity of the −118/+62 FGF-BP promoter construct (Fig. 7*A*). In contrast, overexpression of LAP in ME-180 cells resulted in a much lesser 8-fold increase in basal activity of the −118/+62 construct.

The expression vector CMV-LIP was then introduced into MDA-MB-468 cells in increasing concentrations (2 μg and 4 μg), along with constant amounts of CMV-LAP (5 μg) and FGF-BP promoter constructs, to ascertain the effects of decreasing the ratio of LAP:LIP on the FGF-BP promoter. Cotransfection of 2 μg of LIP along with LAP, conferred a LAP:LIP ratio of ~2 (Fig. 7*B*), and this change in LIP:LAP ratio reduced the superinduction of the −118/+62 construct by 50% (Fig. 7*C*). Increasing LIP to 4 μg conferring a LAP:LIP ratio of ~1 (Fig. 7*B*), and this significantly decreased the superinductive effect of LAP to a level 70% below the level of induction seen with LAP alone (Fig. 7*C*). The effects observed because of the changes in LAP:LIP ratio were primarily limited to the C/EBP site, because transfection with the ΔC/EBP construct in a constant activity level

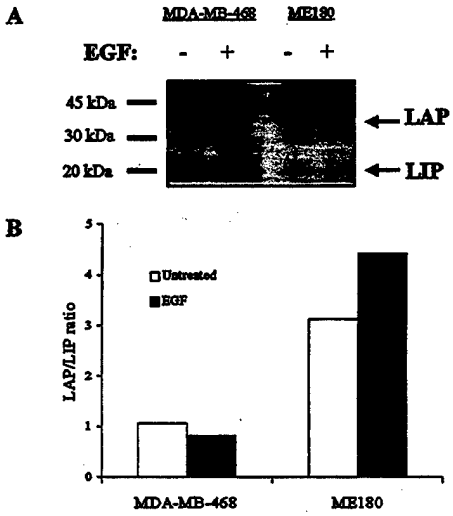

Fig. 6. Expression of C/EBPβ in ME-180 and MDA-MB-468 cells. *A*, a representative Western blot analysis of C/EBPβ protein levels using 40 μg of nuclear extracts from untreated and EGF-treated MDA-MB-468 and ME-180 cells. C/EBPβ was specifically recognized using a polyclonal antibody specific for the COOH terminus of the protein [C/EBPβ (C-19)]. The positions of LAP (*35 kDa*) and LIP (*20 kDa*) isoforms are indicated by *arrows*. *B*, ratios of LAP to LIP in MDA-MB-468 and ME-180 cells. Levels of LAP and LIP were quantified from multiple exposures of Western blot analyses using densitometry and corrected for levels of the M_r 46,000 nonspecific band. Values are expressed as actual ratios of LAP to LIP for each cell line.

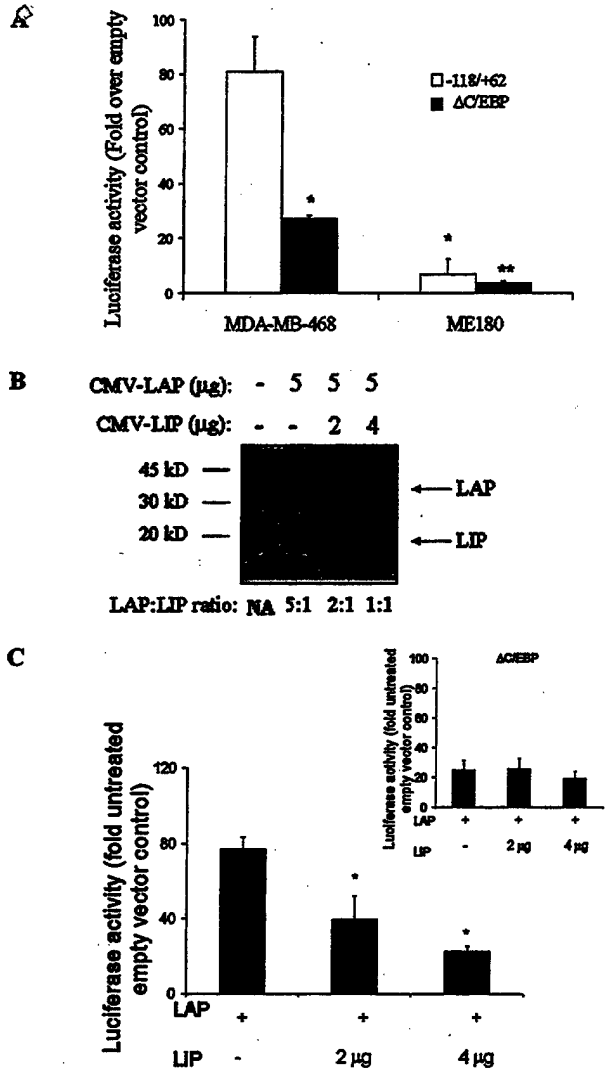

Fig. 7. Effects of LAP and LIP overexpression on the FGF-BP promoter activity. *A*, MDA-MB-468 cells and ME-180 were cotransfected with the indicated FGF-BP promoter constructs and 5 μg CMV-LAP. Relative luciferase activity of the cells transfected with ΔC/EBP (■) or −118/+62 (□) constructs are expressed as fold over control (empty vector transfected cell lines). *B*, shown is a representative Western blot of C/EBPβ protein levels in MDA-MB-468 cells transiently transfected with CMV-LIP and CMV-LAP. The levels of LAP and LIP were quantified from multiple exposures of Western blot analyses using densitometry, and corrected for levels of the M_r 46,000 band. Values are expressed as relative ratios of LAP to LIP for each transfection condition. *C*, MDA-MB-468 cells were cotransfected with the −118/+62 or ΔC/EBP (*C, inset*) FGF-BP promoter constructs, 5 μg CMV-LAP, and the indicated amounts of CMV-LIP or empty vector (pcDNA3). MDA-MB-468 cells were treated were kept in serum-free IMEM for 16 h. Values are expressed as the mean of at least three experiments, each done in triplicate wells; *bars*, ±SE. Statistically significant differences relative to −118/+62 (*) or MDA-MB-468/ΔC/EBP (**) are indicated ($P < 0.05$, *t* test).

80% below the level seen with the −118/+62 construct (Fig. 7*C*, *inset*). Interestingly, there is an apparent increase in the expression of LAP, concurrent with the increase in LIP, although the amount of transfected LAP DNA remains constant (Fig. 7*B*). This phenomenon may be accounted for by differences in transfection efficiencies between LAP-LIP-transfected cells or by the possible ability of LAP protein to be stabilized by increases in LIP expression. These scenarios remain to be studied.

Binding of C/EBPβ-LAP and -LIP to the C/EBP Site on the FGF-BP Promoter. To additionally investigate the interactions of C/EBPβ-LIP and -LAP with the C/EBP site we performed gel mobility shift analysis. As seen in Fig. 5*C* and Fig. 8 (*Lanes 1* and *9*), incubation of nuclear extracts from untreated and EGF-treated MDA-MB-468 with the radiolabeled −55/−30 oligonucleotide probe resulted in the formation of four complexes a-d. However, it should be noted that frequently in different preparations of nuclear extracts, one or more of the complexes was indistinguishable, and EGF treatment of cells resulted in no consistent differences in the mobility or the amount of any of the complexes (Fig. 8, *Lanes 1* and *2 versus 9* and *10*). To improve the resolution and to help identify components of these complexes, we examined binding to the FGF-BP promoter C/EBP element in extracts from cells in which levels of LIP or LAP had been increased by transient overexpression. Increasing levels of LIP, which functionally results in FGF-BP promoter repression (Fig. 7*C*), enhanced both the c and d complexes in the untreated and EGF-treated extracts (Fig. 8, *Lanes 3* and *11*). In contrast, the overexpression of LAP significantly increased the b complex and also slightly increased the c complex (Fig. 8, *Lanes 6* and *14*). We also determined that an antibody to C/EBP supershifted the b, c, and d complexes produced after overexpression of LIP or LAP (Fig. 8, *Lanes 5, 8, 13* and *16*).

The next question was then to determine how EGF and p38 MAPK signaling affected the binding of these complexes. Under conditions of basal levels of LIP and LAP, inhibition of p38 MAPK produced no consistent change in complex binding either in the presence or absence of EGF, although again in many of the extracts the levels of binding to the complexes were low and somewhat variable (Fig. 8, *Lanes 2 and 10*). Furthermore, under conditions of LIP overexpression, inhibition of p38 MAPK slightly decreased binding on the d complex (Fig. 8, *Lanes 4* and *12*). In contrast, inhibition of p38 MAPK with SB202190 decreased the LAP-induced binding of the c complex in basal and slightly increased the binding in EGF-treated conditions (Fig. 8, *Lanes 7 versus 15*). These data suggest that binding

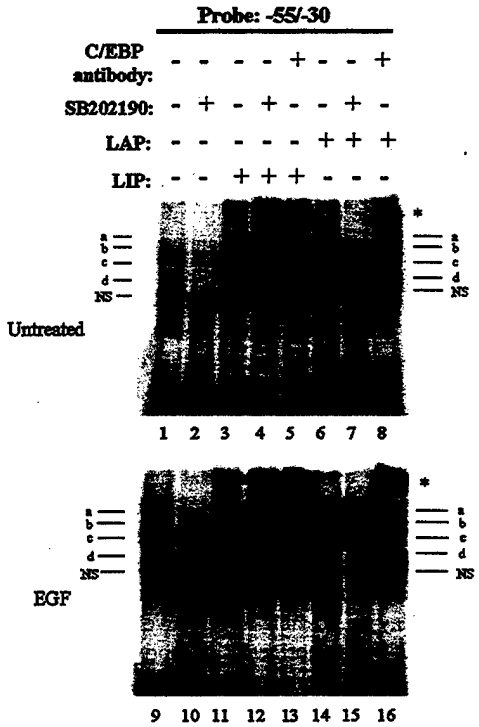

Fig. 8. Binding of C/EBPβ-LAP and -LIP to the C/EBP site on the FGF-BP promoter. ^{32}P-labeled −55/−30 FGF-BP promoter sequence was incubated in the presence of nuclear extracts of MDA-MB-468 cells transfected with: empty vector, CMV-LAP, or CMV-LIP constructs. MDA-MB-468 cells were pretreated with vehicle alone (Me_2SO) or 10 μM SB202190 for 1 h and then treated with or without 10 ng/ml EGF for 1 h. Binding reactions were incubated with a C/EBP supershift antibody where indicated. Specific binding is indicated by *bars* (*a–d*) to either side of each panel, nonspecific binding is indicated (*NS*), and supershifted complexes are indicated by *.

of the c complex can be changed by activation of the p38 MAPK signaling cascade. Interestingly, the binding of the b complex is differentially regulated under basal *versus* EGF-induced conditions. If EGF is present, then inhibition of the p38 MAPK increases binding of complex b (Fig. 8, *Lanes 14 versus 15*), whereas in the absence of EGF, inhibition of p38 MAPK decreases binding of b (Fig. 8, *Lane 6 versus 7*). This suggests that other EGF-induced signaling pathways can alter the susceptibility of the b complex to regulation by p38 MAPK. In summary it seems that basal repression of the promoter by LIP is well correlated with the formation of the d complex. Whereas inhibition of p38 MAPK had some effect on the binding of the d complex, the effect of p38 MAPK is mainly on the b and c complexes, the DNA binding of which can be modulated by p38 MAPK signaling especially by ongoing EGF stimulation.

DISCUSSION

In this study, we show that FGF-BP is highly expressed in invasive breast carcinoma, relative to normal breast tissues and *in situ* carcinoma, and that this pattern of expression is recapitulated in the MDA-MB-468 human breast cancer cell line. Previous studies from our laboratory have demonstrated that FGF-BP is also highly expressed in SCC and colon cancer (12, 15). However, in both of these tumor types we have observed that FGF-BP gene expression is turned on at early dysplastic stages of disease (15),[6] whereas in breast cancer high FGF-BP gene expression is confined to invasive disease. This suggests that angiogenesis in late-stage breast disease may be controlled by a different set of growth factors than early breast cancer. This switching of rate-limiting angiogenic factors has precedent, for instance during colon cancer progression FGF-BP plays a role in early angiogenesis in the polyp and early dysplastic lesions, but vascular endothelial growth factor is a predominant factor during later stages (49, 50).

A unifying factor in terms of FGF-BP regulation in both breast and SCC is its dependence on high EGFR signaling for high levels of FGF-BP expression. In breast cancer, 30% of tumors have increased EGFR and HER2 signaling, and this is associated with a poor prognosis (28, 51–54). FGF-BP may well be a critical gene target for the EGFR/HER2 signaling in breast cancer, enhancing the angiogenic phenotype in late-stage disease. The involvement of the p38 MAPK signaling pathway, as a predominant mechanism for activating FGF-BP gene expression, is also common to SCC and breast cancer cells. Interestingly, activation of PKC is also a requirement for activation of FGF-BP gene expression in these two cell types, suggesting its involvement as another dominant regulator of FGF-BP transcription. PKC has been shown to be associated with the activation of p38 MAPK signaling (55, 56). Therefore, EGF-induced signaling through PKC may activate p38 MAPK-mediated FGF-BP transcription. A number of genes have been reported that can be selectively activated by EGF induction of p38 MAPK (57–59), and along with FGF-BP, these genes may represent a subset that are activated to initiate a particular EGF-induced phenotype. The selective use of p38 MAPK signaling for expression of an angiogenic molecule in invasive disease indicates that it may be possible to selectively target signaling pathways to abrogate the tumorigenic phenotype without necessarily dampening all of the proliferative signaling.

The data presented here suggest that the AP-1 and C/EBP sites in the FGF-BP promoter can be regulated by p38 MAPK. The factors binding to the AP-1 site are c-fos, Fos-B, and JunB, all of which can be phosphorylated and activated by p38 MAPK signaling (60). The pattern of AP-1 activation and binding to the FGF-BP promoter is similar to that observed in SCC and represents a conserved transcriptional target for p38 MAPK induction of FGF-BP in different tumor types. In contrast, the targeting of p38 MAPK signaling to the C/EBP site in the FGF-BP promoter, specifically to C/EBPβ, is less well defined. However, at this detection level, a major problem we found in this analysis was that the C/EBP-binding species in MDA-MB-468 extracts were frequently faint and indistinct, thereby making clear conclusions about the changes in factor binding after p38 MAPK activation difficult.

The overexpression of C/EBPβ-LIP and -LAP helped to determine whether these isoforms were part of complexes a-d. From gel-shift analysis we can conclude that complex b contains LAP, complex c contains LIP and LAP, and complex d contains LIP. Given the relative mobility of the LIP and LAP homo- and heterodimers reported previously (61), it could be postulated that complex b represents LAP homodimers, complex c represents LIP/LAP heterodimers, and the d complex is a LIP homodimer. However, because C/EBP family members can heterodimerize with other C/EBP family members (62) and with other leucine zipper family members such as Fos and Jun (62), we cannot rule out that the a-d complexes represent heterodimers with these proteins. Nevertheless, the b and c complexes are clearly regulated by p38 MAPK signaling. The c complex has the DNA binding activated by p38 MAPK, which suggests that if the c complex is responsible for EGF-induced gene activation, it is likely not a LIP/LAP heterodimers, because this is a repressive transcription complex (20). The DNA binding of the b complex is increased by p38 MAPK in the presence of EGF-induced signaling but not when EGF signaling is absent. If the b complex is indeed the LAP/LAP homodimer, it can activate transcription from a C/EBPβ site (21), but our data suggest that p38 MAPK could be involved only when other signaling pathways in the cell are induced. In this regard, it has been reported that p38 MAPK can phosphorylate LAP (63), and this might be one possible mechanism of activation of the LAP homodimer. However, signaling through p38 MAPK can result in the phosphorylation of a number of other leucine zipper transcription factors, including ATF-2 (64, 65), Elk-1 (48), c-Jun (64), and CHOP (66). Therefore, we cannot rule out the possibility that heterodimeric complexes of these factors with LAP are playing a role in the EGF and p38 MAPK induction of the FGF-BP promoter at the C/EBP element. Overall, the regulation of FGF-BP transcription by EGF at the FGF-BP promoter C/EBP element appears to be complex, potentially dependent not only on the relative amounts of the C/EBPβ isoforms and their heterodimerization partners, but also on the activity of p38 MAPK and other signaling pathways in the cell.

Perhaps the most significant observation in our study was the difference seen in the regulation of the basal activity of the FGF-BP promoter in MDA-MB-468 cells on deletion of the C/EBP site, which resulted in a significant increase in basal promoter activity (80-fold). This is in contrast to ME-180 SCC cells where deletion of the same site did not result in any change in basal activity (16). These data suggest that although the C/EBP site is a necessary element for EGF-induced FGF-BP promoter activity in both SCC and breast cancer cells, this site has a unique dual role in the regulation of promoter activity specific to breast cancer cells. This also suggests that a cell type-specific repressive mechanism is present that can silence this promoter until an inductive signal, such as signaling through p38 MAPK, is received. Because LIP levels are high in the MDA-MB-468 cells and the LIP/LIP homodimer is a high affinity repressor (20), this complex could be responsible for this basal repressive activity. The d complex is a good candidate for the LIP/LIP homodimer because it has fast mobility (61) and is selectively increased by LIP overexpression. In addition, the d complex is unaffected by inhibition of the p38 MAPK pathway, which suggests that

[6] R. Cabal-Manzano, unpublished observations.

simple removal of the repressor may not explain the activation by EGF, but that it must be replaced by an active transcription complex in order for FGF-BP gene expression to be induced. The repressive mechanism may not operate in SCC cells because the LIP levels are not high enough.

In conclusion, this study characterizes the signal transduction and transcriptional mechanisms that are important in the basal control and EGF induction of FGF-BP expression in breast cancer cells. Understanding the regulatory pathways involved in the expression of FGF-BP is important, especially because deregulated FGF-BP expression is rate-limiting in tumor formation and tumor angiogenesis (12, 14). We have now observed a link between EGF signaling and FGF-BP gene induction in both SCC (16) and breast cancer cells involving p38 MAPK signaling via AP-1 and C/EBP induced transcription. Although the phosphorylation site of C/EBPβ in response to p38 MAPK has not been defined *in vivo*, it is tempting to speculate that p38 MAPK can directly phosphorylate C/EBPβ and, thus, activate this molecule. We have also demonstrated the ability for the differential binding of C/EBP factors, specifically C/EBPβ-LAP and LIP, to regulate both unstimulated and EGF-stimulated promoter activity of the human FGF-BP gene in human breast cancer cells.

Whereas FGF-BP expression is associated with the malignant progression to invasive breast cancer, it is absent from most breast cancer cell lines assayed. This phenomenon may be explained by increased methylation of the FGF-BP gene in breast cancer cell lines *versus* tissues or the *in vitro* growth conditions in contrast to intact tissues. In addition, as demonstrated by this study, differences in LAP:LIP ratios differentially modulate FGF-BP promoter activity. The MDA-MB-468 cell line, which expresses FGF-BP, has a LAP:LIP ratio of 5:1, whereas the other cell lines that do not express FGF-BP may have LAP:LIP ratios that do not favor expression. These differences would be important to investigate to additionally understand the role of FGF-BP in human breast cancer.

Although many studies demonstrate that p38 MAPK has a role in angiogenesis (67) and the regulation of expression of angiogenic factors such as vascular endothelial growth factor (68), a role for C/EBP factors in the process of angiogenesis is not well characterized. This study suggests that along with its well-defined role in mammary gland development, C/EBPβ may well play a role in the pathology of breast cancer, particularly through the control of angiogenesis in the invasive phenotype.

ACKNOWLEDGMENTS

We thank Drs. Graciela Piwien-Pilipuk and Jessica Schwartz (University of Michigan at Ann Arbor, Ann Arbor, MI) for kindly providing expression plasmids for C/EBPβ-LAP and -LIP; Drs. Andrew Paterson and Jeffrey Kudlow (University of Alabama at Birmingham, Birmingham, AL) for kindly providing suggestions on the transfection of MDA-MB-468 cells; Dr. Violaine Harris for kindly providing suggestions and FGF-BP promoter luciferase reporter constructs; Dr. Ranjan Ray for sharing unpublished data; and the Riegel and Wellstein laboratories for providing helpful discussions.

REFERENCES

1. Folkman, J., and Klagsburn, M. Angiogenic factors. Science (Wash. DC), *235:* 442–447, 1987.
2. Liotta, L. A., Steeg, P. S., and Stetler-Stevenson, W. G. Cancer metastasis and angiogenesis: an imbalance of positive and negative regulation. Cell, *64:* 327–336, 1991.
3. Folkman, J. How is blood vessel growth regulated in normal and neoplastic tissue? G. H. A. Clowes memorial Award lecture. Cancer Res., *46:* 467–473, 1986.
4. Fidler, I. J., ar.1 Ellis, L. M. The implications of angiogenesis for the biology and therapy of cancer metastasis. Cell, *79:* 185–188, 1994.
5. Baird, A., and Klagsbrun, M. The fibroblast growth factor family. Cancer Cells (Cold Spring Harbor), *3:* 239–243, 1991.
6. Gospodarowicz, D., Ferrara, N., Schweigerer, L., and Neufeld, G. Structural characterization and biological functions of fibroblast growth factor. Endocr. Rev., *8:* 95–114, 1987.
7. Vlodavsky, I., Folkman, J., Sullivan, R., Fridman, R., Ishai-Michaeli, R., Sasse, J., and Klagsbrun, M. Endothelial cell-derived basic fibroblast growth factor: synthesis and deposition into subendothelial extracellular matrix. Proc. Natl. Acad. Sci. USA, *84:* 2292–2296, 1987.
8. Rogelj, S., Klagsbrun, M., Atzmon, R., Kurokawa, M., Haimovitz, A., Fuks, Z., and Vlodavsky, I. Basic fibroblast growth factor is an extracellular matrix component required for supporting the proliferation of vascular endothelial cells and the differentiation of PC12 cells. J. Cell Biol., *109:* 823–831, 1989.
9. Saksela, O., Moscatelli, D., Sommer, A., and Rifkin, D. B. Endothelial cell-derived heparan sulfate binds basic fibroblast growth factor and protects it from proteolytic degradation. J. Cell Biol., *107:* 743–751, 1988.
10. Kiefer, M. C., Stephans, J. C., Crawford, K., Okino, K., and Barr, P. J. Ligand-affinity cloning and structure of a cell surface heparan sulfate proteoglycan that binds basic fibroblast growth factor. Proc. Natl. Acad. Sci. USA, *87:* 6985–6989, 1990.
11. Wu, D. Q., Kan, M. K., Sato, G. H., Okamoto, T., and Sato, J. D. Characterization and molecular cloning of a putative binding protein for heparin-binding growth factors. J. Biol. Chem., *266:* 16778–16785, 1991.
12. Czubayko, F., Smith, R. V., Chung, H. C., and Wellstein, A. Tumor growth and angiogenesis induced by a secreted binding protein for fibroblast growth factors. J. Biol. Chem., *269:* 28243–28248, 1994.
13. Tassi, E., Al-Attar, A., Aigner, A., Swift, M. R., McDonnell, K., Karavanov, A., and Wellstein, A. Enhancement of fibroblast growth factor (FGF) activity by an FGF-binding protein. J. Biol. Chem., *276:* 40247–40253, 2001.
14. Czubayko, F., Liaudet-Coopman, E. D., Aigner, A., Tuveson, A. T., Berchem, G. J., and Wellstein, A. A secreted FGF-binding protein can serve as the angiogenic switch in human cancer. Nat. Med., *3:* 1137–1140, 1997.
15. Kurtz, A., Wang, H. L., Darwiche, N., Harris, V., and Wellstein, A. Expression of a binding protein for FGF is associated with epithelial development and skin carcinogenesis. Oncogene, *14:* 2671–2681, 1997.
16. Harris, V. K., Coticchia, C. M., Kagan, B. L., Ahmad, S., Wellstein, A., and Riegel, A. T. Induction of the angiogenic modulator fibroblast growth factor-binding protein by epidermal growth factor is mediated through both MEK/ERK and p38 signal transduction pathways. J. Biol. Chem., *275:* 10802–10811, 2000.
17. Harris, V. K., Liaudet-Coopman, E. D., Boyle, B. J., Wellstein, A., and Riegel, A. T. Phorbol ester-induced transcription of a fibroblast growth factor- binding protein is modulated by a complex interplay of positive and negative regulatory promoter elements. J. Biol. Chem., *273:* 19130–19139, 1998.
18. Poli, V. The role of C/EBP isoforms in the control of inflammatory and native immunity functions. J. Biol. Chem., *273:* 29279–29282, 1998.
19. Diehl, A. M. Roles of CCAAT/enhancer-binding proteins in regulation of liver regenerative growth. J. Biol. Chem., *273:* 30843–30846, 1998.
20. Descombes, P., and Schibler, U. A liver-enriched transcriptional activator protein. LAP, and a transcriptional inhibitory protein, LIP, are translated from the same mRNA. Cell, *67:* 569–579, 1991.
21. Descombes, P., Chojkier, M., Lichtsteiner, S., Falvey, E., and Schibler, U. LAP, a novel member of the C/EBP gene family, encodes a liver-enriched transcriptional activator protein. Genes Dev., *4:* 1541–1551, 1990.
22. Seagroves, T. N., Krnacik, S., Raught, B., Gay, J., Burgess-Beusse, B., Darlington, G. J., and Rosen, J. M. C/EBPβ, but not C/EBPα, is essential for ductal morphogenesis, lobuloalveolar proliferation, and functional differentiation in the mouse mammary gland. Genes Dev., *12:* 1917–1928, 1998.
23. Zahnow, C. A., Cardiff, R. D., Laucirica, R., Medina, D., and Rosen, J. M. A role for CCAAT/enhancer binding protein β-liver-enriched inhibitory protein in mammary epithelial cell proliferation. Cancer Res., *61:* 261–269, 2001.
24. Zahnow, C. A., Younes, P., Laucirica, R., and Rosen, J. M. Overexpression of C/EBPβ-LIP, a naturally occurring, dominant- negative transcription factor, in human breast cancer. J. Natl. Cancer Inst., *89:* 1887–1891, 1997.
25. D'Amico, T. A., and Harpole, D. H., Jr. Molecular biology of esophageal cancer. Chest Surg. Clin. N. Am., *10:* 451–469, 2000.
26. Nemunaitis, J., and O'Brien. J. Head and neck cancer: gene therapy approaches. Part II: genes delivered. Expert Opin. Biol. Ther., *2:* 311–324, 2002.
27. Sartorelli, A. C. The 1985 Walter Hubert lecture. Malignant cell differentiation as a potential therapeutic approach. Br. J. Cancer, *52:* 293–302, 1985.
28. Sainsbury, J. R., Farndon, J. R., Needham, G. K., Malcolm, A. J., and Harris, A. L. Epidermal-growth-factor receptor status as predictor of early recurrence of and death from breast cancer. Lancet, *1:* 1398–1402, 1987.
29. Piccart, M., Lohrisch, C., Di Leo, A., and Larsimont, D. The predictive value of HER2 in breast cancer. Oncology, *61*(Suppl. 2)*:* 73–82, 2001.
30. Unger, E. R., Budgeon, L. R., Myerson, D., and Brigati, D. J. Viral diagnosis by *in situ* hybridization. Description of a rapid simplified colorimetric method. Am. J. Surg. Pathol., *10:* 1–8, 1986.
31. Panoskaltsis-Mortari, A., and Bucy, R. P. *In situ* hybridization with digoxigenin-labeled RNA probes: facts and artifacts. Biotechniques, *18:* 300–307, 1995.
32. Baldino, F., Jr., Chesselet, M. F., and Lewis, M. E. High-resolution *in situ* hybridization histochemistry. Methods Enzymol., *168:* 761–777, 1989.
33. Kozak, M. Possible role of flanking nucleotides in recognition of the AUG initiator codon by eukaryotic ribosomes. Nucleic Acids Res., *9:* 5233–5262, 1981.
34. Kozak, M. Point mutations define a sequence flanking the AUG initiator codon that modulates translation by eukaryotic ribosomes. Cell, *44:* 283–292, 1986.
35. Raja, R. H., Paterson, A. J., Shin, T. H., and Kudlow, J. E. Transcriptional regulation of the human transforming growth factor- α gene. Mol. Endocrinol., *5:* 514–520, 1991.

36. Harris, V. K. Transcriptional regulation of the angiogenic factor FGF-BP in squamous cell carcinoma. Ph. D. Thesis. Washington, DC: Georgetown University, 1998.
37. Harris, V. K., Kagan, B. L., Ray, R., Coticchia, C. M., Liaudet-Coopman, E. D., Wellstein, A., and Tate Riegel, A. Serum induction of the fibroblast growth factor-binding protein (FGF-BP) is mediated through ERK and p38 MAP kinase activation and C/EBP-regulated transcription. Oncogene, *20:* 1730–1738, 2001.
38. Bonfil, R. D., Vinyals, A., Bustuoabad, O. D., Llorens, A., Benavides, F. J., Gonzalez-Garrigues, M., and Fabra, A. Stimulation of angiogenesis as an explanation of Matrigel-enhanced tumorigenicity. Int. J. Cancer, *58:* 233–239, 1994.
39. Filmus, J., Pollak, M. N., Cailleau, R., and Buick, R. N. MDA-468, a human breast cancer cell line with a high number of epidermal growth factor (EGF) receptors, has an amplified EGF receptor gene and is growth inhibited by EGF. Biochem. Biophys. Res. Commun., *128:* 898–905, 1985.
40. Shao, Z. M., Wu, J., Shen, Z. Z., and Barsky, S. H. Genistein inhibits both constitutive and EGF-stimulated invasion in ER-negative human breast carcinoma cell lines. Anticancer Res., *18:* 1435–1439, 1998.
41. Davies, S. P., Reddy, H., Caivano, M., and Cohen, P. Specificity and mechanism of action of some commonly used protein kinase inhibitors. Biochem. J., *351:* 95–105, 2000.
42. Kobayashi, E., Ando, K., Nakano, H., Iida, T., Ohno, H., Morimoto, M., and Tamaoki, T. Calphostins (UCN-1028), novel and specific inhibitors of protein kinase C. I. Fermentation, isolation, physico-chemical properties and biological activities. J. Antibiot. (Tokyo), *42:* 1470–1474, 1989.
43. Cuenda, A., Rouse, J., Doza, Y. N., Meier, R., Cohen, P., Gallagher, T. F., Young, P. R., and Lee, J. C. SB 203580 is a specific inhibitor of a MAP kinase homologue which is stimulated by cellular stresses and interleukin-1. FEBS Lett., *364:* 229–233, 1995.
44. Kumar, S., McDonnell, P. C., Gum, R. J., Hand, A. T., Lee, J. C., and Young, P. R. Novel homologues of CSBP/p38 MAP kinase: activation, substrate specificity and sensitivity to inhibition by pyridinyl imidazoles. Biochem. Biophys. Res. Commun., *235:* 533–538, 1997.
45. Duncia, J. V., Santella, J. B., III, Higley, C. A., Pitts, W. J., Wityak, J., Frietze, W. E., Rankin, F. W., Sun, J. H., Earl, R. A., Tabaka, A. C., Teleha, C. A., Blom, K. F., Favata, M. F., Manos, E. J., Daulerio, A. J., Stradley, D. A., Horiuchi, K., Copeland, R. A., Scherle, P. A., Trzaskos, J. M., Magolda, R. L., Trainor, G. L., Wexler, R. R., Hobbs, F. W., and Olson, R. E. MEK inhibitors: the chemistry and biological activity of U0126, its analogs, and cyclization products. Bioorg. Med. Chem. Lett., *8:* 2839–2844, 1998.
46. Amoui, M., Draber, P., and Draberova, L. Src family-selective tyrosine kinase inhibitor, PP1, inhibits both Fc εRI- and Thy-1-mediated activation of rat basophilic leukemia cells. Eur. J. Immunol., *27:* 1881–1886, 1997.
47. Harris, V. K., Coticchia, C. M., List, H. J., Wellstein, A., and Riegel, A. T. Mitogen-induced expression of the fibroblast growth factor-binding protein is transcriptionally repressed through a non-canonical E-box element. J. Biol. Chem., *275:* 28539–28548, 2000.
48. Raingeaud, J., Whitmarsh, A. J., Barrett, T., Derijard, B., and Davis, R. J. MKK3- and MKK6-regulated gene expression is mediated by the p38 mitogen-activated protein kinase signal transduction pathway. Mol. Cell. Biol, *16:* 1247–1255, 1996.
49. Shaheen, R. M., Davis, D. W., Liu, W., Zebrowski, B. K., Wilson, M. R., Bucana, C. D., McConkey, D. J., McMahon, G., and Ellis, L. M. Antiangiogenic therapy targeting the tyrosine kinase receptor for vascular endothelial growth factor receptor inhibits the growth of colon cancer liver metastasis and induces tumor and endothelial cell apoptosis. Cancer Res., *59:* 5412–5416, 1999.
50. Brown, L. F., Berse, B., Jackman, R. W., Tognazzi, K., Manseau, E. J., Senger, D. R., and Dvorak, H. F. Expression of vascular permeability factor (vascular endothelial growth factor) and its receptors in adenocarcinomas of the gastrointestinal tract. Cancer Res., *53:* 4727–4735, 1993.
51. Berger, M. S., Locher, G. W., Saurer, S., Gullick, W. J., Waterfield, M. D., Groner, B., and Hynes, N. E. Correlation of c-erbB-2 gene amplification and protein expression in human breast carcinoma with nodal status and nuclear grading. Cancer Res., *48:* 1238–1243, 1988.
52. Guerin, M., Barrois, M., Terrier, M. J., Spielmann, M., and Riou, G. Overexpression of either c-myc or c-erbB-2/neu proto-oncogenes in human breast carcinomas: correlation with poor prognosis. Oncogene Res., *3:* 21–31, 1988.
53. van de Vijver, M. J., Peterse, J. L., Mooi, W. J., Wisman, P., Lomans, J., Dalesio, O., and Nusse, R. Neu-protein overexpression in breast cancer. Association with comedo-type ductal carcinoma *in situ* and limited prognostic value in stage II breast cancer. N. Engl. J. Med., *319:* 1239–1245, 1988.
54. Paik, S. Clinical significance of erbB-2 (HER-2/neu) protein. Cancer Investig., *10:* 575–579, 1992.
55. Efimova, T., LaCelle, P., Welter, J. F., and Eckert, R. L. Regulation of human involucrin promoter activity by a protein kinase C. Ras, MEKK1, MEK3, p38/RK, AP1 signal transduction pathway. J. Biol. Chem., *273:* 24387–24395, 1998.
56. Nagao, M., Yamauchi, J., Kaziro, Y., and Itoh, H. Involvement of protein kinase C and Src family tyrosine kinase in Gαq/11-induced activation of c-Jun N-terminal kinase and p38 mitogen-activated protein kinase. J. Biol. Chem., *273:* 22892–22898, 1998.
57. Lange, C. A., Richer, J. K., Shen, T., and Horwitz, K. B. Convergence of progesterone and epidermal growth factor signaling in breast cancer. Potentiation of mitogen-activated protein kinase pathways. J. Biol. Chem., *273:* 31308–31316, 1998.
58. Hazzalin, C. A., Cano, E., Cuenda, A., Barratt, M. J., Cohen, P., and Mahadevan, L. C. p38/RK is essential for stress-induced nuclear responses: JNK/SAPKs and c-Jun/ATF-2 phosphorylation are insufficient. Curr. Biol., *6:* 1028–1031, 1996.
59. Talukder, A. H., Jorgensen, H. F., Mandal, M., Mishra, S. K., Vadlamudi, R. K., Clark, B. F., Mendelsohn, J., and Kumar, R. Regulation of elongation factor-1α expression by growth factors and anti-receptor blocking antibodies. J. Biol. Chem., *276:* 5636–5642, 2001.
60. Hazzalin, C. A., Cuenda, A., Cano, E., Cohen, P., and Mahadevan, L. C. Effects of the inhibition of p38/RK MAP kinase on induction of five fos and jun genes by diverse stimuli. Oncogene, *15:* 2321–2331, 1997.
61. Piwien-Pilipuk, G., Van Mater, D., Ross, S. E., MacDougald, O. A., and Schwartz, J. Growth hormone regulates phosphorylation and function of CCAAT/enhancer-binding protein β by modulating Akt and glycogen synthase kinase-3. J. Biol. Chem., *276:* 19664–19671, 2001.
62. Lekstrom-Himes, J., and Xanthopoulos, K. G. Biological role of the CCAAT/enhancer-binding protein family of transcription factors. J. Biol. Chem., *273:* 28545–28548, 1998.
63. Engelman, J. A., Lisanti, M. P., and Scherer, P. E. Specific inhibitors of p38 mitogen-activated protein kinase block 3T3–L1 adipogenesis. J. Biol. Chem., *273:* 32111–32120, 1998.
64. Derijard, B., Raingeaud, J., Barrett, T., Wu, I. H., Han, J., Ulevitch, R. J., and Davis, R. J. Independent human MAP-kinase signal transduction pathways defined by MEK and MKK isoforms. Science (Wash. DC), *267:* 682–685, 1995.
65. Raingeaud, J., Gupta, S., Rogers, J. S., Dickens, M., Han, J., Ulevitch, R. J., and Davis, R. J. Pro-inflammatory cytokines and environmental stress cause p38 mitogen-activated protein kinase activation by dual phosphorylation on tyrosine and threonine. J. Biol. Chem., *270:* 7420–7426, 1995.
66. Wang, X. Z., and Ron, D. Stress-induced phosphorylation and activation of the transcription factor CHOP (GADD153) by p38 MAP kinase. Science (Wash. DC), *272:* 1347–1349, 1996.
67. Mudgett, J. S., Ding, J., Guh-Siesel, L., Chartrain, N. A., Yang, L., Gopal, S., and Shen, M. M. Essential role for p38α mitogen-activated protein kinase in placental angiogenesis. Proc. Natl. Acad. Sci. USA, *97:* 10454–10459, 2000.
68. Jung, Y. D., Liu, W., Reinmuth, N., Ahmad, S. A., Fan, F., Gallick, G. E., and Ellis, L. M. Vascular endothelial growth factor is upregulated by interleukin-1 β in human vascular smooth muscle cells via the P38 mitogen-activated protein kinase pathway. Angiogenesis, *4:* 155–162, 2001.